MODELLING OF MASS TRANSFER IN PACKING MATERIALS WITH CELLULAR AUTOMATA

Alma Margaretha Engelbrecht

Thesis submitted in partial fulfilment
of the requirements for the degree

MASTER OF SCIENCE IN ENGINEERING
(CHEMICAL ENGINEERING)
at the Department of Process Engineering
Stellenbosch University

Supervised by: Prof C Aldrich
Prof A J Burger

December 2008

Declaration

By submitting this thesis electronically, I declare that the entirety of the work contained therein is my own, original work, that I am the owner of the copyright thereof (unless to the extent explicitly otherwise stated) and that I have not previously in its entirety or in part submitted it for obtaining any qualification.

Date: December 2008

Synopsis

The general objective for this thesis is to assess the ability of cellular automata to model relatively complex processes or phenomena, in particular thermodynamic scenarios. The mass transfer in packing materials of distillation columns was selected as an example due to the sufficient level of complexity in the distillation process, and its importance in a wide range of applications.

A literature survey on cellular automata that summarizes the information currently available in formal publications and the internet is included to provide a general overview on the basic theoretical principles and the application of cellular automata models in the process engineering industry. The literature study was also used to identify potential requirements for the new research project.

The study objective includes the construction of a cellular automata model that is able to represent transition of solutes from the fluid on the micro-surfaces of packing materials to the by-passing vapour stream, as well as the steady-state equilibrium between evaporation and condensation. Iterated model parameters sufficient for the realistic modelling of mass transfer as a result of thermodynamic driving forces, are required to meet this objective. The model behaviour was compared and the parameters subsequently adjusted according to the behaviour that is theoretically expected from the system being simulated. Qualitative (although sometimes in a quantitative format) rather than quantitative observations and comparisons were made seeing that the model has not yet been calibrated.

The model that has been developed to date is not able to simulate the individual effects of chemical and thermodynamic properties although a realistic simulation of the cumulative effect exerted by these factors, or change thereof, on a system has been achieved. The accuracy of the results that have been obtained by using iterated parameters cannot be guaranteed for scenarios that deviate too much from the systems that have already been modelled successfully.

The trade-off between the ability of the model to incorporate the effect of polarization, its ability to represent separation, in particular the condensation of hydrophilic substances, for strong hydrophilic packing materials and its ability to incorporate a large number of species limits the range of scenarios that can be successfully modelled.

The model is able to represent the effect of a declining driving force (difference between the component vapour pressure of the gas phase and that of the liquid phase) that is typical of a system which is allowed to reach equilibrium after an initial disturbance. The model is also able to represent an additional driving force for separation caused by the effect of intermolecular forces.

The model also displays the potential ability to represent the effect of different surface structures of the packing material on the extent of separation achieved at steady state as well as the rate at which such steady state conditions have been achieved. The model must be correctly scaled to minimize inaccurate results.

Although several adjustments are needed to eliminate some limitations, the model has proven itself worthy of further development due to its capability to represent the basic characteristics of mass transfer in packing materials.

Opsomming

Die algehele doelwit van hierdie tesis is die beoordeling van sellulêre automata se vermoë om relatief komplekse prosesse en verskynsels, veral dié wat verband hou met termodinamika, te modelleer. Die massa-oordag in die pakkingsmateriaal binne-in distillasiekolomme was as 'n voorbeeld gekies weens die genoegsaam komplekse aard daarvan, asook die belangrike rol wat die distillasieproses in verskeie toepassings daarvan speel.

'n Literatuuroorsig is ingesluit waarin die inligting oor sellulêre automata wat tans in formele publikasies en op die internet verkrygbaar is, opgesom word. Die doel hiervan is om as algemene oorsig oor die basiese teorie en die toepassing van sellulêre automata modelle in die prosesingenieurswese-industrie, te dien. Die literatuuroorsig word ook aangewend as 'n hulpmiddel waarmee potensiële vereistes vir die nuwe navorsingsprojek geïdentifiseer word.

Die studiedoelwit sluit die konstruksie van 'n sellulêre automata model wat daartoe instaat is om die oorgang van opgeloste stowwe vanuit die vloeistoflagie op die mikro-oppervlaktes van die pakkingsmateriaal na die verbygaande gasstroom, sowel as die gestadigde ekwilibrium tussen verdamping en kondensasie te modelleer, in. Hiervoor word geïtereerde modelparameters voldoende vir die realistiese modellering van massa-oordrag as gevolg van termodinamiese dryfkragte, benodig. Die gedrag van die model word met die teoreties verwagte gedrag van die stelsel wat gesimuleer word, vergelyk en die parameters word daarvolgens aangepas. Aangesien die model nog nie gekalibreer is nie, word daar van kwalitatiewe (soms gekwantifiseerde) eerder as inherent kwantitatiewe waarnemings en vergelykings gebruik gemaak.

Die model is tot dusver nog nie daartoe instaat om die uitwerking van 'n individuele chemiese of termodinamiese eienskap te modelleer nie. 'n Realistiese model van die gesamentlike effek van hierdie faktore, of verandering daarin, is egter wel verkry. Die akkuraatheid van resultate wat met die hulp van geïntereerde parameters verkry is, kan nie vir scenarios wat te veel van die gemodelleerde scenario afwyk, gewaarborg word nie.

Die onvermoë van die model om polarisasie, sommige skeidingsmeganismes (veral waar kondensasie van hidrofiliese dampe vir 'n sterk hidrofiliese pakkingsmateriaal ter sprake is) en 'n groot aantal chemiese spesies terselfdertyd te akkomodeer, beperk die scenarios wat suksesvol gemodelleer kan word.

Die model kan die uitwerking van 'n afnemende dryfkrag (verskil tussen die dampdruk van 'n komponent in die gasfase en die ooreenstemmende druk in die vloeistoffase), tipies van 'n stelsel wat toegelaat word om te stabiliseer nadat dit aanvanklik versteur is, uitbeeld. Die model kan ook die addisionele dryfkrag as gevolg van intermolekulêre kragte, inkorporeer.

Die model het ook die potensiaal getoon om die uitwerking van verskillende oppervlakkonfigurasies in die pakkingsmateriaal op die skeidingstempo en graad van skeiding wat by gestadigde toestande verkry word, suksesvol uit te beeld. Die skaal van die model moet egter korrek gekies word om onakkuraathede uit te skakel.

Op hierdie stadium is daar nog verskeie verstellings aan die model nodig om bogenoemde beperkings uit te skakel. Die model het egter reeds genoeg potensiaal getoon om die verdere ontwikkeling daarvan te regverdig.

Quote

Admission of ignorance is often the first step in education.

– Stephen Covey

Acknowledgements

The author acknowledges the help of Ben Bredenkamp, researcher at the University of Stellenbosch, for the following:

- Assistance with Matlab Coding used for simulating the mass transfer in packing materials with cellular automata.

- Advice regarding the implementation of the programme and the subsequent interpretation of the results.

Table of Contents

1. Introduction

Quantitative problems are often classified into the following three regimes: Problems of simplicity, problems of disorganized complexity and problems of organized complexity.

Problems of simplicity refer, as the name implies, to simple mathematical problems that involve only a few variables, usually two. On the other hand, a problem of disorganized complexity deals with a very large number of variables of which the individual properties are either erratic or unknown while the entire system can be characterized by orderly and analyzable average properties (Weaver, 1948).

Problems of organized complexity refer to the "middle region" of problems in which the number of variables is too large for the problem to be considered simple, yet it possesses organized features which renders it unsuitable for random sampling. Therefore statistical methods through which disorganized complex problems can be dealt with cannot be directly applied. These organized complex problems simultaneously deal with a sizable number of factors which are interrelated into a complicated organic whole (Weaver, 1948).

Electronic computing devices have proven themselves to be an increasingly useful tool for dealing with the latter kind of problems, due to their increased ability to store large amounts of information, to perform complicated calculations and the decreased need for direct human input (Weaver, 1948).

1.1 Continuous and Discrete Models of Complex Problems

Solutions for organized complex problems are often pursued by means of modelling. A model usually strives to simplify such a problem by incorporating only a few variables strategically selected from the total "pool" of variables inherent to the problem. The model uses the information available from the selected variables to define and subsequently solve the problem.

Continuous models that incorporate differential equations form part of the classical modelling strategy represented by Arrow (a) in Figure 1. These models proved to be extremely useful, especially when calculations still had to be performed by hand before the computer age. Continuous models, especially those that incorporated partial differential equations, played a significant role in the development of modern physics (Schatten, 2006).

Most differential equations have no closed form solution. Computers are now commonly used to solve these equations by substituting the symbolic calculations with numerical approximations (Schatten, 2006). This converts the results again to a discrete form as shown in Figure 1 (Greenspan, 1973).

Toffoli commented on this approach as follows: *"... we start ... with mathematical machinery that probably has much more than we need, and we have to spend much effort disabling these 'advanced features' so that we can get our job done in spite of them."* (Toffoli, 1984) The rapid development in electronic computers over recent decades made the use of discrete models as opposed to continuous models an increasingly feasible and attractive alternative.

Cellular Automata is an example of a discrete modelling system that involves a system in which space, time, and the states of the system are discrete.

Each point in a regular spatial lattice, called a cell, can have any one of a finite number of states. The states of the cells in the lattice are updated according to a set of local rules. The state of a cell at a given time depends only on its own state and the states of its local neighbours during the previous time slot. All cells on the lattice are updated synchronously in discrete time steps (Gutowitz, 1999).

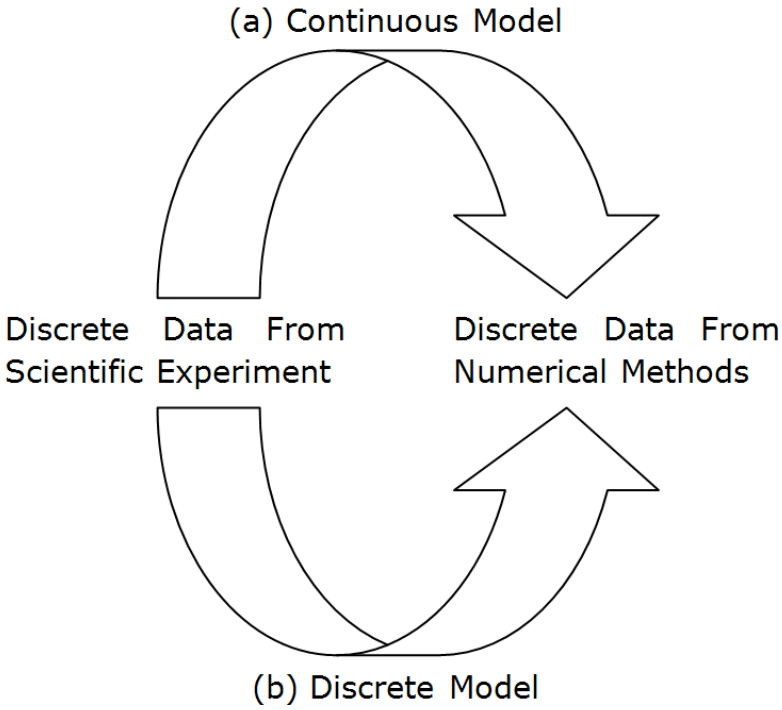

Figure 1: Solution of complex problems by means of (a)continuous modelling and (b) discrete modelling

A discrete model provides a more consistent modelling approach by keeping the data in the discrete form as shown by Arrow (b) in Figure 1 (Greenspan, 1973).

A further advantage of cellular automata with respect to systems of differential or partial differential equations is the inherent dynamic stability. The addition of new features or interactions never leads to structural instabilities. (Ganguly et al., 2003)

The use of cellular automata has some disadvantages as well: It is very difficult to produce quantitative results without compromising the inherent strength of cellular automata which lies in the simplicity of the rules (Schatten, 2006). Cellular automata allows for a finite number of rules while there is no limit to the possible number of differential equations in a continuous model. However, the number of differential equations that can actually be solved is small (Schatten, 2006).

Whether continuous or discrete models are superior for solving complex problems remains a question with no simple answer and the subject of numerous academic debates. This study is not intended to support either side of the argument, but merely explores the capability of cellular automata to model thermodynamical scenarios that are usually modelled with more conventional methods.

1.2 Motivation for Modelling of Mass Transfer in Packing Materials with Cellular Automata

Cellular automata are simple models that enable the analyst to represent well-understood local effects, such as the chemical or steric interaction between molecules themselves and between molecules or particles and their environment, which can lead to very complex behaviour on a macroscopic scale.

A thorough understanding of the selective vaporization (stripping) of solutes from the thin liquid film on the micro surfaces of rigid structures, such as the packing materials found in distillation columns, is important for the effective recovery of volatile chemicals. These chemicals are often (by-) products from a vast range of chemical processes, of which some are of vital economic or environmental importance. The distillation process is dynamic and depends on the structure of the packing material, as well as the chemical and thermodynamic properties of the materials being transported or separated.

Previous work on the modelling of various other chemical and physical, including thermodynamical, phenomena with cellular automata does exist. Refer to Section 2.6.1 for examples in this regard. Work by the Process Engineering Department as well as published results from other institutions and persons are applicable in this regard (to be discussed and referenced in Section 2.6). However, there appears to be no previous research on the modelling of mass transfer in packing materials, or any equivalent system in terms of type and complexity, with cellular automata.

1.3 Objectives for this Study

The general objective for this study is to explore the capability of cellular automata to model relatively complex processes or phenomena, in particular thermodynamic scenarios (usually modelled with more conventional methods). The mass transfer in packing materials of distillation columns was selected as an example due to the sufficient level of complexity in the distillation process, and its importance in a wide range of applications.

The specific objectives for this study are as follows.

1.3.1 Literature Review

A literature review on cellular automata is required for the following purposes:

- The literature survey will summarize the information currently available in books, published journal articles and the internet.
- The literature survey must provide a general overview on cellular automata that includes the basic theoretical principles and must provide some insight on the application of cellular automata models in the process engineering industry.

- The literature study will serve as a gap analysis in which potential requirements for the new research project are identified.

1.3.2 Construction of a Suitable CA Model to Simulate the Mass Transfer in Packing Materials

The study objective includes the construction of a cellular automata model that is suitable for the modelling of mass transfer in packing materials. The model was implemented in the form of a computer programme that receives input from the user (model parameters) from which it will calculate the required output (model results). The model parameters will typically consist of the board dimensions, the number and type of cells present and the rules according to which these cells move (or exchange positions).

This study will subsequently aim towards model parameters that are sufficient for the realistic modelling of mass transfer (including selective evaporation and condensation) as a result of the thermodynamic driving forces to which these parameters correspond. The potential ability of the model to represent the effect of the packing material structure on the rate and steady state level of separation achieved will also be investigated.

1.3.3 Evaluation of the Model Behaviour

The general integrity and scope of the model needs to be evaluated. The ability of the model to represent simple mass transfer scenarios will therefore be tested.

The model behaviour will be compared to the behaviour that is theoretically expected from the system being simulated. The model in its current format has not yet been calibrated. Therefore qualitative (although sometimes in a quantitative format) rather than quantitative observations and comparisons are expected.

Criteria need to be established according to which the model output can be compared to the behaviour that is theoretically expected. The necessary qualitative and quantitative output required for such criteria also need to be identified and incorporated into the computer programme.

2. Overview on Cellular Automata

The primary objective of this chapter is to provide a general overview on cellular automata, which includes the history and development, definition and characterization, possible structural variations, dynamics, behavioural classification and applications thereof.

Cellular Automate involves a system in which space, time, and the states of the system are discrete. Each point in a regular spatial lattice, called a cell, can have any one of a finite number of states. The states of the cells in the lattice are updated according to a set of local rules. The state of a cell at a given time depends only on its own state and the states of its local neighbours during the previous time slot. All cells on the lattice are updated synchronously. Thus the state of the entire lattice advances in discrete time steps (Gutowitz, 1999). The overall structure can be viewed as a parallel processing device (Ganguly et al., 2003).

2.1 History and Development of Cellular Automata

During the past 70 years there has been three periods of heightened interest in cellular automata which were a result of three outstanding contributions. The first of these contributions, which played a key role in the development of cellular automata, is John von Neumann's self-reproducing automaton (von Neumann, 1966), the second, Martin Gardner's popularization of John Conway's *Game of Life* (Gardner, 1970) and the third, Stephen Wolfram's classification of automata (Sarkar, 2000; Wolfram, 1984).

The history of cellular automata has accordingly been divided in three sections: Classical era during which the predominant influence was the initial work of von Neumann, the Gardner era during which Cellular Automata was popularized by John Conway's *Game of Life* (amongst other factors) and finally the modern era which was characterized by the work of Wolfram and by developments on other fronts of Computer Science (Sarkar, 2000).

2.1.1 Classic Era - Early Development of Cellular Automata

Stanislaw Ulam, while working at the Los Alamos National Laboratory during the 1940’s, modelled the growth of crystals with a simple lattice network. At the same time, John von Neumann, Ulam's colleague, was working on the problem of self-replicating systems which included physical systems like factories and machinery (von Neumann, 1966; Toffoli et al., 1987).

The concept of cellular automata (CA) was initiated in the early 1950's by J. Von Neumann and Stan Ulam (Ganguly et al., 2003). Ulam suggested that an abstract mathematical model would be more suitable to demonstrate the possibilities of universal construction and self reproduction. Von Neumann subsequently developed his design around a mathematical abstraction. Von Neumann's simplified cellular

automata were two dimensional, with a numerically implemented self-replicator (Wolfram, 2002).

The result was a universal copier and constructor which operated as cellular outomata with small neighbourhoods (only orthogonal cells that touch side by side were neighbours). Each cell would exhibit one of twenty nine states. Von Neumann mathematically proved that a particular pattern would make endless copies of itself within the given cellular universe. This is known as the tessellation model (Wolfram, 2002). In the context of cellular automata, 'universal' refers to the ability to model any other automata.

The details of von Neumann's construction were unpublished at the time of his death in 1957. His work was edited and published posthumous by A. W. Burks. During 1964-1965, Codd worked out a variant on von Neumann's CA which required only eight states per cell (Codd, 1968).

The principal results of the time were demonstrations on the existence of universal constructors as well as Moore's *Garden of Eden theorem.* The *Garden of Eden theorem* showed configurations in certain automata which could only be initial states. Such a pattern could never again be repeated during the course of the automaton's evolution (Moore, 1962; Myhill, 1963).

The *classical era* was preceded by even earlier work on automata theory. Examples include the studies of Warren S. McCulloch and Walter Pitts in 1943 on neural nets (McCulloch et al., 1943).

2.1.2 Gardner Era - Popularization of Cellular Automata

Public awareness of cellular automata can be attributed to John Horton Conway's interest in simplifying and exploring the capabilities of von Neumann's configuration (Gardner, 1970; Dewdney, 1989, 1990). One of the most common examples of cellular automata is the Game of Life (written by John Conway) in which complex patterns emerge from a (supposedly infinite) square lattice of simple two state (living and dead) automata whose next state is determined solely by the current states of its four closest neighbours and itself.

Conway's results were presented in 1970 as an ecological game called *Life*, a two-state, two-dimensional cellular automaton, in Martin Gardner's monthly *Mathematical Games* column in the *Scientific American*. The rules were as follows: If a black cell has 2 or 3 black neighbours, it stays black. If a white cell has 3 black neighbours, it becomes black. In all other cases, the cell stays or becomes white. McIntosh appropriately describes the significance of the *Game of Life*: Conway carefully composed the evolutionary rules of this game. Extremes in which live cells multiplied and grew without bound, or in which live cells dwindled and eventually died, were avoided. The ultimate fate of his delicately balanced creation remained uncertain. Uncommon combinations capable of unlimited growth were always possible. Small patterns were able to delay thousands of generations before their final behaviour finally emerged (McIntosh, [1]).

Possibly because it was viewed as a largely recreational topic, little follow-up work was done. In 1969, however, German computer pioneer Konrad Zuse published his book *Calculating Space.* He proposed that the physical laws of the universe are

discrete by nature, and that the entire universe is just the output of a deterministic computation by means of a giant cellular automaton. His first paper on this topic dates back to 1967. (Schmidhuber, 2003)

2.1.3 Modern Era - Wolfram's Research on Cellular Automata

In 1983 Stephen Wolfram published the first of a series of papers which investigated a very basic but essentially unknown class of cellular automata, which he termed *elementary cellular automata*. The unexpected complexity of the behaviour of these simple rules led Wolfram to suspect that complexity in nature may be due to similar mechanisms.

Although both von Neumann and Conway were aware that alternative rules of evolution existed, they concentrated on one single rule by exploring its consequences in detail which served their purposes. Wolfram, on the contrary, was one of the first to compare the evolutionary histories of large numbers of different rules, with the intent of classifying them according to their long term behaviour (McIntosh, [1]).

Additionally, during this period Wolfram formulated the concepts of intrinsic randomness and computational irreducibility, and suggested that rule 110, an example of cellular automata within Wolfram's classification scheme (Wolfram, 2002), may be universal—a fact proved by Matthew Cook in the 1990s. Universal cellular automata are able to model the behaviour of any other cellular automata. In 2002 Wolfram published his results in his book, *A New Kind of Science*, in which he emphasized the significance of cellular automata for all disciplines of science.

In his book, *The Lifebox, the Seashell and the Soul*, Rucker expanded upon Wolfram's theories on universal automata. A cellular automata model was used to explain how simple rules can generate complex results (Rucker, 2005; McIntosh, [1]).

2.2 Definition and Characterization of Cellular Automata

An informed choice of the configuration, local rules, boundary conditions, etc. is impossible to make without a prior knowledge of the inherent characteristics of cellular automata which includes the versatility and limitations thereof. The optimal exploitation of the cellular automata as a modelling technique will therefore be highly unlikely without a proper introduction to this relatively new concept.

2.2.1 Definition of Cellular Automata

Cellular automata are, in contrast to partial differential equations, which can describe continuous dynamical systems, discrete dynamical systems (Schatten, 2006).

Cellular automata consist of regular grids of cells. Each cell can be in one of a finite number of possible states, updated synchronously in discrete time steps according to a local, identical interaction rule. The state of a cell is determined by the previous state of itself as well as that of the surrounding neighbourhood of cells.

2.2.2 Characterization of Cellular Automata

Figure 2 shows the four features by which cellular automata are characterized, namely the state of the cell, the neighbourhood of the cell, the geometry of the underlying medium (grid) which contain the cells and the local transition rules (Sarkar, 2000).

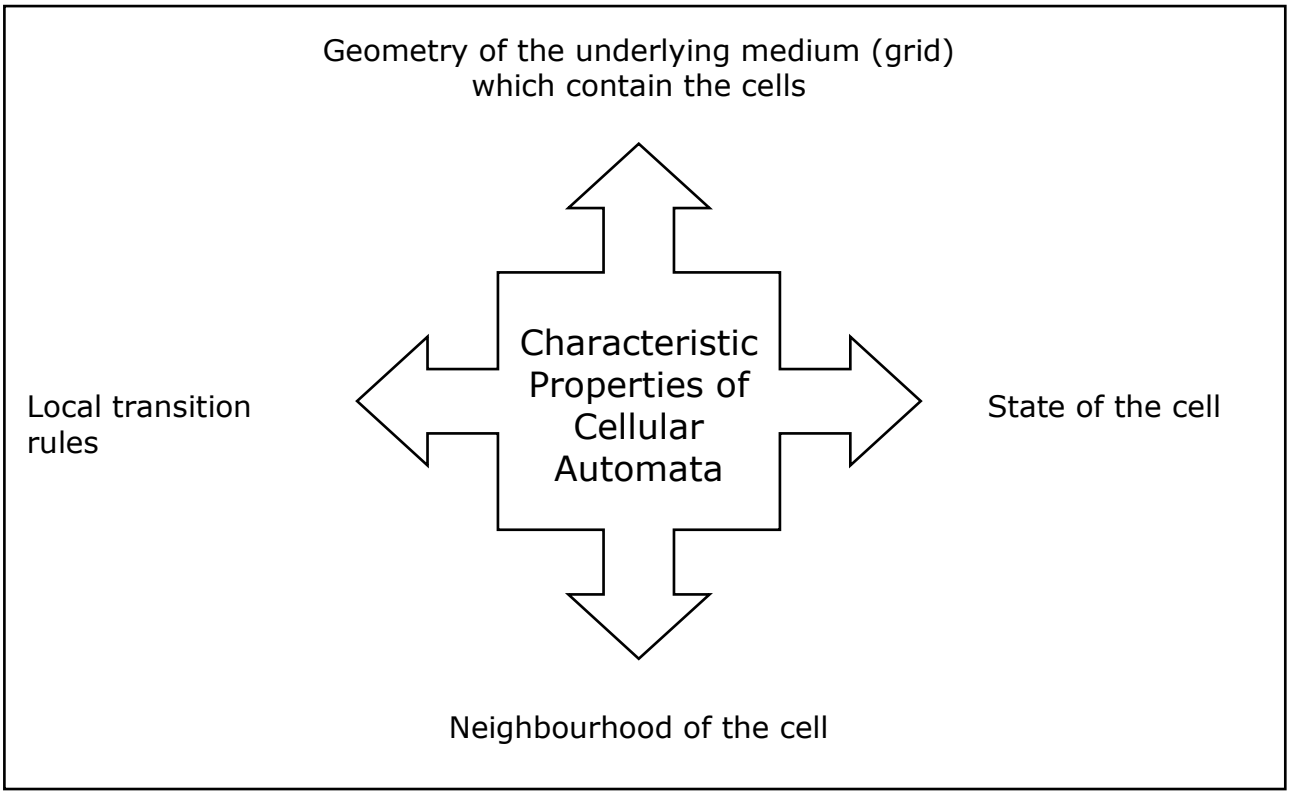

Figure 2: Features by which cellular automata are characterized

The defining role of the above mentioned properties in the structure and state transitions of cellular automata is discussed in Section 2.3 and 2.4 respectively.

2.3 Structural Variations of Cellular Automata

Different structural variations of cellular automata have been proposed to ease the design and behavioural analysis thereof and to increase its versatility for modelling purposes (Ganguly et al., 2003).

One of the defining specifications of a cellular automaton is the type of grid on which it is constructed and subsequently computed. A grid is defined as an intersection of infinite lines according to some rules (Wolfram, 2002; Gardner, 1970; Weisstein, [6]). Cellular automata may be constructed on Cartesian grids in arbitrary numbers of dimensions, with a lattice containing an integer number of cells as the most common choice for a grid (Wolfram, 1994). The simplest "grid" consists of a one dimensional line of cells.

Secondly, the number of possible states a cellular automaton (cell) may assume must also be specified. This number is typically an integer, with 2 (binary) being the simplest choice.

Thirdly, the neighbourhood over which cells affect one another must be specified. The simplest choice is "nearest neighbours," in which only cells directly adjacent to a given cell may be affected at each time step.

Ulam, suggested that von Neumann, who was the first to define cellular automata, should mathematically abstract this concept (Wolfram, 2002; Gardner, 1970; Weisstein, [6]). Von Neumann initially viewed them as three dimensional models, but then turned to two dimensional models after he had realized that they were complex enough for the purposes of his work. Although cellular automata may be constructed on Cartesian grids in an arbitrary number of dimensions (Wolfram, 1994), the most popular dimensions of cellar automata have ever since been one and two dimensional automata.

2.3.1 One Dimensional Cellular Automata

Because of its inherent simplicity, the one dimensional CA with two states per cell became the most studied variant of CA. The neighbourhood size generally varies from three (simplest) to five or seven cells (Ganguly et al., 2003).

The simplest type of cellular automaton is a binary, nearest-neighbour, one dimensional automaton. Such automata are called *elementary cellular automata* (Wolfram 1983, 2002). There are 256 such automata, each of which can be indexed by a unique binary number whose decimal representation is known as the "rule" for the particular automaton (Wolfram, 1994).

In general terms the number of rules can be calculated by k^{kn}, where *k* is the number of possible states for the cell and *n* is the number of neighbours (including the centre cell itself) (Schatten, 2006).

An illustration of Rule 30 is shown in Figure 3 (a)-(d) on the following page with the results it produces after 15 time-steps starting from a single black cell in Figure 4.

One dimensional cellular automata are represented as a row of cells. The progression of each state is observed by stacking each row on top of each other after applying the rule once after each step (Wolfram, 2002) as shown in Figure 4.

For a binary automaton, 0 is commonly depicted as a white cell whereas 1 is depicted as a black cell. However, *totalistic cellular automata* may also have a continuous range of ***k*** possible values (states). In these automata, the average or the sum of the adjacent cell states determines the evolution of a specific cell. For these automata, the set of rules describing the behaviour can be encoded as a (***3k-2***)-digit ***k***-ary number known as a "code" (Wolfram, 2002).

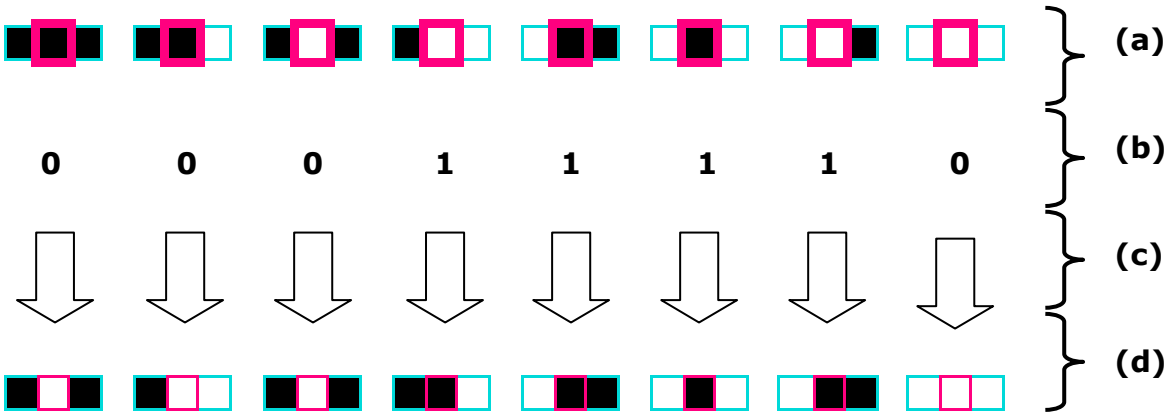

(a) *All possible state and neighbourhood configurations for one dimensional, binary cellular automata in a three cell neighbourhood*

(b) *Binary representation of Rule 30 with white and black cells as results represented by 0 and 1 respectively*

(c) *Application of Rule 30 on the centre cells (pink border) of the configurations in (a) yielding the result in (d).*

(d) *Result of Rule 30 for all the possible neighbourhood configurations in (a)*

Figure 3: Application of Rule 30 on one dimensional cellular automata

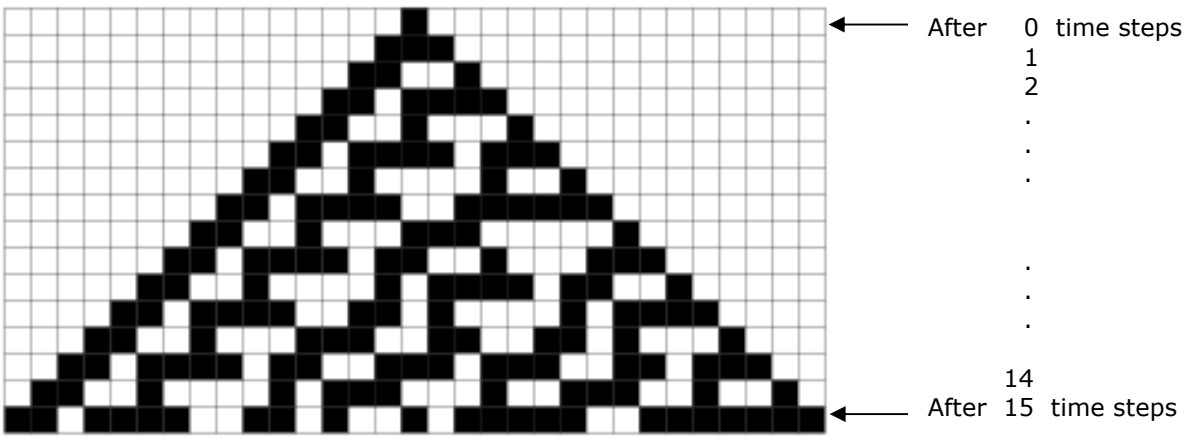

Figure 4: Result for a Rule 30 automaton of a single black cell in 15 time steps (Wolfram, 2002)

2.3.2 Two Dimensional Cellular Automata

Due to the simplicity and symmetry of the resulting patterns, square, triangular, and hexagonal grids are commonly utilized in two dimensional cellular automata. Researchers in cellular automata therefore tend to stick to these grids for their models. An example of a more exotic two dimensional grid is the Penrose tiling, which is per definition a general class of grids with a non-repeating pattern which can extend over an infinite area (Peterson, 1988).

Two Dimensional CA with Triangular Cells

A triangular grid, also called an isometric grid (Gardner, 1983), consists of a regular arrangement (tessellation) of equilateral triangles as shown in Figures 5 and 6. A triangular grid therefore consists of three equidistant sets of parallel lines, all at 60-degree angles from each other (Peterson, 1988).

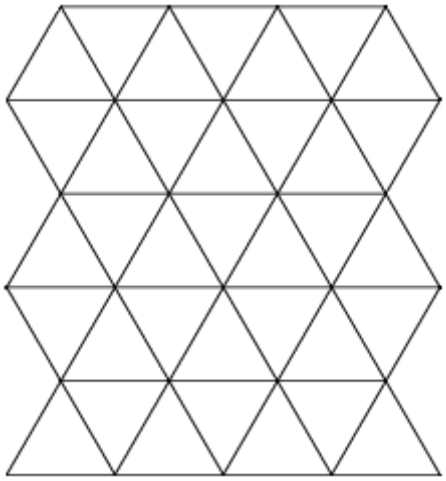

Figure 5: Two dimensional isometric grid

The total number of triangles (including inverted ones) in Figure 6 is calculated as follows (Wolfram, 1994):

$$N(n) = \begin{cases} (1/8)(n+2)(2n+1)n & \text{for n even} \\ (1/8)((n+2)(2n+1)n-1) & \text{for n odd} \end{cases} \quad \textbf{(1)}$$

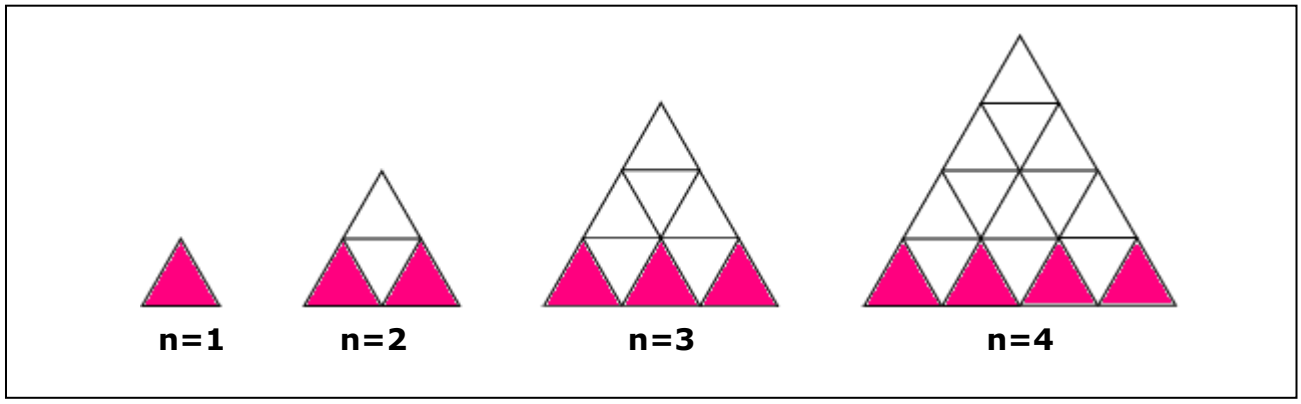

Figure 6: Triangular isometric grid with a total side length of n constituent cellular side lengths

Hexagonal Two Dimensional Cellular Automata

A hexagonal grid is a two dimensional grid formed by a tessellation of regular hexagons (Figure 7). Note the absence of single contact points between gridlines characteristic of isometric and orthogonal grids. Boards consisting of hexagonal grids are therefore often found in strategy and role-playing games (Wolfram, 1994).

Figure 7: ***Hexagonal grid with a centre cell (light grey) surrounded by its six nearest neighbours (black)***

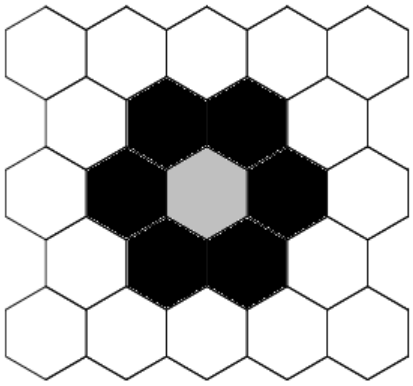

Two Dimensional CA with Squared (Orthogonal) Cells

A square grid is defined as two sets of an infinite number of parallel lines that are equidistant from each other and perpendicular (Peterson, 1988). This grid coincides with the traditional two dimensional, orthogonal Cartesian planes which render it the most popular grid for cellular automata models.

All two-dimensional CA consisting of squared cells are assumed to have either a five-cell neighbourhood or a nine-cell neighbourhood, with two or more possible states per cell. The two variations of neighbourhood configurations (five and nine) are termed Von Neumann and Moore neighbourhoods respectively and are shown in Figure 8 (a) and (b) on the following page. The extended generalizations of these two configurations are termed the R-radial and R-axial neighbourhoods (Figure 8 (c) and (d)) respectively. For both Von Neumann and Moore neighbourhood, R = 1.

For a two-dimensional CA with a Moore neighbourhood (R=1) and two possible states per cell, k=2 and n=9. Therefore the number of possible rules can be calculated as follows:

$$k^{kn} = 2^{(2x9)} = 536870912 \qquad \textbf{(2)}$$

A comprehensive study of all rules in higher dimensional automata is therefore not easily achievable (Schatten, 2006).

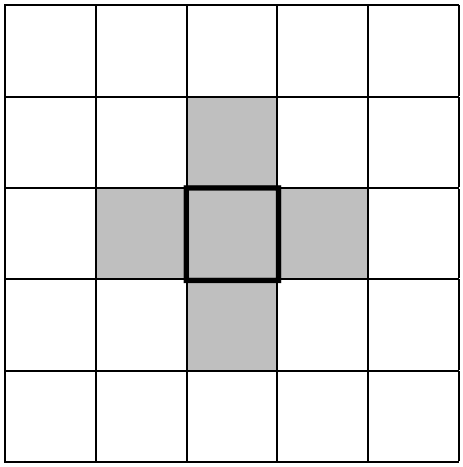

(a) Von Neumann neighbourhood (grey) for centre cell (black border) with R = 1

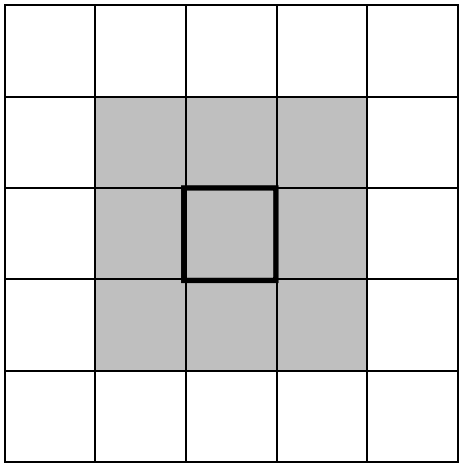

(b) Moore neighbourhood (grey) for centre cell (black border) with R = 1

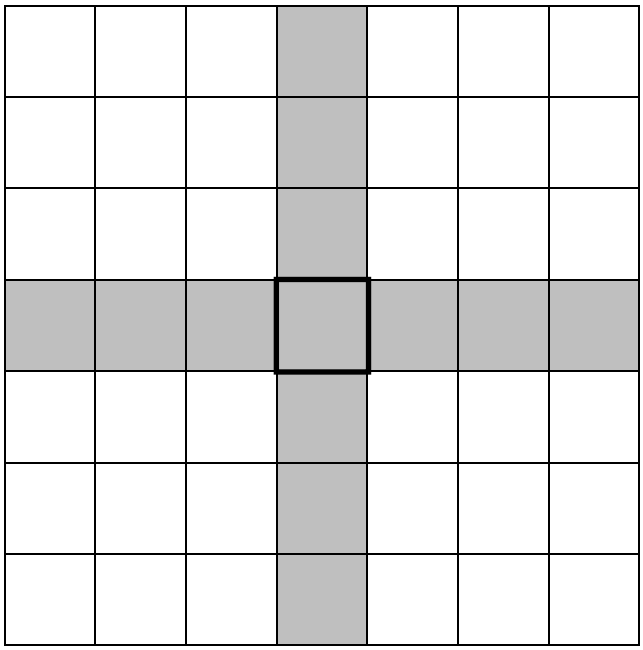

(c) Expanded Von Neumann neighbourhood (in grey) for centre cell (black border) with R = 3

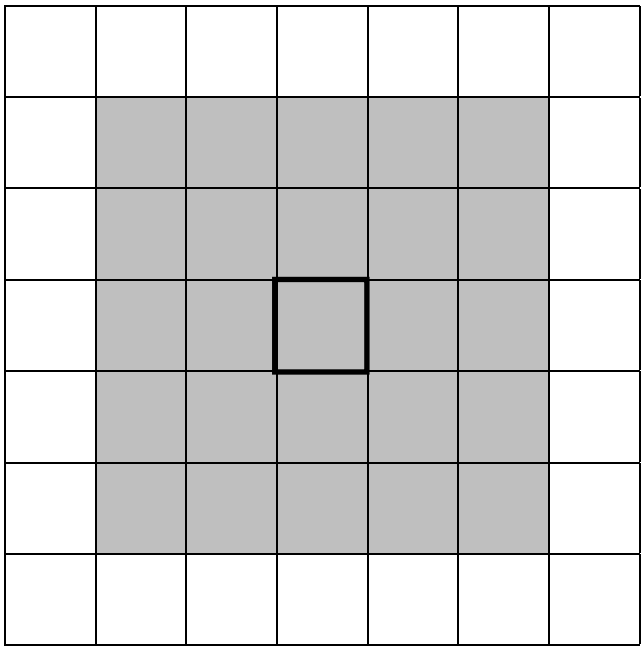

(d) Extended Moore neighbourhood (in grey) for centre cell (black border) with R = 2

Figure 8: ***Different neighbourhood configurations for two dimensional cellular automata***

2.3.3 Boundary Configurations of Multi-Dimensional CA

Cellular automata grids may consist of a multi (possibly infinite) dimensional structure. Cellular automata are often simulated on a finite grid rather than an infinite one. For example, in two dimensions a grid would often be considered as a rectangle instead of an infinite plane.

Cellular automata generally poses a problem where cells on the edges of finite grids are considered seeing that the rules for their behaviour are usually based on their interaction with their surroundings (neighbours) of the cells within the grid, which differs from those on the edge of the grid.

The behaviour of the cells on the edges of the grid will affect the behaviour of all the other cells within the grid. A possible solution is to define neighbourhoods differently for these cells. One could formally consider the fact that they have fewer neighbours. Therefore a separate set of rules for the cells on the edges of the grid needs to be defined which could also become tedious. For finite grids, it is more feasible to apply one of the following boundary configurations:

Fixed Boundary Configuration

A grid has a fixed boundary in a given dimension if the cells on the edges of the grid in that dimension are considered as if they are adjacent to cells in a pre-specified unchanging state for the full duration of the computation (Peterson, 1988).

Null Boundary Configuration

A variation of the fixed boundary configuration is the null boundary configuration in which the boundary cells are assumed to be in a quiescent state (Peterson, 1988) or, for numerically calibrated states, in which they have a zero value.

Periodic Boundary Configuration

A grid has a periodic boundary in a given dimension if it is considered to be folded in this dimension. The right most cell is the neighbour of the left most one and vice versa for this dimension. Two dimensional grids are usually visualized as a *toroidal* arrangement: When one cell disappears over a given edge of the board, another cell comes in at the corresponding position at the opposite edge of the board. This can be visualized as taping the left and right edges of the rectangle to form a tube, then taping the top and bottom edges of the tube to form a torus as in Figure 9. The same principle applies for grids in any other dimension.

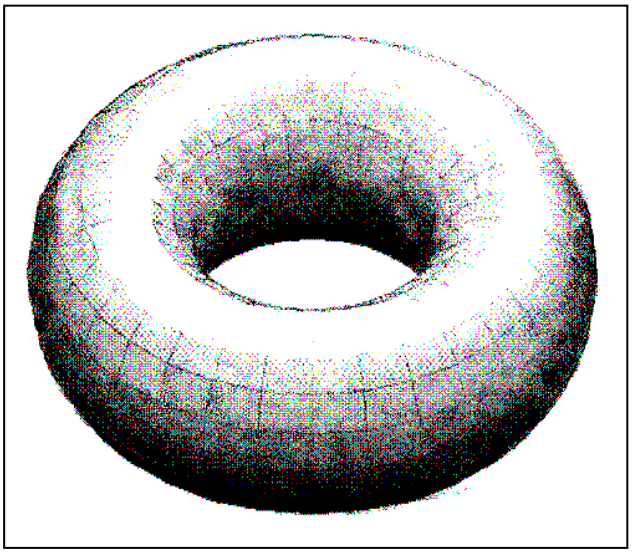

Figure 9: Toroidal shape

Other Possible Boundary Configurations

It is also possible for one end of a grid to have periodic boundary condition and the other end to have fixed boundary condition (Bardell, 1990). Although there are other possibilities for boundary conditions (Martin et al., 1984), the above mentioned configurations are the most widely known and applied.

2.4 Systematic State Transitions (Rule-based Dynamics) of Cellular Automata

The states of the cells in the lattice of a cellular automaton are updated according to a set of local rules which in turn depends on the previous states of the cells and that of their local neighbours (refer to the definition of CA in Section 2.2). The following sub-sections elaborate on various possibilities for rule configurations that can be applied on cellular automata.

2.4.1 Uniform, Hybrid and Tessellation Cellular Automata

The local rules applied to each cell can either be the same for every cell (uniform CA) or differ from one another (hybrid CA). Therefore cellular automata where each cell has its own local rule are considered hybrid.

It is possible for a cell to change its local rule at each time step. In the VLSI (very large-scale integration) context, this is called a programmable CA. This type of structure is also called a tessellation automata or time-varying CA in a more theoretical context (Sarkar, 2000).

2.4.2 Deterministic and Stochastic Cellular Automata

The local rule is usually assumed to be deterministic. This is not necessarily true for all CA. There are variations in which the rule sets are probabilistic or fuzzy (Ganguly et al., 2003). The rule sets are generally defined and adapted according to the design requirements of the applications.

Standard rule sets which have been used for different applications do exist. Wolfram rules (Wolfram, [7]) are examples of these rule sets. The vast number of possible configurations of cellular automata contributes to the modelling power and versatility thereof.

2.4.3 Iterative Cellular Automata

This is a CA where only one particular cell is given an input. It has been shown that this class is an inherently slower device than the usual CA because the input is provided one symbol at a time to a particular cell. Normally the input for a CA is the initial configuration itself (Sarkar, 2000).

2.4.3 One-Way Cellular Automata

A one-way CA allows only one-way communication. For example, in a one dimensional array each cell depends either only on itself and its left neighbour or on itself and its right neighbour. However, both-side dependence is not allowed. This lack of two-way flow of information can be considered as a restriction on the power of the automaton. However, there are results which indicate otherwise (Sarkar, 2000).

2.4.4 Reversible (Invertible) Cellular Automata

Another variation of cellular automata, is the reversible (invertible) CA. For this type of CA, the time-based development of the system is completely reversible. Therefore at any time step, the rules allow the development of the CA to go forward or backward in time without losing any information (Schatten, 2006).

Rule *r* is therefore invertible if another rule, called the inverse rule, exists which drives the CA backward. For example, if application of *r* to a configuration *c* produces a configuration *d*, then application of the inverse rule to *d* produces *c*. A CA is called invertible if its local rules are invertible (Sarkar, 2000).

2.5 Classification of Cellular Automata according to its Dynamic Behaviour

Various classification schemes for cellular automata, based on the dynamic behaviour thereof, exist. The three most well-known schemes namely the classification by Wolfram, Culik II and Yu's classification scheme as well as Eppstein's classification, are briefly discussed in the sub-sections to follow.

2.5.1 Wolfram's Classification Scheme

Stephen Wolfram proposed a classification scheme which divided cellular automata rules into four categories according to the evolution results from a "disordered" initial state (Wolfram, 1984). His classification is therefore based on entropy measures and identifies the following four classes (Sarkar, 2000).

Class I Evolution leads to a homogeneous state

After a finite number of time steps, Class I CA evolve from almost all initial states to a unique homogeneous state, in which all cells/sites have the same value.

Class II Evolution leads to series of fixed configurations or oscillators

After a finite number of time steps, Class II CA evolve from almost all initial states to a set of separated simple stable or periodic structures.

Class III Evolution leads to a chaotic pattern

From almost all possible initial states, evolution of infinite class III CA leads to aperiodic ("chaotic") patterns. After sufficiently many time steps, the statistical properties of these patterns are typically the same for almost all initial states. In particular, the density of non-zero sites typically tends to a fixed non-zero value.

Class IV Evolution leads to complexity

Evolution leads to complex localized structures, sometimes long-lived (e.g. for one dimensional cellular automata, Wolfram's Rule 20 52 and 110). With class IV cellular automata, complex behaviour, stable or periodic structures which persist for an infinite time and propagating structures are formed. It is believed that this class is capable of universal computation.

(Wolfram, 1984; Sarkar, 2000)

Wolfram's classification scheme was influential, but it failed to capture the idea of universal computation. Systems capable of universal computation have been found in all four of Wolfram's categories. Since universal computation is such a fundamental feature of cellular automata, a classification scheme that provides no assistance in identifying it seems to be of only rather limited interest (Wolfram, 1984). Work in this regard that followed Wolfram's proposal in 1984, concentrated on formalizing the intuitive classifications by Wolfram et al. (Sarkar, 2000).

2.5.2 Culik II and Yu's Classification Scheme

Culik II and Yu (1988) proposed the following classification scheme with **r** being the local rule in a cellular automaton.

Class I

Rule **r** is in Class I if every finite configuration, i.e. configurations in which only a finite number of cells are in non-quiescent states, evolves to a stable configuration in finitely many steps.

Class II

Rule **r** is in Class II if every finite configuration evolves to a periodic configuration in a finite number of steps.

Class III

Rule **r** is in Class III if it is decidable whether a configuration occurs in the orbit of another.

Class IV

Class IV comprises of all local rules that are not included in Classes I, II or III.

(Sarkar, 2000)

The above classification considers only finite configurations. Infinite configurations in general cannot be finitely described, and hence cannot be approached by conventional computability theory.

Braga et al. (1995) provided a classification of CA based on pattern growth. Certain shift-like dynamics in the evolution can be discovered by examining the local rule. A subsequent grouping of rules exhibiting similar dynamics yields a classification which is close to that of Wolfram (Sarkar, 2000; Culik II et al, 1990).

2.5.3 Eppstein's Classification Scheme

John Conway's *Game of Life* has fascinated and inspired many enthusiasts, due to the emergence of complex behaviour from a very simple system. One of the many phenomena that have been regarded as particularly interesting in the *Game of Life* is the existence of "gliders": small patterns that move across the grid. According to some authors, for example Wolfram, gliders and other complex behaviours occurring in the *Game of Life* are unusual, (Eppstein, [4]).

Others, for example David Eppstein, question whether gliders are really that rare. Eppstein claims that he has investigated whether gliders exist in many semi-totalistic rules similar to the *Game of Life*, where the behaviour of a cell depends only on its own state and the number of live neighbours. According to Eppstein, the results show that the existence of gliders is commonplace, contradicting Wolfram and calling into question his classification of cellular automata.

The classification scheme proposed by Eppstein as an alternative to that of Wolfram is summarized below.

Contraction (pattern shrinkage) impossible

If a rule dictates that any pattern expands to infinity in all directions, no gliders can exist. Therefore the question of whether a pattern lives or dies cannot be universal. If a rule dictates that a pattern can never shrink, no pattern can die or move. Universal computation could still occur in other ways. For example, the boundary of an expanding pattern could simulate the behaviour of a one dimensional universal automaton.

Expansion (pattern growth) impossible

If a rule dictates that any pattern remains bounded by the dimensions of the original pattern, no gliders can exist. Therefore, the question of whether a pattern lives or dies is again not universal as no gliders can exist.

Both expansion and contraction possible

Gliders can exist only in the remaining cases. Although investigations have shown that a large fraction of the remaining cases does indeed support gliders, their universality still needs to be proven.

(Eppstein, [4], [5]; Wolfram, 1984)

Eppstein's classification scheme attempts to improve on Wolfram's scheme, but this scheme may have some limitations as well. Some of the one dimensional rules are universal. A two dimensional plot of the history of their evolution is also a CA - and is also universal. However, a two dimensional plot of the evolution of a one dimensional CA fulfils the "contraction impossible" condition above since cells are only added. This suggests that the description of these rules as not being universal is mistaken. While they can not contain gliders, they can still contain "pseudo-propagating" structures that are capable of achieving the same effect (Eppstein, [4], [5]; Wolfram, 1984).

2.6 Applications of Cellular Automata

The simple structure of cellular automata has attracted researchers from various disciplines, including physical and social sciences, since the original concept was proposed by Von Neumann and Ulam. Cellular automata have become popular due to their inherent potential to model complex systems, including different sophisticated natural phenomena, in spite of their structural simplicity (Ganguly et al., 2003).

Researchers from diverse application fields have intuitively identified cellular automata dynamics with problems in their own fields. Examples include modelling of biological systems from the level of intracellular activity to the levels of clusters of cells, and population of organisms. Cellular automata have also been used to model the kinetics of molecular systems and crystal growth in chemistry. In physics, the applications cover the study of dynamical systems starting from the interaction of particles to the clustering of galaxies.

In computer science, cellular automata based methods have been employed to model the Von Neumann (self-reproducing) machines as well as the parallel processing architecture. Beyond the domain of natural science, cellular automata have also been used to study problems in other diverse fields, for example, whether the membership of NATO should be more restricted or not (Ganguly et al., 2003). Some examples of applications are summarized with references in the following subsections.

2.6.1 Cellular Automata as a Modelling Method for Physical, Chemical and Biological Phenomena

The idea to develop cellular automata as an alternative to differential equations for modelling laws in physics has lead to the investigation of cellular automata models.

The following examples were primarily selected from various journal articles. These articles describe previous work done on the modelling of various physical, chemical and biological systems through the use of cellular automata. Cellular automata have proven itself as a robust modelling method for these examples, amongst many others (Ganguly et al., 2003).

Initial Modelling Attempt on a Biological System

One of the early attempts to use cellular automata for modelling of biological systems was by Lindenmayer (1968), who proposed a model for the growth of filamentary organisms. Dynamic cellular automata, where cells may appear or disappear with time, were used (Sarkar, 2000).

The key idea was to consider one sequence (1 dimensional array) of cells from the organisms at a time. Cell division was modelled by allowing a cell to be replaced by more than one cell, each in a pre-specified state. If a cell has a neighbourhood consisting of its left neighbour, then after division, the same neighbourhood holds. This model is for non-branching filamentary organisms (Sarkar, 2000).

It is also possible to extend the model to include branching organisms by incorporating both left and right neighbours. Two output functions are defined for this model, the left and the right output. The input to the left cell in the next step is the left output and similarly for the right cell. For the branching organism, the local rule specifies the first cell of the branch to be created. So if the local neighbourhood of a cell is conducive, a new branch is created, which is then considered attached to the basal cell. A cell may give rise to several branches, and in the model it is not possible to distinguish between the relative orientations of the branches. It is also possible for the branches to give rise to new branches (Sarkar, 2000).

Cellular Automata Models of Biochemical Phenomena

Kier, Cheng and Testa (1999) describes the use of kinematic, asynchronous stochastic cellular automata to model water and several other solution phenomena generally encountered in complex biological systems. The experiments were designed and executed in order to assess the ability of the dynamic simulations (including cellular automata) to model certain physical properties observed in solutions.

The simulation results have shown significant similarities to the properties of real physical solutions. These include solution behaviour, dissolution, immiscible systems, micelle formation, diffusion, membrane passage, enzyme activity and acid dissociation.

A Cellular Automata Model of Membrane Permeability

In this study also by Kier and Cheng (1997) a cellular automata model of a semi-permeable membrane separating two compartments of water has been created. The water is stationary in both compartments except for spontaneous diffusion through the membrane. In one compartment, the properties of a polar solute have been assigned to cells near the membrane surface.

The increased concentration of solute cells caused an increase in the preferential diffusion of water from the opposite compartment into the membrane. Therefore the simulation of the osmotic effect is found to increase with the concentration of solute cells.

The lipophilicity of the solute cells has been varied in a subsequent study in order to observe the effect on their diffusion into and through the semi-permeable membrane. The diffusion increases with increasing lipophilicity up to a certain point on the lipophilicity scale, after which a sharp decline in the membrane passage of the solute is observed. At this specific point, also called the critical value of lipophilicity, the

solute concentration within the membrane itself increases dramatically with small changes in the lipophilicity of the solute. At the same critical value there is a significant decrease in the water flow through the membrane in both directions.

Kier and Cheng (1997) showed that dramatic changes in membrane permeability may occur due to minor changes in the molecular structure of the solute which may lead to some physical property changes in the membrane. Changes in the solute must therefore be carefully monitored and accounted for during the simulation.

Direct Simulation of a Permeable Membrane

Brosa (1990) used cellular automata to compute flow through a permeable membrane separating two parallel adjoining water channels. The water in both channels was flowing in the same direction. The membrane constituted of scattering centres formed by the cellular automata. This modelling technique was in direct contrast with classical hydrodynamics which represents a membrane by means of the boundary condition in Equation 3.

$$V^{II}(r) = 0 \qquad \textbf{(3)}$$

The Navier-Stokes equation available from other sources was compared with the output of the cellular automata.

The results from the cellular automata and Navier-Stokes equation agreed well under certain limitations. The boundary condition (3) derived from classical hydrodynamics which stated that the membrane only allowed flow perpendicular to its surface, had to be discarded. Furthermore the membrane was restricted to a small but finite thickness.

The study by Brosa (1990) clearly confirms the statement that cellular automata can provide a more realistic picture than classical hydrodynamics of liquid phenomena, for example flow through a porous membrane, given that certain limits to the model are not transgressed.

The Cellular Automata Model for Lipid Membranes

A published study by Kubica (1994) incorporated the cellular automata method to model the effect of amphiphilic molecules on lipid membranes. Different types of molecular aggregation based on the different affinities of the interacting molecules (depending on their "head" and alkyl chain length) were proposed as an explanation of the differences in permeability of a lipid membrane modified with a mixture of amphiphilic cationic and anionic modifiers.

It was shown within these models that a mixture of opposite-charged amphiphilic molecules can increase the permeability of a membrane modified with only one type of modifier when the mixture contains long and short alkyl chain amphiphiles. It can however decrease the membrane permeability when all modifier molecules have long alkyl chains. These results agreed with experimental data.

The correlation between the simulation and experimental results indicates that the cellular automata describes (suggests) a possible mechanism of action for the above mentioned modifiers.

2.6.2 Other Applications of Cellular Automata

Although the modelling of different physical systems is the most widely explored application of cellular automata, there are many other applications which serve as a further proof of the versatility thereof (Ganguly et al., 2003).

CA as Parallel Computing Machine

In computer design, the application of CA was proposed for building parallel multipliers, prime number sieves, parallel processing computers and sorting machines (Ganguly et al., 2003).

Two-dimensional CA have been used extensively for image processing and pattern recognition (Ganguly et al., 2003).

The MPP (Massively Parallel Processor) of Goodyear Aerospace Corporation was one of the fastest computers of the early 1980s. CA based machines termed as CAMs (CA Machines) have been developed by Toffoli and others. The structure of such machines having a high degree of parallelism (with local and uniform interconnection) is ideally suited for simulation of complex systems. A CAM can achieve simulation performance of at least several orders of magnitude higher than that can be achieved with a conventional computer at comparable cost. CAMs were developed as a result of over a decade of machine and modelling research by the Information Mechanics Group at the Massachusetts Institute of Technology (Ganguly et al., 2003).

Recently, researchers have started exploring the cellular automaton as a typical computing device. It has been presented as a nanometre-scale classical computer (Ganguly et al., 2003).

Application of Cellular Automata in Social Sciences

Sakoda was the first person to develop a CA based model in social sciences. Sakoda published the article `The Checkerboard Model of Social Interaction' in 1971 (Sakoda, 1971). The basic design of the model was already present in his unpublished dissertation of 1949. The central goal of his model was to understand group formation (Ganguly et al., 2003).

Another early example of CA based modelling was provided by Thomas Schelling. Schelling analyzed segregation processes among individuals belonging to two different classes : black and white (Ganguly et al., 2003, Schelling, 1969).

Neither Sakoda nor Schelling ever referred explicitly to CA. The formal concept of CA was not known to this group of researchers in early seventies. The first person who explicitly classifed checkerboard models under CA framework was the economist Peter S. Albin in his essays and his book `The Analysis of Complex Socioeconomic Systems'. He was also the first to stress the enormous potential of CA and finite automata for understanding social dynamics (Ganguly et al., 2003).

CA based models have been used more extensively in behavioural and social sciences by a vast number of analysts ever since (Ganguly et al., 2003).

Application of Cellular Automata in Games

The following three games are, amongst others, examples of games which are based on cellular automata (Ganguly et al., 2003).

Game of Life

This game was originally proposed by Conway. Refer to Section 2.1.2 for more detail on the prominent role of this game in the history and popularization of cellular automata.

The original motivation was to design a simple set of rules to study the macroscopic behaviour of a population. The criterion for the rules was that the growth or decay of the population should not be easily predictable. After extensive experimentation, Conway selected the following set up.

The population is represented by a Moore neighbourhood in a two dimensional infinite array of cells. Each cell can be in state 1 (alive) or 0 (dead). The local rules for each cell have been described as follows.

- *Survival*

  If a cell is in state 1 (alive) and has 2 or 3 neighbours in state 1, the cell survives by remaining in state 1.

- *Birth*

  If a cell is in state 0 and has exactly 3 neighbours in state 1, the cell evolves to state 1 in the next time step.

- *Death*

  A cell in state 1 dies (goes to state 0) from loneliness if it has 0 or 1 neighbours. It may also die from suffocation if it has 4 or more neighbours.

As with many CA evolutions, the "Game of Life" shows extensive variation in the growth patterns of the initial cell population.

Research at the Massachusetts Institute of Technology has shown that there is a simple initial configuration that grows without limit. The configuration grows into a "glider gun" and, after 40 steps, fires the first "glider," and thereafter continues firing gliders after every 30 moves.

It has been informally proved that the "Game of Life" is capable of universal computation.

(Sarkar, 2000)

Interesting Properties and Phenomena Exhibited by the "Game of Life"

The popularity of Conway's "Game of Life" can be attributed to the many interesting structures that can be created with these simple rules. There are numerous possible configurations that exhibit a wide variety of behaviours which include the following examples.

Oscillators

Oscillators, which oscillate periodically from one shape to another; still life, which are oscillators of period one (unchanging); guns, which "shoot" an object repetitively; spaceships, which are moving objects with periodic form; and many other interesting examples (Wolfram, 2002; Gardner, 1970; Weisstein, [6]).

Garden of Eden Configurations

The game of life also has the interesting property of "fatherless states". Also called "garden of Eden" configurations, they are states of the automata that cannot be reached through the progression of any other state. There currently exists three known "garden of Eden" configurations (Wolfram, 2002; Gardner, 1970; Weisstein, [6]).

Firing Squad Problem

This game was first proposed by Myhill in 1957 but the first publication was in 1962 by Edward Moore (Moore, 1962). In this synchronization problem, **n** soldiers (out of which one is a general) are standing in a row. The soldiers (including the general) can communicate only with their immediate left and right neighbours. The general gives the command to fire. The soldiers and the general are all required to fire simultaneously and for the first time.

In CA terms, the problem is to design a cell and a local rule, which evolves to a configuration from which all cells enter a pre-designated state all at once and for the first time, starting from an initial configuration, where only one cell is on and the other **n - 1** cells are off. The idea is to design a cell which is independent of the number of soldiers, and hence will work for an array of an arbitrary length. In case the general is one of the end cells, the minimum time required for synchronization is **2n - 2** steps.

Waksman provided a solution in **2n - 2** steps in 1966. The solution depends predominantly on signals propagating through the array at different speeds. A signal is essentially a symbol which passes from one cell to its neighbour in a particular direction (left or right). A signal propagates at the maximum possible speed if it moves one cell at each step (Waksman, 1966).

It is possible for a cell to suppress a signal for a fixed number of time steps. The speed of the signal determines its geometry — the angle that it makes with the horizontal.

A minimum state solution to the problem is provided by Mazoyer (Mazoyer, 1987). Solutions where the general can be any cell, also exists. Culik II (1990) considered several other variations, and has used the results to disprove a conjecture that real-time one-way CA cannot accept certain languages.

The problem has also been generalized to higher dimensions (Nguyen and Hamacher 1974; Shinahr 1974) and node static and dynamic CA (Herman et al. 1974; Varshavsky et al. 1970 cited by Sarkar, 2000).

A generalization to arbitrary graphs, called the Firing Mob problem, has been introduced in Culik II and Dube (1991), where an efficient solution is also provided (Sarkar, 2000). The introduction to Culik II and Dube (1991) also contains a brief history of the Firing Squad problem and also the solutions attempted by various researchers.

The central result, that it is possible to design such a CA, is called the Firing Squad Theorem, and used in language and pattern-recognition studies of CA (Smith III 1972; Culik II 1989 cited by Sarkar, 2000).

(Sarkar, 2000)

Queen Bee Problem

This "de-synchronization" problem is related to the Firing Squad Problem. This problem incorporates the design of a CA with cells that evolve from an configuration in which all cells are initially in the same state, to a configuration with only one cell in a pre-designated state. (Smith III, 1976 cited by Sarkar, 2000)

(Sarkar, 2000)

$\sigma(\sigma^+)$ – Game

This game was first proposed by Sutner (1990) and is based on the battery operated toy, MERLIN. It is a two-person game and is played on a two dimensional finite grid, where each node has a bulb that can be either on or off.

A move is made by choosing a node and, as a result, the states of all the bulbs in orthogonal neighbourhood positions toggle. A configuration of the game is a state of the grid where some of the bulbs are on and others are off. Player A chooses two configurations, the initial and the target configurations. Player B has to make a sequence of moves starting from the initial configuration to reach the target configuration.

Choosing a node twice is the same as not choosing it at all. The order in which the nodes are chosen is not important.

The study of the σ-game reduces to the study of linear, 2-dimensional CA (Barua and Ramakrishnan, 1996; Sutner, 1990). The corresponding game where the state of the chosen bulb also changes is called the σ^+-game.

Both the σ and σ^+-games have been studied on 2 dimensional and multidimensional grids.

(Sarkar, 2000)

VLSI Application of Cellular Automata

Because of its simplicity, regularity, modularity and the inherent structural ability to form cascades with local neighbourhood, additive CA are ideally suited for VLSI (very large scale integration) implementation. Different applications ranging from VLSI test domains to the design of a hardwired version of different CA based schemes have been proposed (Ganguly et al., 2003).

Pattern Recognition

Although this is also, like VLSI application, an important application of cellular automata in various research domains (Ganguly et al., 2003), including neural networks, its significance has limited applicability for the purposes of this thesis and will therefore not be discussed in further detail.

2.7 Research Areas Insufficiently Addressed by Literature

From the literature available to date, it can be seen Cellular automata are occasionally used to model some phenomena related to chemical engineering (refer to Section 2.6.1 for some examples with references), especially where discrete entities like particles, micro-organisms, chemical species like atoms, ions or molecules are considered. There are no examples in which cellular automata feature as a modelling technique for any large scale chemical operation like distillation. Cellular automata are at this stage still under-exploited in the process engineering industry as opposed to other modelling techniques like CFD-modelling.

At the time this study was undertaken, CA models that specifically deal with the mass transfer in packing materials were non-existent. Information on the modelling of other systems involving mass transfer (e.g. filtration) with cellular automata, proved to be useful only as background knowledge. The modelling examples in the literature are often based on assumptions that do not accommodate the full spectrum of possible dynamic behaviour for these systems and are therefore not yet suitable for any large scale, industrial application. In spite of limiting assumptions, principles that were adapted from these models served as ideas for the simulation programme used in this study. Several adjustments and modifications were therefore necessary to meet the needs of the new project.

The shortcomings in the currently available information suggest the need for new simulation models as well as the comparison of the new modelling results with practical (real life) results in order to obtain the necessary models for the phenomena that are involved. The rectification of these insufficiencies for the mass transfer in packing materials corresponds to the general objective for this project.

Discrete modelling techniques like cellular automata are normally not considered for application to large scale chemical processes, especially those that have been successfully modelled with continuous modelling techniques. It is however expected that modelling with cellular automata will become increasingly important in applications like nanotechnology where the behaviour of small, discrete units (or groups thereof) need to be modelled.

3. Methodology

The attempt to simulate the mass transfer within the microstructure of packing materials in distillation columns (as defined in Appendix A1) is based on a simple, two dimensional cellular automata model. The simulation procedure has been divided in two stages, namely the construction and the implementation stages, which are discussed in the following sub-sections.

3.1 Construction of the Cellular Automata Model

A *Matlab* programme that simulates the selective evaporation of a solute from a solution on the surface of packing material was used to model the effect of different types of microstructures. Cellular automata were used to simplify the otherwise complicated model. For the purposes of this experiment, "type" refers to the pre-allocated identity of a cell, e.g. Type 3 is water according to Table 1 below. The following steps were followed during the construction phase.

3.1.1 Initialization of the Two Dimensional Board

The system is divided in a gas phase (G) typically containing non polar gas, usually air, and water vapour, a thin liquid film (L) typically consisting of a non-polar solute dissolved or suspended in a polar solvent and a section which represents the solid packing material surface (PM). These respective phases are represented (modelled) on a two dimensional grid (board) of 300x300 cells as shown in Figure 10. The rigid surface structure may have various possible geometries of which some will be discussed in Section 4.2.

Figure 10 depicts typical starting conditions (before mass transfer commences) for the system according to the colour coding in Table 1.

Table 1: Colour key for cell types used in cellular automata model

Type 1: Void cells
Type 2: Non polar gas (air)
Type 3: Polar liquid (water)
Type 4: Non polar liquid (alcohol)
Type 5: Packing material
Type 6: Polar vapour (water)

A discussion on the composition of each phase will follow in Section 3.2. The distinction between the water vapour and liquid enables the identification of newly formed vapour and condensate at the end of each simulation run.

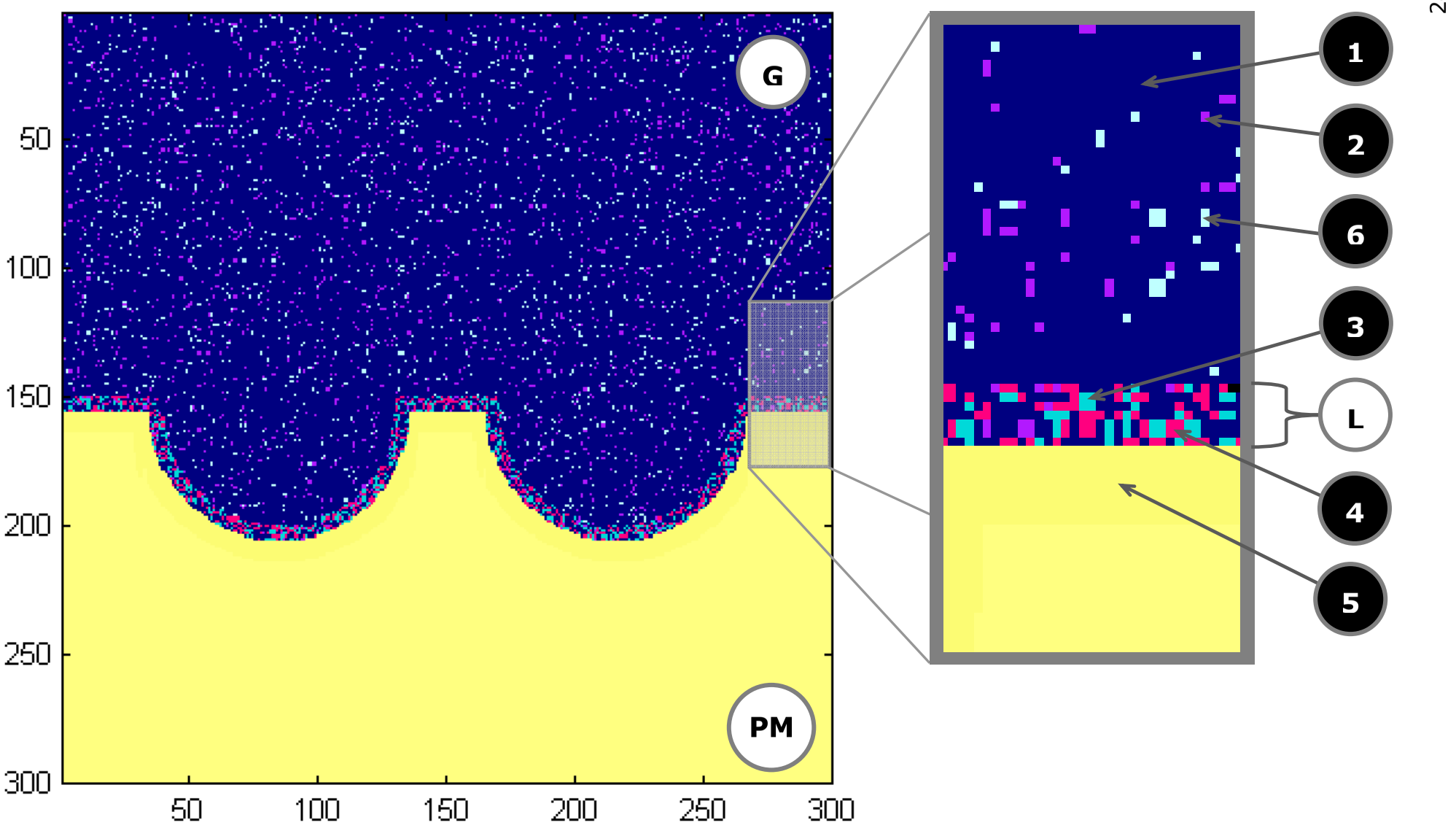

Figure 10: ***Populated board just before simulation commences***

The board is populated by each cell type according to a specified ratio for the number of void cells relative to the number of cells for all the other types. Each cell represents a molecule or group of molecules, depending on the scale of the model, for a certain type. A single cell will therefore retain its identity/type, e.g. water (Type 3), for the full duration of an experimental run, although its position might change during the simulation process. The position of a cell on the board is indexed by a single number x as shown in Figure 11.

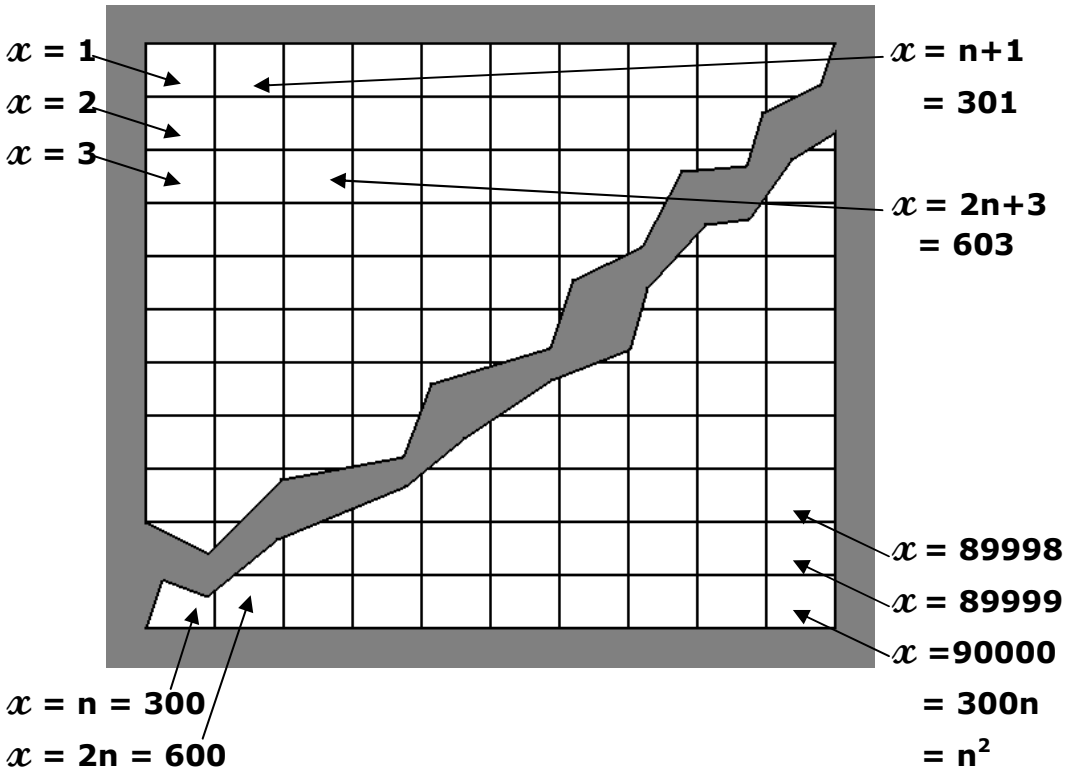

Figure 11: Examples of single-number Indexing on a 300x300 board

Each cell (excluding the cells on the edges of the board) has a Moore neighbourhood which is defined as shown in Figure 12a.

The numbers in the centre of each cell indicate the increase or decrease in index number with respect to that of the centre cell. For example, if the index of the centre (grey) cell were 615, then the index of the neighbour of the top left hand side (North West) of the centre cell will be 115-n-1. For a 300x300 board, n = 300. Therefore the index of this neighbour would be 615-300-1 = 314.

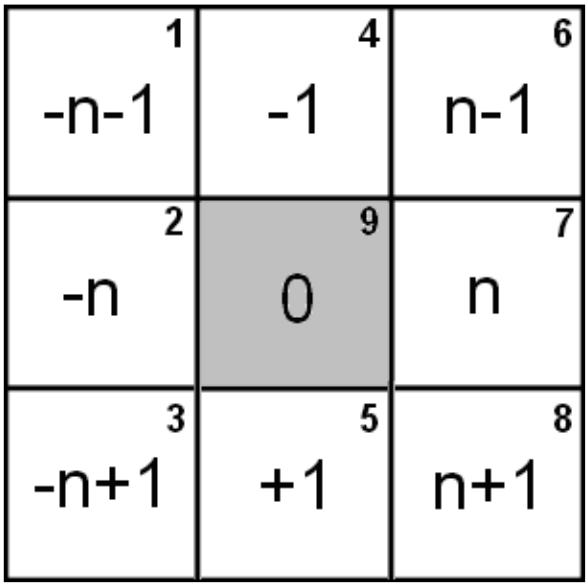

Figure 12 (a): Central Cell (grey) in the Moore neighbourhood (white) that is used in the current model as opposed to the Von Neuman neighbourhood in Fig. (b)

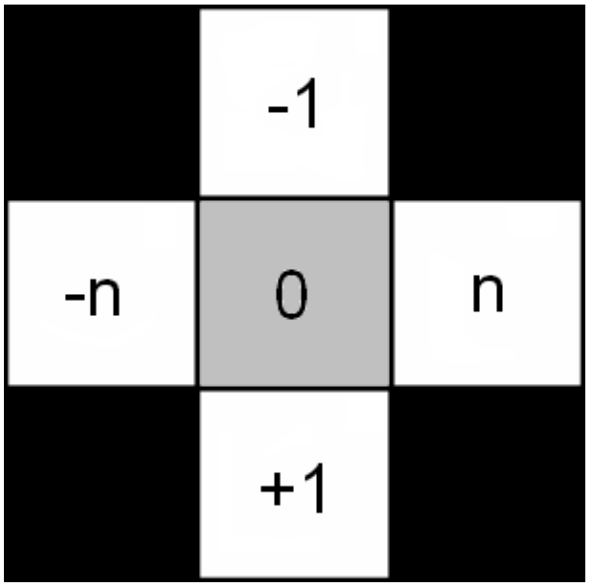

Figure 12 (b): Central Cell (grey) in a Von Neuman neighbourhood (white)

Figure 12 (a) and (b) illustrates the nearest neighbours of the cell. The nearest neighbours include all the cells that are located within the R=1 neighbourhood. (Refer to Section 2.3.2.)

3.1.2 Definition of Parameters for Cell Movements

The programme was set in *Matlab* according to the following principles (rules) which describe the movement of each cell (cellular automaton), depending on its type and location. The actual movement is initiated by a programme "trigger" that is discussed in Section 3.2.1.

Definition of Boundary Conditions: Stationary Edges

To avoid the occurrence of mobile cells with undefined neighbours, the cells on the edges of the board remain stationary and do not participate in any movement. These cells form the boundaries of the system and their contribution to the system as a whole is considered negligible for the purposes of this study. A cell is considered to be part of the boundaries when it lies within a distance of R cells from the closest edge of the board, where R is the size of the neighbourhood that influences the movements of the cell.

Directional Bias (Movement due to External Directional Forces)

The numbers in the top right hand corner of each cell in Figure 12 (a) depicts the sequence in which the neighbourhood cells appear in the vector ($\bar{\mathbf{V}}$) for R =1. $\bar{\mathbf{V}}$ determines the direction in which a centre cell will move and is therefore called the *directional bias*.

$$\bar{\mathbf{V}} = [-n-1, -n, -n+1, -1, +1, n-1, n, n+1, 0] \quad \textbf{(4)}$$

To illustrate the concept of the directional bias, the following vector serve as an example.

$$\bar{\mathbf{V}}_{\text{Example}} = [\ 3,\ 1, 1\ ,\ 3\ ,\ 1, 3\ ,\ 1\ ,\ 1\ ,\ 1\ ] \quad \textbf{(5)}$$

For this example, the centre cell (cell x) will be three times likely to move into position x–n-1, x-1 or x+n-1 than any of the other surrounding positions. This directional bias is illustrated in Figure 13. Note that the cell's current position (centre position = x+0) also counts as one of the "other directions" in the vector. Therefore the probability for the cell remaining in the same position has been accounted for.

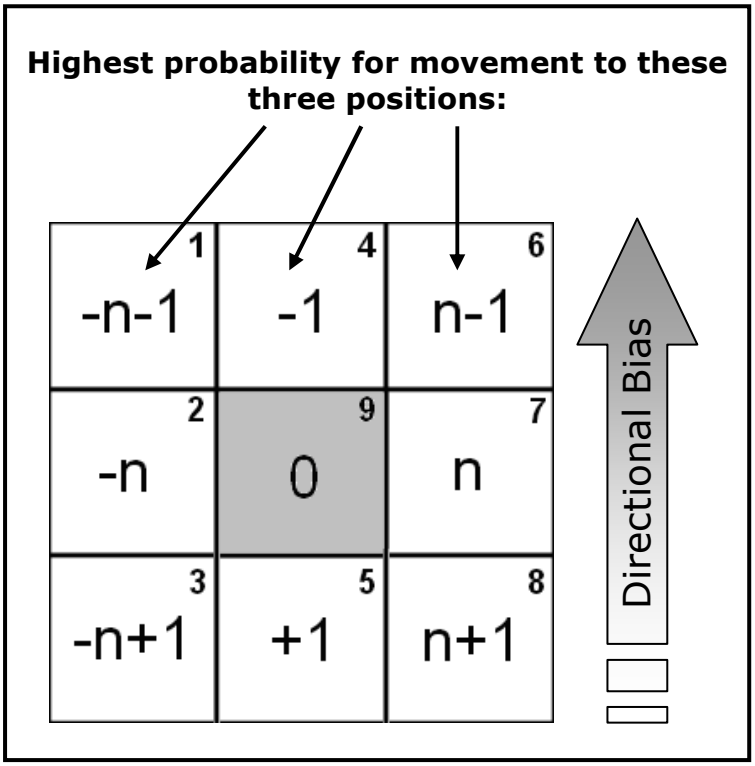

Figure 13: Graphic Depiction of the Directional Bias for the Movement of the Centre Cell within its Neighbourhood.

The directional bias shown in Figure 13 is pre-defined by the user of the programme and can therefore be used to represent the effect of any external force/influence on the movement within the system. An example of such a driving force is an induced pressure drop by means of a pump or an inclined flow duct. Note that the directional bias does not apply to the stationary cells within the system boundaries.

Type Bias (Cell Movement due to Internal Driving Forces)

The effect of the internal driving forces within the system itself, e.g. difference in vapour pressure between the liquid film layer and the surrounding gas phase, is modelled by means of a user-defined matrix, namely the Type Bias. To construct the Type Bias, the swapping probability of a cell needs to be defined.

The swapping probability (β_y), also called the score, is a single scalar value that defines the probability for a neighbour (Cell y) of the centre cell (Cell x) which is surrounded by a specific combination of neighbours to swap with Cell x. Cell y is defined in terms of x according to the Moore Neighbourhood, therefore y = x-n-1, x-n, x-n+1, x-1, x+1, x+n-1, x+n or x+n+1 (eight neighbouring positions), or y =x+0 (current position of Cell x) for R=1. Note that the total number of neighbours for Cell x, including Cell x itself, is related to the size of neighbourhood as follows:

$$N = (2xR+1)^2 \quad \textbf{(6)}$$

Therefore N=9 for R=1. According to Equation 6, an exponential increase occurs in the number of neighbours that have to be considered when R is increased. The effect of the extended neighbourhood sometimes needs to be accounted for (Section 3.2.4) to improve the accuracy of the model.

The drastic increase in the number of cells to be accounted for, will cause an increased number of calculations. This has resulted in a trade-off between accuracy and processing speed required for the simulation programme.

A weight (α) is attributed to each neighbour of Cell y, depending on the type of that neighbour. For R=1 the Swapping Probability for Cell y is defined in terms of α as follows:

$$\beta_y = (\alpha_{y-n-1})(\alpha_{y-n})(\alpha_{y-n+1})(\alpha_{y-1})(\alpha_{y+1})(\alpha_{y+n-1})(\alpha_{y+n})(\alpha_{y+n+1}) \quad \textbf{(7)}$$

Note that the Moore neighbourhood that influences the movement of Cell y may vary in size (R≥1), but only the nearest, adjacent neighbours (R=1) of Cell x are considered for a possible swap with Cell x. This increases the flexibility and calculation speed of the model and prevents unrealistic behaviour resulting from cells that "jumps over one another" to swap with non-adjacent neighbours.

The neighbour (Cell y) with the highest score (β_y) will be the most likely to exchange positions (swap) with Cell x. Table 2 shows an example where the current position of Cell x (y = x+0) has a β_y of 6, Neighbour y = x+1 has a β_y of 3, while the rest of the neighbours all have a β_y of approximately 1.5. χ_y is the % Chance for Cell x to swap with Cell y and can be written as follows:

$$\chi_y = \frac{100 \times \beta_y}{\{(\beta_{x-n-1}) + (\beta_{x-n}) + (\beta_{x-n+1}) + (\beta_{x-1}) + (\beta_{x+1}) + (\beta_{x+n-1}) + (\beta_{x+n}) + (\beta_{x+n+1}) + (\beta_{x+0})\}} \% \quad \textbf{(8)}$$

Table 2: ***% Chance for neighbours to swap positions with Cell x, based on the Swapping Probability of each neighbour***

y*	β_y	χ_y for $x \in y$	χ_y for $x \notin y$
x-n-1	1.5	7.69%	11.11%
x-n	1.5	7.69%	11.11%
x-n+1	1.5	7.69%	11.11%
x-1	1.5	7.69%	11.11%
x+1	3.0	15.38%	22.22%
x+n-1	1.5	7.69%	11.11%
x+n	1.5	7.69%	11.11%
x+n+1	1.5	7.69%	11.11%
x+0= x	6.0	30.77%	undefined for $x \notin y$

**Value of y identifies Cell y, a neighbour of Cell x, by specifying its position*

According to the swapping probabilities, Cell x is two times more likely to stay in the current position (Position x +0) than to swap with Neighbour x+1 and four times more likely to stay in Position x +0 than to swap with any other neighbour. Table 2 shows that there is a 30.77% chance that Cell y will stay in its current position. If one assumes that a swap does take place ($x \notin y$), there is a 22.22% chance that Cell x+1 will swap with Cell x and a 11.11% chance for each of the other neighbouring cells to swap with Cell x.

Note that this results in a stochastic model as opposed to a deterministic model in which Cell x would have a 100% chance to stay in position when β_y for y = x+0 exceeds the β_y for all the other neighbours. A deterministic model will always select the neighbour with the biggest β_y to swap with Cell x. For such models, it will make no difference whether the second largest β_y differs slightly from the largest β_y or whether there is an orders of magnitude difference present. The stochastic approach enables the model to account not only for the presence of a difference between the β_y's of the respective neighbours, but also for the severity of that difference. The stochastic model is therefore expected to yield more realistic results and has become the preferred choice for the purposes of this study.

The Type Bias Matrix ($\overline{\Omega}$) is a collection of possible weights from which every α is selected according to the type of the neighbour involved. For six possible types of cells, the matrix is defined as follows:

$$\overline{\Omega}_y = \begin{Bmatrix} \alpha_{1,1} & \alpha_{1,2} & \alpha_{1,3} & \alpha_{1,4} & \alpha_{1,5} & \alpha_{1,6} \\ \alpha_{2,1} & \alpha_{2,2} & \alpha_{2,3} & \alpha_{2,4} & \alpha_{2,5} & \alpha_{2,6} \\ \alpha_{3,1} & \alpha_{3,2} & \alpha_{3,3} & \alpha_{3,4} & \alpha_{3,5} & \alpha_{3,6} \\ \alpha_{4,1} & \alpha_{4,2} & \alpha_{4,3} & \alpha_{4,4} & \alpha_{4,5} & \alpha_{4,6} \\ \alpha_{5,1} & \alpha_{5,2} & \alpha_{5,3} & \alpha_{5,4} & \alpha_{5,5} & \alpha_{5,6} \\ \alpha_{6,1} & \alpha_{6,2} & \alpha_{6,3} & \alpha_{6,4} & \alpha_{6,5} & \alpha_{6,6} \end{Bmatrix} \quad \textbf{(9)}$$

where $\alpha_{i,j}$ represents the weight with

i = Cell type for Cell $\boldsymbol{y}$

j = Cell type for the neighbour of Cell $\boldsymbol{y}$

For example, if Cell $\boldsymbol{y}$ represents water (Type 3) and its neighbour represents a void cell (Type 1), the allocated weight for the interaction with that neighbour will be as follows:

$\alpha_{i,j} = \alpha_{3,1}$

Trial runs were done in order to fine-tune the value of each $\alpha_{i,j}$-combination for a feasible model.

3.2 Implementation of the Cellular Automata Model

To implement the model, the board has to be populated, and the construction of the Directional Bias and Type Bias needs to be completed. The number of time steps allowed for each run as well as the trigger cell type must be selected. In addition, parameters have to be selected to evaluate the performance of the model.

3.2.1 Selection of a Trigger Cell Type

To run the programme code which was constructed as described in Section 3.1, a "trigger type" must be selected. For this series of experiments, the empty type (Type 1) has been selected to serve as trigger for the whole board. The purpose of the trigger type is to identify a single cell type for which the Swapping Probability of its neighbours (β_y) has to be calculated. Only cells from this type (in this case Type 1) will be considered as "Cell x" during the simulation. This prevents clashes between multiple Swapping Probabilities that would have been calculated for cells from different types if no trigger type were selected.

Therefore only Type 1 cells will actively exchange their positions with other cells. The non-trigger type cell types move merely as a result from the movements of the trigger type cells. The cells will all move according to their respective Swapping Probabilities. The Directional Bias (defined in Section 3.1.2) therefore applies to the trigger type cells only.

The programme evaluates the board on a cell-by-cell basis in random order (not the same order in which the board has been indexed) to ensure that the program mechanism does not contaminate the results with regards to directional flow. For each cell in the trigger type, the new position is calculated as described in Section 3.1.2. When the new position has been calculated for all the trigger-type cells, the programme counts one time step after which the procedure is repeated for the next time step. The duration of each run is specified by the user in terms of the number of time steps required.

To ensure that all cells are provided sufficient opportunity to be displaced to a more favourable position by the trigger type cells, all non-trigger type cells (except for the rigid packing material structure which is considered immobile for the purposes of this simulation) must have at least 4 (~45%) trigger type cells in its nearest (R=1) neighbourhood.

3.2.2 Distribution of Cell Types amongst the Phases

For this simulation, the trigger type consists of empty cells (Type 1), which means that the density of the other types should be relatively low.

To speed up the calculations, the programme will not consider another trigger type cell to swap with the cell that is currently being considered (Cell x). This results in the programme "ignoring" any empty cell with only empty cells in its nearest neighbourhood, seeing that a swap in this case will have no effect on the overall configuration of the neighbourhood.

To benefit from this "speed up" effect, both the gas and liquid phases have been populated with a relatively high density of Type 1 cells (low density of all other types) as shown in Table 3.

Table 3: Initial Phase Population for the Cellular Automata Model

	Vapour Phase (G)	*Liquid Film Layer (L)*	*Structured Packing (PM)*
Type 1: Void cells	*94.00%*	*48.00%*	*0.00%*
Type 2: Non polar gas (air)	*3.33%*	*4.00%*	*0.00%*
Type 3: Polar liquid (water)	*0.00%*	*24.00%*	*0.00%*
Type 4: Non polar liquid (alcohol)	*0.00%*	*24.00%*	*0.00%*
Type 5: Packing material	*0.00%*	*0.00%*	*100.00%*
Type 6: Polar vapour (water)	*2.67%*	*0.00%*	*0.00%*
	100.00%	*100.00%*	*100.00%*

The composition in Table 3 forms part of the initial conditions that will apply for all simulations, including the theoretical examples in this chapter, unless otherwise specified.

Cells with no empty spaces in its nearest neighbourhood will automatically not be considered for a swap with an empty cell. This also improves the calculation speed of the programme significantly. Therefore, the packing material, which does not need to move for the purposes of this simulation, has been modelled with no spaces. This is not an accurate mechanical model for the micro structure of a solid phase, but is only used to model the influence of the packing material on the mass transfer behaviour of the liquid and vapour phases, and is therefore considered sufficient as the solid packing material itself does not move.

3.2.3 Selection of a Directional and Type Bias

For a realistic model of the mass transfer between the vapour and liquid film phases, the Type Bias must be strong enough to induce the selective evaporation of the non-polar alcohol molecules (Type 4 cells) from the polar water molecules (Type 3 cells) in the liquid film layer, even for a neutral Directional Bias. The alcohol must diffuse amongst the non polar air (Type 2) and water (Type 6) molecules in the vapour phase, leaving behind the pre-existing liquid water (Type 3) and newly condensated water (Type 6 cells that migrated to the liquid phase). An iterative procedure was used to find such a Type Bias.
The Directional Bias for the entire system was set as follows.

$$\overline{\mathbf{V}}_{\text{System}} = [1, 1, 1, 1, 1, 1, 1, 1, 1] \qquad \textbf{(10)}$$

This (neutral) Directional Bias therefore dictates that the trigger type cells will not exhibit a specific preference for any flow direction except for the "swapping" with non-trigger type cells induced by the Type Bias.

The Type Bias for the simulation was selected by means of an iterative procedure which involved several trial runs.

The first iteration for a Type Bias was constructed according to the following principles.

- Some types pf cells will have a great affinity for a neighbour of another type. These cells will have an inherent reluctance to exchange positions with an empty cell which would cause them to separate from these neighbours.

- Other cell types may repel one another. If a cell is repelled by its neighbour, it will have a higher likelihood to swap positions with an empty cell, possibly moving to a more favourable neighbourhood. If the next neighbourhood turns out to be unfavourable, the average swapping probability or mobility (β_y) of the cell with respect to its neighbours will remain relatively high until it reaches a favourable neighbourhood. The β_y-values will now decrease, due to the mathematical relationship with α_{ij} that expresses an increased affinity of a given cell for its neighbouring cells.

The question now arises: How is the affinity of one cell type to another quantified, evaluated and compared to other combinations of cell types? The answer is in the mathematical relationship between α and β in Equation (7) from which the following can be deduced.

For an increasing β-value: $\alpha_{ij} > 1$
For a decreasing β-value: $\alpha_{ij} < 1$
For an unaffected β-value: $\alpha_{ij} \sim 1$

For repulsion between two cells that represent Type *i* and *j* respectively, $\alpha_{ij} > 1$, for a high affinity of Type *i* for Type *j*, $\alpha_{ij} < 1$ and for neutral or no interaction, $\alpha_{ij} \sim 1$.

If there were no phase change present, intermolecular forces would provide the key to a feasible solution. By classifying each possible combination of types according to the strength and direction of their intermolecular interactions, the repulsion and resulting α-value within each possible cell type combination can be evaluated and compared to that of another combination. This approach proved itself to be very useful in a previous study which involved a simple, single phase osmotic system (Engelbrecht, et al., 2006).

For the current system which involves the evaporation of the non-polar alcohol and the possible condensation of the polar water vapour (if we assume that the packing material is hydrophilic), it has become evident from initial trial runs that the above mentioned approach needs some modification to yield satisfactory results.

Table 4 shows the interaction between different cell types and the possible range for the resultant α-values. 'Initial phase' refers to the phase (gas/liquid/solid) of a chemical substance (cell type) at the start of the simulation, while 'Intermolecular force' refer to the physical or chemical forces that would have been exhibited by the different molecules if they were in the same phase.

For the current case study, the presence of the different phases, as well as all possible phase changes, has to be accounted for in addition to the intermolecular force type. The ranking of the interaction parameters is therefore significantly more complicated than before.

Table 4 shows an intuitive approach to the ranking of interactions that are the combined effect of the intermolecular force type (based on the chemical properties of the species under consideration), the phases present at the start of the simulation (initial conditions) and the expected phase changes due to the (component) vapour pressure gradient(s) within the system.

For example, there exist attracting Van der Waals forces between the non polar gas molecules (i,j = 2,2) in Table 4, but the effect of these forces compete with the effect of the kinetic energy that enables the molecules to exist in the low density gas phase. Realistic results were obtained by modelling the total effect of these two opposing factors as slightly repulsive.

Table 4: Proposed Ranking of α–values to be Incorporated in the CA Model

i	*j*	*Molecular Structure / Description & Initial Phase*		*Intermolecular Force Type (Single Phase)*	*Total Force Strength*	*Direction*	*Rank**
		i	*j*				
1	*1*	*Void*	*Void*	*-*	*-*	*-*	*4*
1	*2*	*Void*	*Non Polar Gas*	*-*	*-*	*-*	*4*
1	*3*	*Void*	*Polar Liquid H20*	*-*	*-*	*-*	*4*
1	*4*	*Void*	*Non Polar Liquid*	*-*	*-*	*-*	*4*
1	*5*	*Void*	*Solid, Hydrophilic Packing Material*	*-*	*-*	*-*	*4*
1	*6*	*Void*	*Polar Gas*	*-*	*-*	*-*	*4*
2	*1*	*Non Polar Gas*	*Void*	*-*	*-*	*-*	*4*
2	*2*	*Non Polar Gas*	*Non Polar Gas*	*Van der Waals Forces*	*Weak*	*Repelling*	*3*
2	*3*	*Non Polar Gas*	*Polar Liquid H20*	*Dipole-Induced Dipole*	*Very Strong*	*Repelling*	*2*
2	*4*	*Non Polar Gas*	*Non Polar Liquid*	*Van der Waals Forces*	*Very Strong*	*Attracting*	*7*
2	*5*	*Non Polar Gas*	*Solid, Hydrophilic Packing Material*	*Dipole-Induced Dipole*	*Strongest*	*Repelling*	*1*
2	*6*	*Non Polar Gas*	*Polar Gas*	*Dipole-Induced Dipole*	*Very Strong*	*Repelling*	*2*
3	*1*	*Polar Liquid H20*	*Void*	*-*	*-*	*-*	*4*
3	*2*	*Polar Liquid H20*	*Non Polar Gas*	*Dipole-Induced Dipole*	*Very Strong*	*Repelling*	*2*
3	*3*	*Polar Liquid H20*	*Polar Liquid H20*	*Dipole-Dipole*	*Strong*	*Attracting*	*6*
3	*4*	*Polar Liquid H20*	*Non Polar Liquid*	*Dipole-Induced Dipole*	*Very Strong*	*Repelling*	*2*
3	*5*	*Polar Liquid H20*	*Solid, Hydrophilic Packing Material*	*Strong Dipole-Dipole or Hydrogen Bonding*	*Very Strong*	*Attracting*	*7*
3	*6*	*Polar Liquid H20*	*Polar Gas*	*Dipole-Dipole*	*Strong*	*Attracting*	*6*
4	*1*	*Non Polar Liquid*	*Void*	*-*	*-*	*-*	*4*
4	*2*	*Non Polar Liquid*	*Non Polar Gas*	*Van der Waals Forces*	*Very Strong*	*Attracting*	*7*
4	*3*	*Non Polar Liquid*	*Polar Liquid H20*	*Dipole-Induced Dipole*	*Very Strong*	*Repelling*	*2*
4	*4*	*Non Polar Liquid*	*Non Polar Liquid*	*Van der Waals Forces*	*Weak*	*Attracting*	*5*
4	*5*	*Non Polar Liquid*	*Solid, Hydrophilic Packing Material*	*Dipole-Induced Dipole*	*Strongest*	*Repelling*	*1*
4	*6*	*Non Polar Liquid*	*Polar Gas*	*Dipole-Induced Dipole*	*Very Strong*	*Repelling*	*2*
5	*1*	*Solid, Hydrophilic Packing Material*	*Void*	*-*	*-*	*-*	*4*
5	*2*	*Solid, Hydrophilic Packing Material*	*Non Polar Gas*	*Dipole-Induced Dipole*	*Strongest*	*Repelling*	*1*
5	*3*	*Solid, Hydrophilic Packing Material*	*Polar Liquid H20*	*Strong Dipole-Dipole or Hydrogen Bonding*	*Very Strong*	*Attracting*	*7*
5	*4*	*Solid, Hydrophilic Packing Material*	*Non Polar Liquid*	*Dipole-Induced Dipole*	*Strongest*	*Repelling*	*1*
5	*5*	*Solid, Hydrophilic Packing Material*	*Solid, Hydrophilic Packing Material*	*Strong Dipole-Dipole or Hydrogen Bonding*	*Strongest*	*Attracting*	*8*
5	*6*	*Solid, Hydrophilic Packing Material*	*Polar Gas*	*Strong Dipole-Dipole or Hydrogen Bonding*	*Very Strong*	*Attracting*	*7*
6	*1*	*Polar Gas*	*Void*	*-*	*-*	*-*	*4*
6	*2*	*Polar Gas*	*Non Polar Gas*	*Dipole-Induced Dipole*	*Very Strong*	*Repelling*	*2*
6	*3*	*Polar Gas*	*Polar Liquid H20*	*Dipole-Dipole*	*Strong*	*Attracting*	*6*
6	*4*	*Polar Gas*	*Non Polar Liquid*	*Dipole-Induced Dipole*	*Very Strong*	*Repelling*	*2*
6	*5*	*Polar Gas*	*Solid, Hydrophilic Packing Material*	*Strong Dipole-Dipole or Hydrogen Bonding*	*Very Strong*	*Attracting*	*7*
6	*6*	*Polar Gas*	*Polar Gas*	*Dipole-Dipole*	*Weak*	*Attracting*	*5*

*****1= largest α, 8= smallest α.

Furthermore, the strong attractive forces allocated to the interaction of Type 2 (non polar gas) with Type 4 (non polar liquid) in comparison with the interaction amongst the Type 4 cells themselves, not only represent the effect intermolecular forces, but also the effect of the lower component vapour pressure (for Type 4) exhibited by a mix of Type 4 and Type 2 in comparison with the vapour pressure exhibited by pure Type 4.

The first iteration for the Type Bias Matrix ($\overline{\mathbf{\Omega}}$) therefore represents the cumulative effect of the intermolecular forces, and the vapour pressure gradient within the system. For the finalization of the Type Bias Matrix ($\overline{\mathbf{\Omega}}$), numerical values for each α_{ij} were guessed (according to Table Y) as a first iteration after which the first experimental runs have been executed. Based on the results harvested after each iteration, alterations were made to the α-values for each subsequent set of runs. The simulation output, including the iteration results, are presented, discussed and evaluated in Section 4.1.1.

3.2.4 Extension of the Radius of Influence to Model the Effect of Polarization

The following case study is a simple, yet very typical scenario at the surface of the packing material (Figure 14) which illustrates the effect of a larger R=3 neighbourhood as opposed to that of an R=1 neighbourhood. Refer to Table 1 for the colour key to the different cell types.

In Figure 14, there is a possibility that the empty (Type 1) cell with the yellow border might swap with Cell $\boldsymbol{y}$, the non polar (Type 4) cell just above it, depending on the neighbourhood of $\boldsymbol{y}$.

If the R=1 neighbourhood is considered, and the influence of the empty cells are considered negligible, the current neighbourhood of Cell $\boldsymbol{y}$ (indicated with red dots in the top right hand corners in Figure 14) will be unfavourable (unlikely to retain Cell $\boldsymbol{y}$) due to the reluctance of Cell $\boldsymbol{y}$ to associate with the three water (polar liquid) cells above it, as indicated by Table 4. Therefore Cell $\boldsymbol{y}$ will exhibit a tendency to move away from those three cells and will therefore be very likely to swap with the empty cell below it (marked with a bright yellow border).

The new neighbourhood of Cell $\boldsymbol{y}$ (indicated with blue dots in the bottom right hand corners in Figure 14 after a supposed swap with the empty cell) contains only two polar liquid cells and and therefore appears more favourable for the Type 4 cell. This swap, based on the R=1 radius of influence, results in the downward movement of a non polar cell towards the hydrophilic packing material. This is not the expected behaviour during the distillation of alcohol and water, for example, where the hydrophilic packing material is likely to attract polar water molecules while the non polar alcohol cells are eventually displaced by the water and therefore moving further away from the packing material.

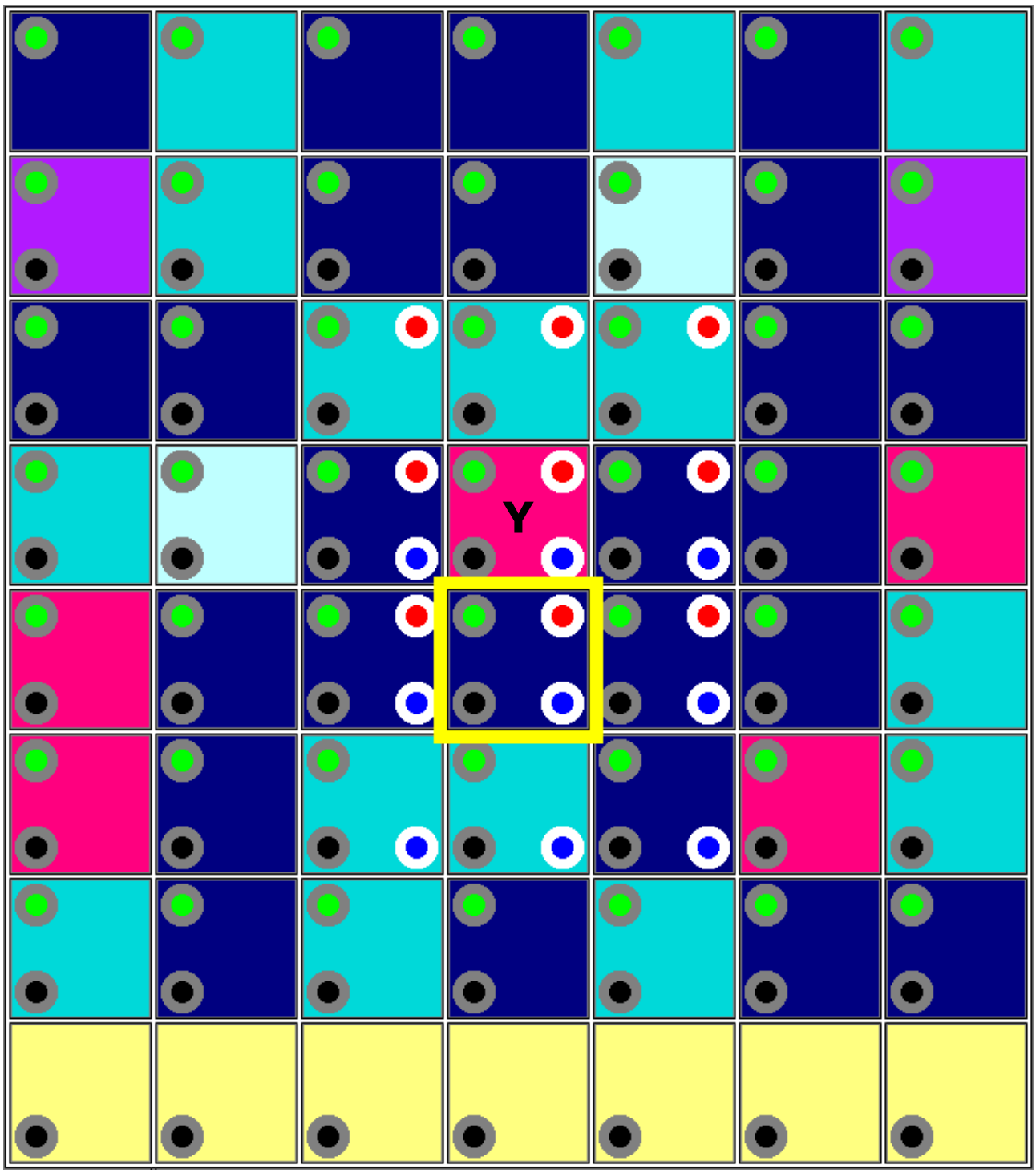

Figure 14: Typical Scenario at the Surface of the Packing Material where R=3 provides a more accurate Model than R=1

This behaviour is a result of the R=1 neighbourhood which fails to discriminate between strongly polarized molecules and less polarized molecules. In reality, the two water cells (representing molecules or groups of molecules, depending on the scale of the model) is likely to be strongly polarized because of their close proximity to the hydrophilic packing material which attracts them either by hydrogen bonding or strong dipole-dipole bonding. The water cells above Cell Y would be much less polarized due to the longer distance between these cells and the packing material.

When the radius of influence is enlarged to R=3, the current position of Cell $\boldsymbol{y}$ remains unfavourable due to the presence of water (polar liquid) cells in the extended neighbourhood (indicated with green dots in the top left hand corners in Figure 14). Therefore Cell $\boldsymbol{y}$ still has a tendency to move to a new position. If Cell $\boldsymbol{y}$ however swaps with the empty cell, it ends up in a new neighbourhood (indicated with black dots in the bottom left hand corners in Figure 14) in which the effect of the highly polar packing material cells will be felt, due to the larger radius of influence. This new neighbourhood is highly unfavourable according to Table 4 and Cell $\boldsymbol{y}$ is therefore very likely to be replaced by one of the empty cells above it, returning to a more favourable position as theoretically expected. The larger neighbourhood therefore ensures that driving forces operating over relatively long distances, are accounted for.

A neighbourhood of R=7 has been very effective during trial runs. Higher values of R result in very large neighbourhoods that radically increase the number of calculations needed as explained in Section 3.1.2. Larger neighbourhoods subsequently increase the number of α_{ij} –values needed to be multiplied with one another for the swapping probability ($\beta_{\boldsymbol{y}}$), seeing that each cell in the neighbourhood has its own α_{ij}.

Preliminary trial runs have shown that α_{ij} –values of different rankings according to Table 4 need to differ by several orders of magnitude for these differences to have an effect and therefore to yield acceptable model behaviour by distinguishing between different cell types. These order-of-magnitude differences together with an increase in neighbourhood size has resulted in very large swapping probabilities to the extent where they are regarded as infinitely large numbers (∞) by the programme. The programme has malfunctioned under these circumstances, producing very unrealistic results, if any.

The programme therefore requires a trade-off between the range of the α_{ij} –values and the neighbourhood size, which limits the efficiency of the model.

3.3 Evaluation Criteria for the Uncalibrated Cellular Automata Model

The model in its current state is uncalibrated with respect to all the quantitative properties being modelled. For example, it has not yet been determined whether each cell on the modelling board represents several molecules or just one molecule. The corresponding temperature range for a specific system density is also still unknown.

Furthermore, the model parameters need some fine tuning to distinguish, for example, between ethanol-water and propanol-water mixtures. Although both are alcohol-water mixtures, some properties will differ, including density at a specific temperature and pressure, boiling point temperature for a given ambient pressure, etc. In order to solve these unknown properties for all possible combinations of chemical species in a wide range of physical and thermodynamic conditions, the model needs extensive calibration against reliable data sources which is beyond the feasible scope of this project. The output from this uncalibrated model can therefore not be directly compared to empirical data.

The uncalibrated model has been subjected to preliminary trials to evaluate the integrity and scope of the model. The ideal model, even in its uncalibrated state, must be capable of representing a wide variety of possible mass transfer scenarios that might occur within the packing material structure: E.g. complete evaporation, selective evaporation (ideal case) and incomplete evaporation due to saturation and condensation. The following measures have been used to evaluate these capabilities.

3.3.1 Evaluation of Graphic Programme Output

The graphic output must agree with quantitative results: E.g. if the numerical results indicate the presence of a significantly sized liquid layer, it must be visible on the graphic output itself. The graphic output (snapshot and movie format) provides an easy and early opportunity to pick up fundamental errors, e.g. the unwanted movement of packing material particles and unlogic behaviour that cannot be explained by the Directional or Type Bias. The latter type of behaviour usually results from programme instabilities (which resulted in programme malfunctioning) due to a large neighbourhood combined with too large α_{ij} –values.

3.3.2 Rate of Separation and Results at Steady State

The selectivity range gives an indication of the capability to model various levels of separation, depending on the programme input which includes the Type Bias and the surface structure of the packing material. The level of separation at steady state, after the completion of a simulation run can be determined by comparing the increase in the number of cells in the vapour phase for Types 2, 3, 4 and 6 respectively.

For strong hydrophilic packing material, a high selectivity that would yield a significant increase for State 2 and 4 in the vapour phase is expected. The number of cells in the vapour phase for Type 6 will typically remain constant. The Type 6 population might even decrease due to condensation which will cause the polar vapour to move over to the liquid phase. A less hydrophilic packing material will cause less "evaporation" of Types 2 and 4 and might even result in increased evaporation for Cell Type 3 (polar liquid), which results in less selectivity, if any.

The model must also be able to represent the effect of the different driving forces on the rate at which steady state is achieved.

3.4 Acquisition of Uncalibrated Model Results

This section explains the mechanism by which quantitative and qualitative properties of the system are obtained and measured. These properties are necessary for the evaluation of the model discussed in Section 3.3.

3.4.1 Measurements Taken from Raw Simulation Output

The total number of time steps (1000 steps unless otherwise indicated) for each run has been divided in 40 intervals. The measurements taken for each interval to obtain numerical properties are listed in Table 5.

Unless otherwise stated, these measurements record the number of cells exhibiting certain properties (e.g. belonging to a specific phase). Measurements (marked with √) are taken for individual clusters exhibiting these specific characteristics. The coordinates (location) and total area of each cluster is also measured for each run. The measurements for all the clusters are added to obtain the total number of cells that exhibit a specific set of characteristics.

Table 5: List of Properties Recorded for Each Simulation

	Neighbourhood in contact with Touch Type cells*	*Neighbourhood not in contact with Touch Type* cells*
Vapour phase	*Touch Type* = Type 6*	
Number of cells for all types	√	√
Number of Type 2 cells	√	√
Number of Type 3 cells	√	√
Number of Type 4 cells	√	√
Number of Type 6 cells	√	√
Coordinates of each cluster	√	√
Size of each cluster	√	√
Total number of clusters		
Liquid phase	*Touch Type* = Type 5*	
Number of cells for all types	√	√
Number of Type 2 cells	√	√
Number of Type 3 cells	√	√
Number of Type 4 cells	√	√
Number of Type 6 cells	√	√
Coordinates of each cluster	√	√
Size of each cluster	√	√
Total number of clusters		
Liquid film phase	*Touch Type* = Type 5*	
Number of cells for all types	√	√
Number of Type 2 cells	√	√
Number of Type 3 cells	√	√
Number of Type 4 cells	√	√
Number of Type 6 cells	√	√
Coordinates of each cluster	√	√
Size of each cluster	√	√
Total number of clusters		

**Input parameter given before simulation commences: See Section 3.4.2 for the definition thereof.*

3.4.2 Definition, Identification and Location of Phases

The respective phases need to be defined in quantitative terms to enable the simulation programme to identify and locate them correctly. Note that pre-defined fixed coordinates (e.g. liquid phase from the 180th row up to the 200th row of cells) are not an option, because the phase boundaries move during evaporation and condensation. The simulation programme now needs to define the sometimes mobile phase boundaries for itself. Table 6 shows the input parameters that have been used to identify clusters of adjacent cells that belong to a specific phase.

Table 6: Input Parameters Used for Phase Identification

Symbol	*Parameter Name*	*Definition*
CT	*Counted Type*	*When a cell is tested to see whether it belongs to a specified phase or not, it must have a minimum number of neighbours from this type before it is considered as part of that phase*
RC	*Radius of Counted Neighbourhood*	*Size of neighbourhood in which CT cells are counted*
TT	*Touch Type*	*The programme output must state how many CT cells contain these cells within their respective R=RC neighbourhoods*
MN	*Minimum Number*	*Minimum number of CT cells needed to positively identify a phase*
MS	*Minimum Cluster Size*	*Minimum size of clusters (smaller sizes are considered negligible)*

The numerical values for the input parameters that have been used in the simulations, from which the results in Chapter 4 were obtained, are presented in Table 7.

Table 7: Quantitative Measures Used for Phase Identification

Parameter	*Vapour phase*	*Liquid layer phase*	*Non-solid phases**
CT	*1*	*3*	*1*
RC	*4*	*4*	*4*
TT	*6*	*5*	*5*
MN	*55*	*10*	*0*
MS	*1*	*1*	*1*

**Note that these measurements account for all cells except those belonging to the packing material.*

The number of cells of a specific type present in the vapour phase is subtracted from the number of cells of the same type in the non-solid phase measurements to yield the total number of cells in the liquid phase for that specific type. The total number of cells in the liquid layer for a certain type does not necessarily equal the total number of liquid phase cells of that type, because suspended liquid droplets may form in the gas phase that are not part of the layer itself.

The numerical values for the input parameters shown in Table 7 have been iterated and verified by means of trial runs with measurements taken at the starting conditions (time = 0 steps). This iterative procedure needs to be repeated until the measured phases at the starting conditions agrees with the initial phase composition and geometry specified in Table 3 and Figure 10 respectively.

The minimum density of a certain type of cell in any given phase is calculated according to Equation 11.

$$\left(\mathrm{MN}/\left(2\mathrm{xRC}+1\right)\right)\times 100\% \qquad \textbf{(11)}$$

Note that the corresponding result from Equation 11 is smaller than the specified density in Table 3 for both the gas and liquid phases. This is due to the fact that the neighbourhoods (with R=RC) of the cells on the borders of a cluster belonging to a certain phase will include cells from the adjacent phase. This decreases the average number of the CT-cells, because the concentration of CT-cells in the neighbourhood of a given cell will only equal the specified concentration if the entire neighbourhood consists of that phase alone. This effect is especially significant when there are multiple clusters present for a single phase (e.g. suspended liquid drops in the gas phase). These differences (see Table 8) render the above mentioned iterative approach unavoidable.

Table 8: Difference in Specified and Iterated Density for RC=4

	Vapour phase	*Liquid film layer*	*Solid packing material*
Specified initial concentration of CT-cells	*94.00%*	*24.00%*	*N/A (100% State 5)*
Concentration of CT-cells that correctly defines the phase (iterated value)	*67.90%*	*12.35%*	*N/A (100% State 5)*

The graphic phase concentration measurements of which examples are shown in Figure 15, can be used as a visual comparison measure for the first few iterations. The numeric results have to be compared with the numeric specifications in Table 3 due to the finer differences encountered in further iterations. Note the inaccuracy of the measurements according to the specified concentrations in comparison with that of the iterated minimum concentrations.

(a) *Initial conditions given in Table 3*

(b) & (c) *Measured concentration of CT-cells for the liquid film layer and vapour phase respectively. Note that the colour gradient is calibrated for an R=4 neighbourhood.*

(d) & (f) *Identification of the liquid film layer (white) according to the iterated MV (d) and specified concentration (f). Note the difference in accuracy: Figure (d) shows a close resemblance to figure (b) while figure (f) fails to identify the film layer.*

(e) & (g) *Identification of the vapour phase according to the iterated MV (e) and specified concentration (g). Note again the difference in accuracy: Figure (e) correctly identified the gas phase while Figure (g) shows non-existing "gaps" within the gas phase.*

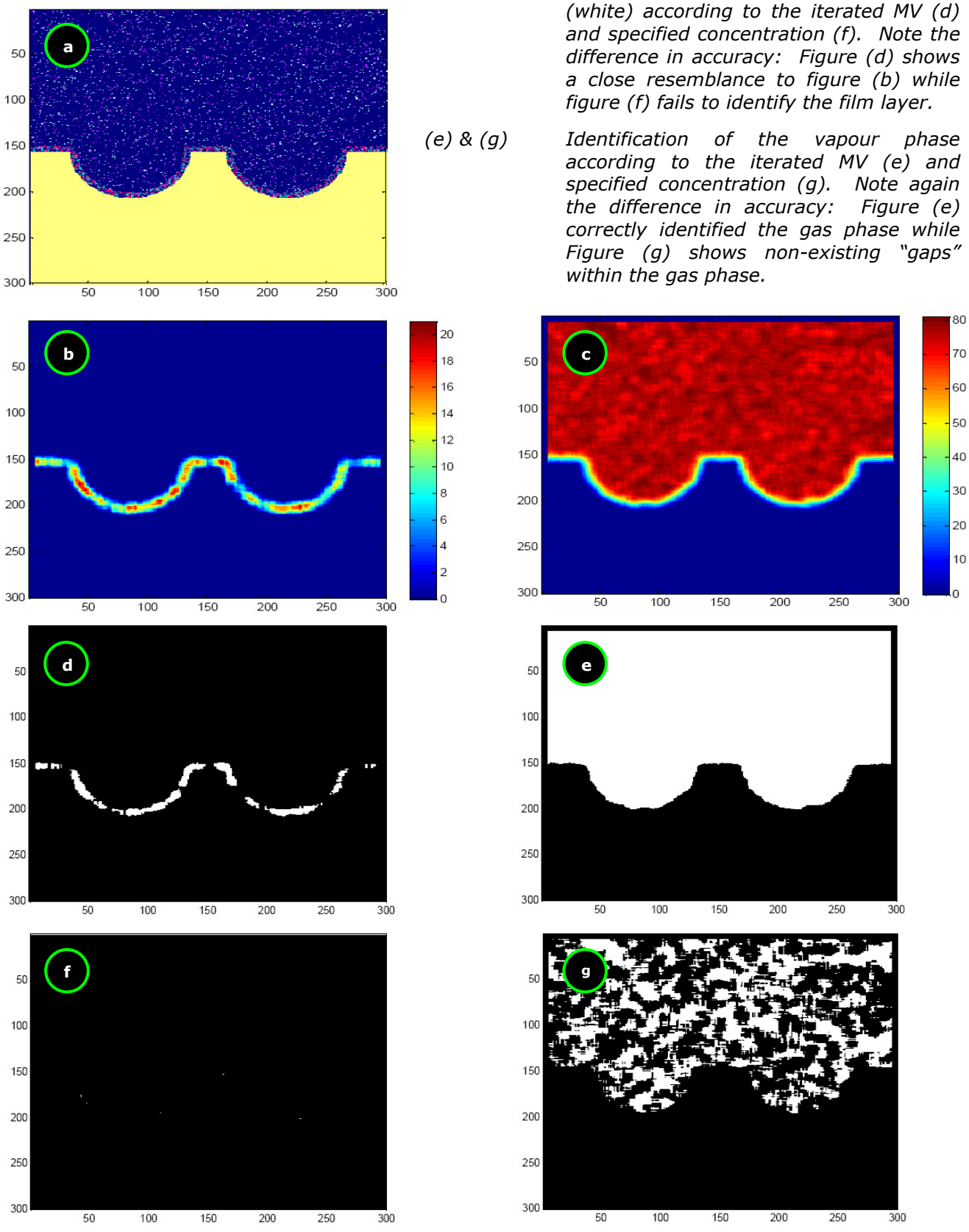

Figure 15: ***Effect of the Definined Minimum Concentrations on the Accuracy of the Model Output***

3.5 Summary of the Method Followed during the Preparation and Execution of the Model

The steps that were followed during the preparation and execution of the cellular automata model are summarized in Table 9.

Table 9: ***Summarized Methodology for Modelling of Mass Transfer in Packing Materials with Cellular Automata***

Procedure	*Paragraph**
Construction	***3.1***
Initialize Board: • *Establish numerical board position index for easy cell location and identification.* • *Divide board in gas (G), liquid (L) and packing material (PM) sections (specification of initial conditions).* • *Identify all possible cell types.*	*3.1.1*
Define Movement Parameters: • *Specify the boundary conditions.* • *Define the directional bias (external influences).* • *Define the type bias (internal influences).* • *Specify radius of influence for the Type Bias.*	*3.1.2*
Implementation	***3.2***
Select cell type for which programme is executed (trigger cells).	*3.2.1*
Define initial concentration of each cell type within each phase.	*3.2.2*
Specify values for all the movement parameters (excluding the boundary conditions which are automatically defined as a function of the radius of influence).	*3.2.3 & 3.2.4*
Iterate and the parameters necessary for the programme to recognize different phases.	*3.4.2*
Execution	***3.4***
Specify total number of time steps for which the simulation should be executed (duration).	*3.4.1*
Specify the time intervals for which measurements must be recorded.	*3.4.1*
Specify the output parameters to be recorded.	*3.4.1*
Execute the programme.	

** Reference to Relevant Discussion or Explanation in Chapter 3*

4. Results for the Qualitative Cellular Automata Model

The model in its current state is not yet calibrated with respect to the quantitative properties being modelled (refer to Section 3.3). The output from this qualitative model can therefore not yet be directly compared to empirical data. Notwithstanding these facts, the qualitative model has been subjected to preliminary trials to evaluate the general integrity and scope of the model.

4.1 Final (Iterated) Type Bias for Hydrophilic Packing Materials of Various Strengths

For a neighbourhood of R=7, the α_{ij} –values (grey shaded) in Table 10, have been used to model the selective vaporization of alcohol from an alcohol-water layer on a hydrophilic packing material surface. These α_{ij} –values for the alcohol-water system, or any suchlike system, have been derived through the iterative procedure described in Section 3.2.3. Equation 12 shows the final Type Bias Matrix ($\overline{\mathbf{\Omega}}$) of which the iterated α_{ij} –values are the elements.

$$\overline{\Omega}_{\gamma} = \begin{Bmatrix} 0 & 0 & 0 & 0 & 0 & 0 \\ 1.5^{0.01} & 1.5^{1} & 1.5^{5} & 1.5^{2} & 1.5^{2} & 1.5^{5} \\ 1.5^{5.99} & 1.5^{5} & 1.5^{0.1} & 1.5^{5} & 1.5^{-12} & 1.5^{0.1} \\ 1.5^{0.01} & 1.5^{2} & 1.5^{5} & 1.5^{2} & 1.5^{5.99} & 1.5^{5} \\ 0 & 0 & 0 & 0 & 0 & 0 \\ 1.5^{5.99} & 1.5^{5} & 1.5^{0.1} & 1.5^{5} & 1.5^{-12} & 1.5^{0.1} \end{Bmatrix} \qquad (\mathbf{12})$$

Note that even very small α_{ij} –values cannot be approximated by zero seeing that this apparently negligible difference would have a profound effect on the swapping probability (β_{γ}) which is the product of all the α_{ij} –values within a given neighbourhood. When these α_{ij} –values are numerically ranked, the iterated ranks of some α_{ij} –values deviate significantly from the theoretical ranks that have been proposed in Section 3.2.3.

4.1.1 Comparison of the Iterated Type Bias with the Theoretical Ranking of the α_{ij} –values

To ease the comparison of the iterated ranking (R_I) with the theoretical ranking (R_T), both ranking systems have been scaled and centred by letting the mean rank equal 0 and the standard deviation equal 1 for both sets. The deviation is the difference between the scaled and centred theoretical ranking (R_{TSC}) and the scaled and centred iterated ranking (R_{ISC}). For a deviation to be considered significant for the purposes of this study, it must fall outside the range (R_{ISC} -R_{TSC})±($0.5\times\sigma_{RISC\text{-}RTSC}$), where $\sigma_{RISC\text{-}RTSC}$ represents the standard deviation of the differences between the scaled iterated and theoretical ranks. Significant differences are underlined in Table 10.

These deviations have resulted from various adjustments that were made during the iterations to obtain a Type Bias Matrix ($\overline{\boldsymbol{\Omega}}$) that yields satisfactory model behaviour.

Modifications to the Type Bias Matrix ($\overline{\boldsymbol{\Omega}}$) were done to ensure that the rigid packing material surface remain stationary throughout all experimental runs. Although intermolecular forces exist between the packing material (Type 5) and the other molecule types, the packing material must influence the movement of the other cell types without losing its own structural integrity. In simple terms: The packing material may cause other cell types to move, but the packing material as such cannot move. This has been achieved by letting all $\alpha_{ij} = 0$ for $i = 5$. Ranking differences ($R_{TSC} - R_{ISC}$) that have resulted from these adjustments are indicated by the blue background fill in Table 10.

The modifications of the Type Bias Matrix ($\overline{\boldsymbol{\Omega}}$) also include the prevention of empty cells swapping with each other by letting all $\alpha_{ij} = 0$ for $i = 1$. This enhances the execution speed of the programme, because unnecessary calculations that do not influence the outcome of the results, have been eliminated (Section 3.2.2). Ranking differences from these adjustments are indicated by the green background fill in Table 10.

Iterations have shown that the model results can be significantly enhanced by assigning non-zero values to α_{ij} for i=2,3,4 or 6, while $j= 1$. These enhancements are based on the fact that fluids with a high volatility due to a low boiling point temperature, tend to evaporate at lower temperatures than less volatile fluids (with high boiling point temperatures). In this study Cell Types 2 and 4 (non polar gas and alcohol) are more volatile than Types 3 and 6 (water vapour and liquid). The less volatile substances are more likely to exist in the more dense phases that have smaller intermolecular spaces, and will therefore repel empty spaces (Type 1 Cells) more aggressively than the more volatile substances.

At ideal operating conditions in a distillation column, the alcohol (Type 4) will tend to evaporate and associate with the stripping agent (non polar gas, Type 2) while the less volatile water vapour (Type 6) will condensate, therefore increasing the number of polar liquid cells. The originally assigned water liquid (Type 3) will typically remain in the liquid phase. For ideal separation, all the alcohol and non polar gas in the system will both end up in the gas phase while all of the water will be in the liquid phase. The gas phase is less dense than the liquid phase and will therefore contain more Type 1 (empty) cells in the cellular automata model.

Due to the high kinetic energy of the gas phase (in comparison with the liquid phase), both the α_{21} and α_{41}–values have been set at 0.1 to model a slightly repulsive effect. The α_{31} and α_{61}–values have been set at 5.99 to model a severely repulsive effect when compared to α_{21} and α_{41}. Ranking differences from these adjustments are indicated by the yellow background fill in Table 10. The system is now able to distinguish between a more dense phase (liquid) and a less dense (gas) phase. This enables the model to identify gas, liquid and solid phases, based on the concentration of empty spaces (Type 1 cells).

Table 10: ***α_{ij}–values for Selective Evaporation of a Non-polar Component from a Polar - Non Polar Liquid Mixture on a Hydrophilic Surface.***

i	*j*	R_T*	R_{TSC}	α_{ij}	R_I	R_{ISC}	R_{ISC} - R_{TSC}
		*Theoretical Rank**	*Scaled and Centered R_T*	*Iterated value*	*Rank for Iterated α_{ij}*	*Scaled and Centered R_I*	*Difference between R_{TSC} and R_{ISC}*
1	1	4.00	-0.01	$1.5^{0.00}$	7.00	0.99	1.00
1	2	4.00	-0.01	$1.5^{0.00}$	7.00	0.99	1.00
1	3	4.00	-0.01	$1.5^{0.00}$	7.00	0.99	1.00
1	4	4.00	-0.01	$1.5^{0.00}$	7.00	0.99	1.00
1	5	4.00	-0.01	$1.5^{0.00}$	7.00	0.99	1.00
1	6	4.00	-0.01	$1.5^{0.00}$	7.00	0.99	1.00
2	1	4.00	-0.01	$1.5^{0.01}$	6.00	0.57	0.58
2	2	3.00	-0.49	$1.5^{1.00}$	4.00	-0.27	0.22
2	3	2.00	-0.97	$1.5^{5.00}$	2.00	-1.10	-0.13
2	4	7.00	1.42	$1.5^{2.00}$	3.00	-0.69	-2.11
2	5	1.00	-1.45	$1.5^{2.00}$	3.00	-0.69	0.76
2	6	2.00	-0.97	$1.5^{5.00}$	2.00	-1.10	-0.13
3	1	4.00	-0.01	$1.5^{5.99}$	1.00	-1.52	-1.51
3	2	2.00	-0.97	$1.5^{5.00}$	2.00	-1.10	-0.13
3	3	6.00	0.94	$1.5^{0.10}$	5.00	0.15	-0.79
3	4	2.00	-0.97	$1.5^{5.00}$	2.00	-1.10	-0.13
3	5	7.00	1.42	$1.5^{-12.00}$	8.00	1.40	-0.02
3	6	6.00	0.94	$1.5^{0.10}$	5.00	0.15	-0.79
4	1	4.00	-0.01	$1.5^{0.01}$	6.00	0.57	0.58
4	2	7.00	1.42	$1.5^{2.00}$	3.00	-0.69	-2.11
4	3	2.00	-0.97	$1.5^{5.00}$	2.00	-1.10	-0.13
4	4	5.00	0.47	$1.5^{2.00}$	3.00	-0.69	-1.15
4	5	1.00	-1.45	$1.5^{5.99}$	1.00	-1.52	-0.07
4	6	2.00	-0.97	$1.5^{5.00}$	2.00	-1.10	-0.13
5	1	4.00	-0.01	$1.5^{0.00}$	7.00	0.99	1.00
5	2	1.00	-1.45	$1.5^{0.00}$	7.00	0.99	2.44
5	3	7.00	1.42	$1.5^{0.00}$	7.00	0.99	-0.43
5	4	1.00	-1.45	$1.5^{0.00}$	7.00	0.99	2.44
5	5	8.00	1.90	$1.5^{0.00}$	7.00	0.99	-0.91
5	6	7.00	1.42	$1.5^{0.00}$	7.00	0.99	-0.43
6	1	4.00	-0.01	$1.5^{5.99}$	1.00	-1.52	-1.51
6	2	2.00	-0.97	$1.5^{5.00}$	2.00	-1.10	-0.13
6	3	6.00	0.94	$1.5^{0.10}$	5.00	0.15	-0.79
6	4	2.00	-0.97	$1.5^{5.00}$	2.00	-1.10	-0.13
6	5	7.00	1.42	$1.5^{-12.00}$	8.00	1.40	-0.02
6	6	5.00	0.47	$1.5^{0.10}$	5.00	0.15	-0.31

***** *Refer to Table Y, Section 3.2 for details on the identification and theoretical ranking of the α_{ij}–values*

It is not always possible to attribute the change in model behaviour that results from an adjustment to an α_{ij} –value to a single, specific physical or theoretical factor or even a combination thereof. This might be resolved by calibration of the model that will allow it to accommodate systems that are chemically and thermodynamically specified.

Further adjustments were done to fine tune the results in an iterative manner (orange background fill in Table 10). The theoretical ground for these adjustments, if any, is likely to emerge during the calibration of the model which falls beyond the scope of this study.

4.1.2 Effect of Hydrophilic Packing Materials on Steady State Conditions and Selectivity Range

The $\alpha_{3,5}$ and $\alpha_{6,5}$ values can be adjusted to model various degrees of hydrophilic behaviour for the packing material (Cell Type 5). The capacity of the model to simulate different degrees of hydrophilicity for the packing material has been investigated.

The physical configuration of the packing material, liquid layer and gas phase, the population of the respective phases and Type Bias used in the experiment are shown in Figure 10, Table 3 and Equation 12 respectively.

Figure 16 shows the number of cells from each cell type that have evaporated from the liquid layer to the gas phase for different values of $\alpha_{3,5}$ and $\alpha_{6,5}$. Note that the expected (desired) end condition for both the Type 3 and Type 6 cells, is water in the liquid phase. Therefore $\alpha_{3,5} = \alpha_{6,5}$. The numerical value of $\alpha_{3,5} = \alpha_{6,5}$ has been varied between slightly smaller than 1 ($\alpha_{3,5} = \alpha_{6,5} = 1.5^m$ for m=-1) which has been expected to produce only a small hydrophilic effect and approximately 0 ($\alpha_{3,5} = \alpha_{6,5} = 1.5^m$ for m=-28) which has been expected to yield a significant hydrophilic effect.

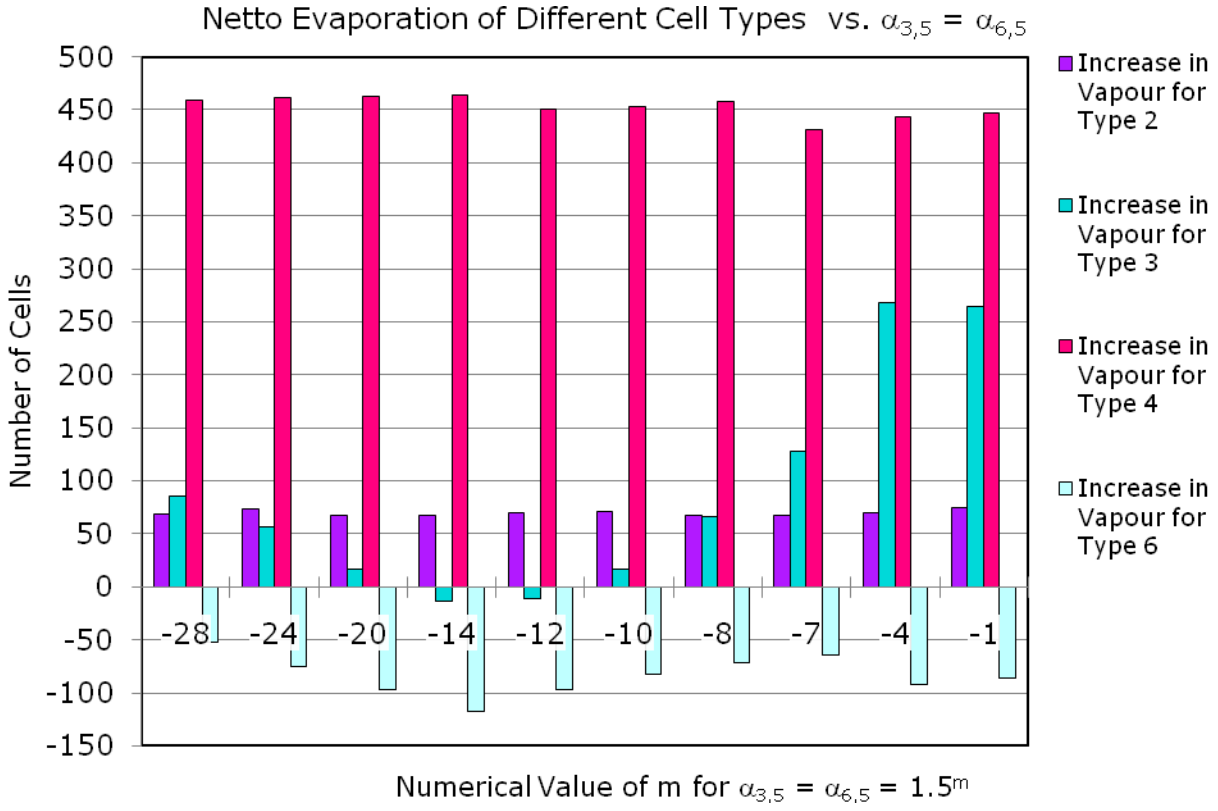

Figure 16: Modelled Separation of Non-polar Solutes (Type 2 and 4) from a Polar Solution (Type 3 and 6) for Different Values of $\alpha_{3,5} = \alpha_{6,5}$

It can be seen in Figure 16 that the evaporation of the non-polar substances remain fairly constant regardless the value of $\alpha_{3,5} = \alpha_{6,5}$ which can be expected as $\alpha_{3,5}$ and $\alpha_{6,5}$ only describes the interaction of the polar substances with the packing material. The behaviour of the polar substances varies significantly with respect to the numeric value of $\alpha_{3,5} = \alpha_{6,5}$, as expected.

For m=-1 decreasing to m=-14, the packing material becomes more hydrophilic which results in an increasing number of Type 6 cells that move from the gas phase towards the more dense liquid phase. The evaporation of the Type 3 cells decreases correspondingly to approximately zero.

Note that according to the definition of the cell types and the initial conditions specified in Table 3 , there are strictly spoken no Type 3 cells (liquid water) present in the initial gas phase and no netto condensation of Type 3 cells is therefore possible. The small amount of condensation shown for m=-12 and m=-14 results from inaccurate measurements due to the fact that the neighbourhoods of the cells on the border of the gas phase will include cells from the adjacent liquid phase (Section 3.4).

Despite these inaccuracies, the results for $-14 \leq m \leq -1$ satisfy intuitive expectations for hydrophilic behaviour. However, when m is decreased further from -14 to -28, the condensation of the Type 6 cells decreases while the evaporation of the Type 3 cells increases, which is the opposite of what has been expected.

The graphic output in Figure 17 shows the typical initial and steady state configurations that have been achieved for different values of m. For $m \geq -4$, the graphic output reflects the results in Figure 16: The hydrophilic effect is too small for the water to remain in a liquid layer on the packing material surface, although the water evaporates at a visibly slower pace than the non-polar solutes.

For $m < -4$, the hydrophilic effect has resulted a thin liquid film layer of water on the packing material surface at steady state. This liquid layer has formed in the region where the R=7 neighbourhood contains a sufficient number of hydrophilic packing material (Type 5) cells to firmly attract the water molecules. For m = -7, the packing material exhibits just enough hydrophilicity for a liquid layer to form where the concentration of Type 5 cells are at a maximum within the R=7 neighbourood, i.e. directly adjacent to the packing material surface.

When m is further decreased, the threshold number of Type 5 cells needed within the R=7 neighbourhood to form a liquid layer, drops and the hydrophilic zone commences further away from the packing material surface. In other words, the hydrophilic zone becomes thicker for a decreasing m-value.

Note the dense outer "rim" (looking like a suspended liquid film layer) that forms at an increasing distance away from the packing material as m decreases to -28. This phenomenon occurs when additional Type 6 (water vapour) cells "condensate" from the gas phase into the hydrophilic zone that has already been populated by the remaining Type 3 cells (due to the hydrophilic attraction by the packing material) while the alcohol (Type 4) cells evaporate. The effect of this apparent bottle neck, called "premature saturation", on the structure of the liquid layer is illustrated in Figure 18.

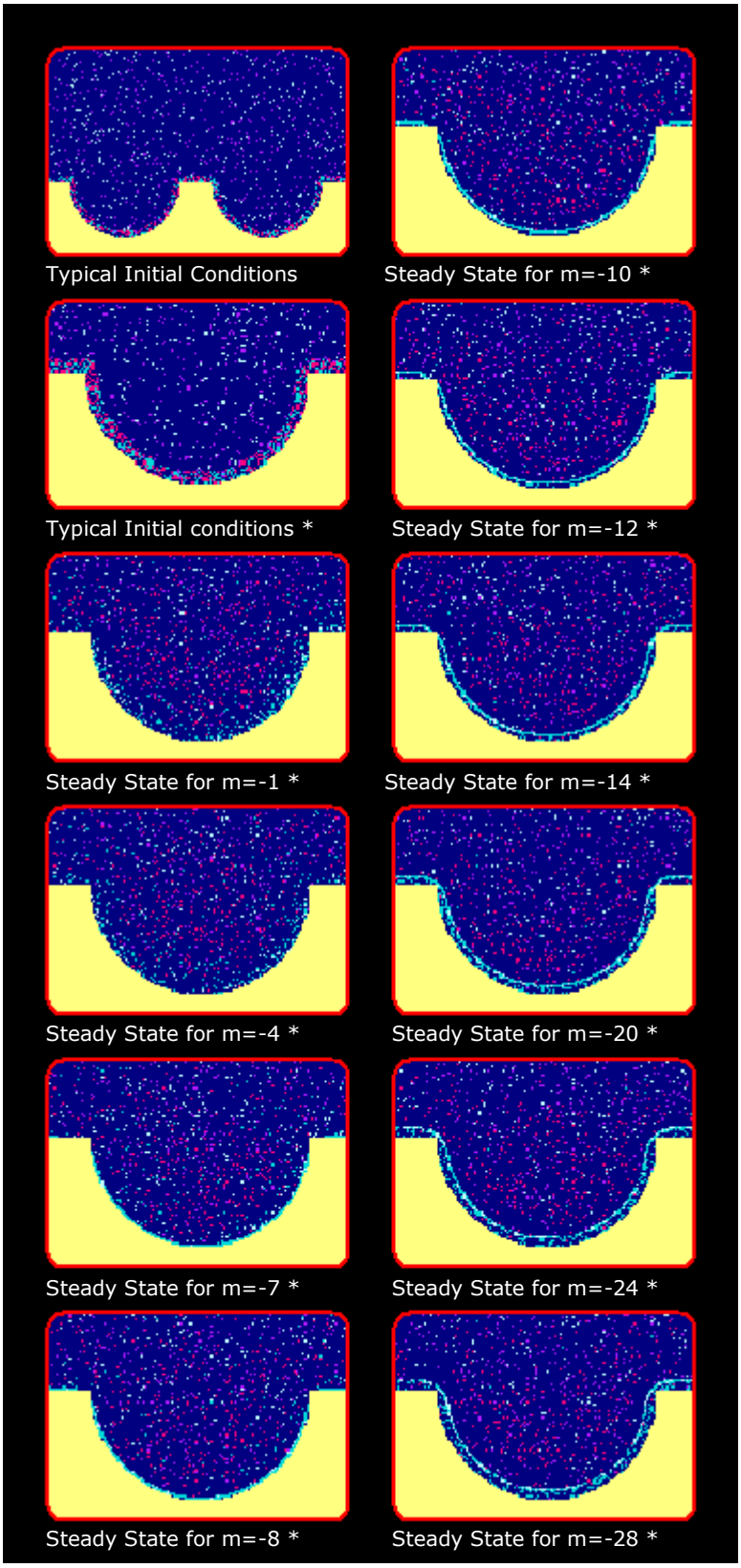

** Cropped and enlarged graphic output*

Figure 17: ***Graphic Output of Initial and Steady State Conditions for*** $\alpha_{3,5} = \alpha_{6,5} = 1.5^m$

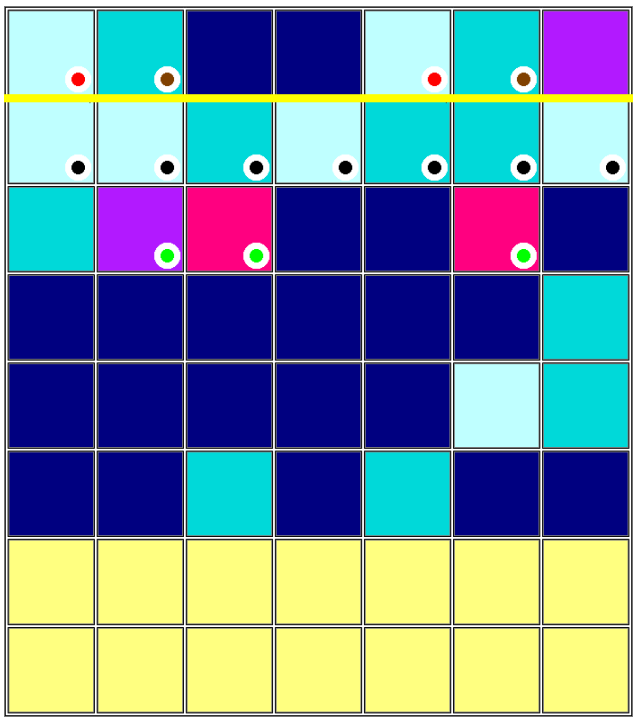

Figure 18 (a): Failure to model the formation of a dense liquid layer due to premature saturation

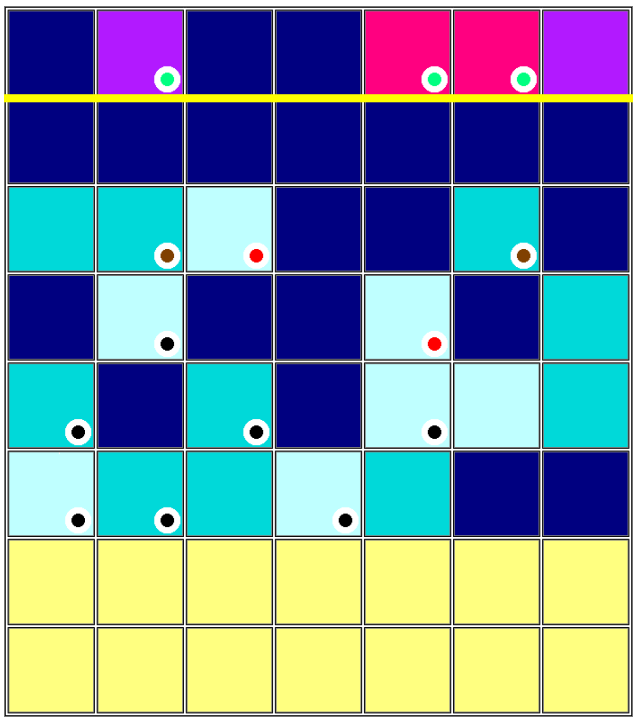

Figure 18 (b): Formation of a dense liquid layer without the effect of premature saturation

In Figure 18 (a) the new water condensate (marked with black dots) "sticks" just within the outer edges (thick yellow line) of the hydrophilic zone instead of making way for "new" Type 6 condensate (red dots) by moving towards the packing material itself to form a dense liquid layer. Note that this premature saturation by the Type 3 and 6 cells, representing polar water molecules, not only limits the condensation of Type 6 cells, but also "traps" some Type 2 and 4 cells that represent non-polar molecules, within the unfavourable hydrophilic zone between the yellow line and the packing material itself. Furthermore, this blockage on the outer edge of the hydrophilic zone "forces" evaporated Type 3 cells to remain in the gas phase instead of returning to the liquid layer (brown dots). Premature saturation therefore effectively limits the ability of the model to yield realistic results in terms of theoretical expectations.

Figure 18 (b) shows the formation of an even liquid layer on the surface of the packing material that would have occurred if the water condensate re-arranged itself within the hydrophilic zone to "stack" on the packing material surface, rather than hovering just beneath the border of the hydrophilic zone as shown in Figure 18 (a). Note that the Type 2 and 4 cells can now freely evaporate, away from the hydrophilic zone. Furthermore, there is now ample room for the new Type 3 and Type 6 condensate. This allows for a dense liquid layer of a maximum thickness equal to that of the hydrophilic zone.

The effect of premature saturation on the model results increases dramatically as the value of m decreases past -20, which is clearly visible in Figure 17 and reflected in the results of Figure 16.

In spite of numerous attempts, the Type Bias cannot be fine tuned to create a sufficient gradient within the hydrophilic zone to prevent premature saturation. For such a gradient, a larger range of $\alpha_{i,j}$-values is needed for the given neighbourhood

size of R=7, that would render the simulation programme unstable. A smaller neighbourhood would allow for a larger range of $\alpha_{i,j}$-values, but this would limit the ability of the current simulation programme to model the effect of polarization (Section 3.2.4).

The trade-off between the neighbourhood size and the allowable range of $\alpha_{i,j}$-values, has resulted in a trade-off between the ability of the model to incorporate the effect of polarization and the ability to represent separation, in particular the condensation of hydrophilic substances, for strong hydrophilic packing materials. The ultimate consequence of this trade-off is a separation model with a limited selectivity range.

The simulation programme needs further modification to avoid these trade-offs that cripples its ability to produce a realistic separation model for scenarios that involves extensive condensation.

4.1.3 Effect of Hydrophilic Packing Materials on Rate at which Steady State is Achieved

The effect of different values for $\alpha_{3,5} = \alpha_{6,5}$ on the rate of separation between non-polar, volatile alcohol and polar, less volatile water has been investigated in this sub-section. The rate of separation can be determined by means of several possible criteria shown in Table 11. These criteria are all based on the number of cells (NOC) for a given type and phase at the initial conditions (specified at the start of the simulation) compared to the average NOC for that type or phase during the subsequent time steps until steady state has been reached.

"Approximate NOC_{AX}" refers to the average NOC of Type A and Phase X for all experimental replicates and surface areas.

Table 11: Comparative Measures for Rate of Separation Achieved

Criterion Description		***Approximate NOC_{AX}***		***% Increase****
Type (A)	*Phase (X)*	*Initial Conditions*	*Steady State*	*Refer to Equation **8, p?***
2	*Vapour*	*1660*	*1730*	*4.21%*
2	*Liquid Layer*	*56*	*11*	*80.36%*
3	*Liquid Layer*	*403*	*353*	*-12.41%*
4	*Liquid Layer*	*335*	*22*	*93.40%*
6	*Vapour*	*1308*	*1225*	*-6.35%*

** Remember that "% Increase" for any substance (Type A) in a given phase (Phase X) is only defined if Type A were present in Phase X at the initial conditions. A negative % Increase-value indicates a decrease in the NOC for Phase X.*

It is generally much easier to distinguish between experimental noise and actual fluctuations in the results for radical changes in experimental (simulated) NOC-values, than for more subtle changes. The approximate NOC_{AX} which undergoes the most radical change (corresponds to the % increase with the biggest absolute numerical value) would therefore be the most suitable criterion to indicate whether (and when) steady state has been reached.

Table 11 shows that the % increase in the NOC for Type 4 (alcohol) in the liquid phase has the biggest absolute value. In other words, the NOC for liquid alcohol has a relatively high initial value and decreases to a very low, steady state value. It is therefore assumed that steady state has been achieved when the approximated NOC for liquid alcohol remains at a low, constant value.

Figure 19 shows the average NOC of Liquid Type 4 for different values of $\alpha_{3,5}$ and $\alpha_{6,5}$ against the elapsed time for the simulation runs. The numerical value of $\alpha_{3,5} = \alpha_{6,5}$ has again been varied between slightly smaller than 1 ($\alpha_{3,5} = \alpha_{6,5} = 1.5^m$ for m=-1) and approximately 0 ($\alpha_{3,5} = \alpha_{6,5} = 1.5^m$ for m=-28).

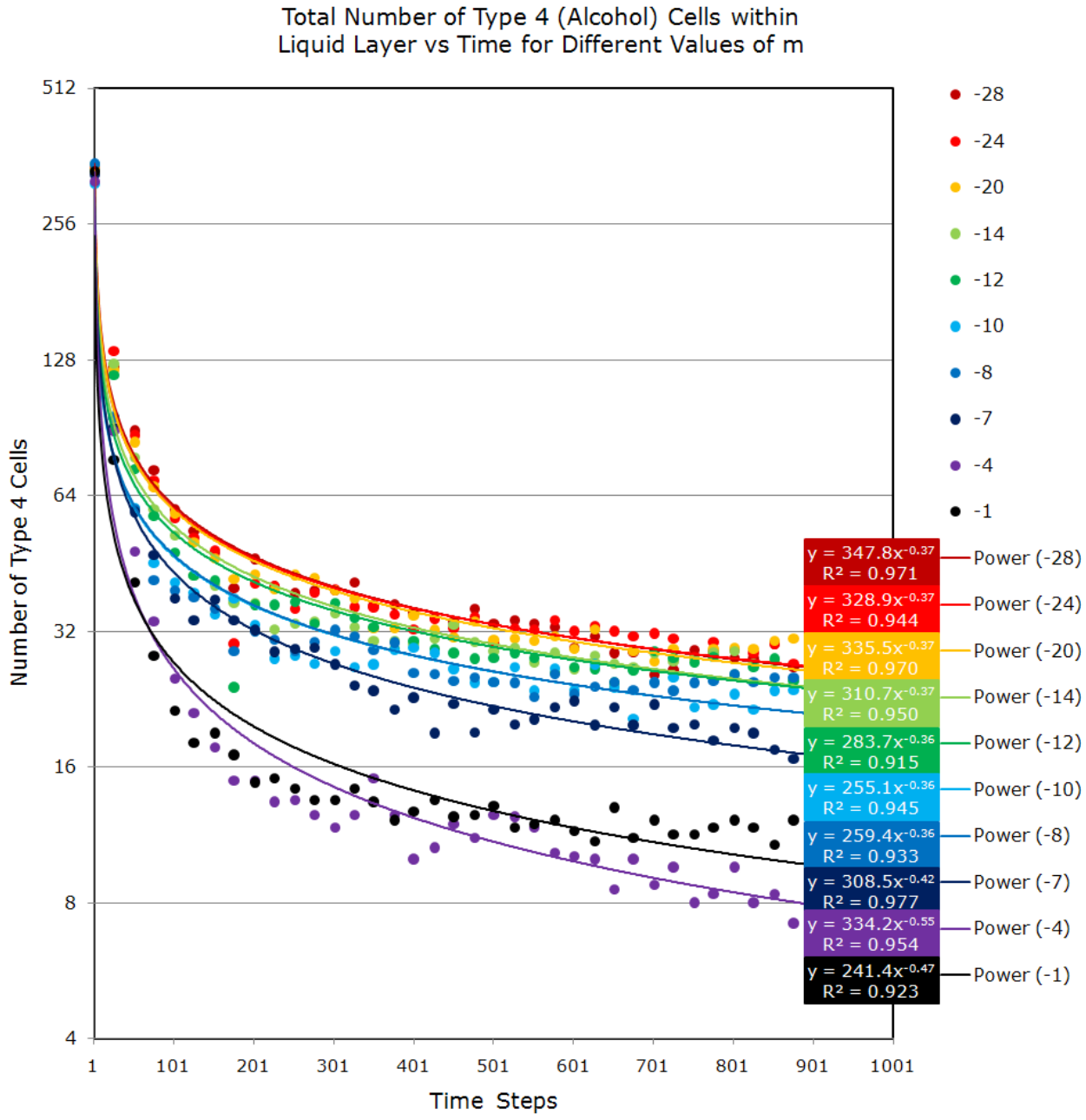

Figure 19: Average number of liquid alcohol cells as a function of time for different values of $\alpha_{3,5} = \alpha_{6,5} = 1.5^m$

The initial conditions (Time Steps = 1) in Figure 19 typically represents a system of which the equilibrium has been disturbed (e.g. fresh air is rapidly pumped over packing material that has been wetted by an alcohol solution). This results in a large initial driving force, in this case the difference in the low alcohol vapour pressure in the gas phase (air) and the relatively high alcohol vapour pressure exerted by the liquid phase (alcohol solution).

The number of liquid Type 4 cells in Figure 19 decreases almost logarithmically with time for all values of m. This behaviour conforms to the theoretical expectations for a system in which the vapour pressure of the liquid phase exceeds that of the gas phase. Such a system will spontaneously strive towards a dynamic steady state equilibrium in which the difference between the component vapour pressure of the gas phase and that of the liquid phase has been minimized through the selective evaporation of the alcohol.

Note that evaporation of the alcohol causes the difference between the component vapour pressures, exerted by the two respective phases, to decrease over time. This is reflected in the absolute value for the slope of curve in Figure 19 that decreases with time for all values of m. This corresponds to the decrease in the rate of alcohol evaporation that is expected for a driving force that declines over time until it reaches zero at steady state.

Figure 19 shows that the model is capable of representing the effect of a declining driving force that is typical of a system which is allowed to reach equilibrium.

Figure 20 represents the effect of packing materials with varying degrees of hydrophilicity on the rate of alcohol evaporation simulated by the decrease in Type 4 cells for the modelled liquid phase.

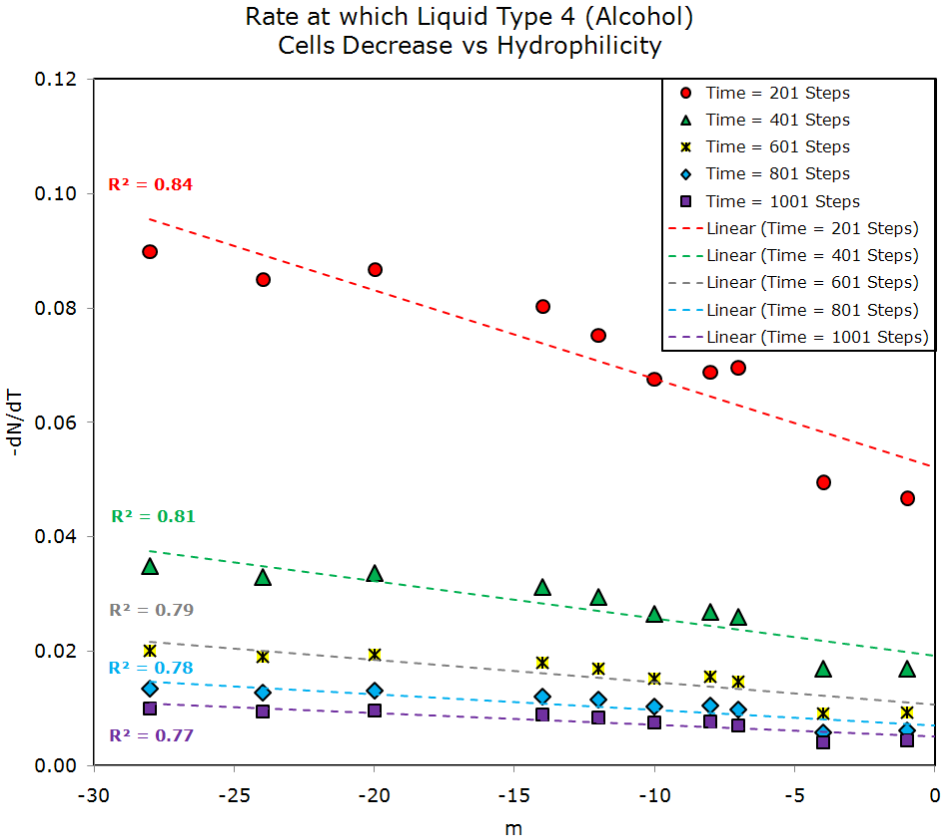

Figure 20: Rate of evaporation for liquid alcohol (Type 4) cells as a function of packing material hydrophilicity (m)

Figure 20 presents an almost linear relationship between the rate of alcohol evaporation and the hydrophilic strength of the packing material. An increase in the hydrophilic strength (corresponds to an increasingly negative m-value) results in a subsequent increase in the rate of alcohol evaporation.

Note that this linear relationship flattens out with an increase in the number of time steps elapsed, which confirms the relationship of the driving force and the subsequent alcohol evaporation rate with time shown in Figure 19.

Figure 20 implies that the hydrophilic strength of the packing material not only affects the total separation that has been achieved after steady state has been reached, but that it also affects the rate of separation.

According to the relationship between the alcohol evaporation rate and the hydrophilic packing material strength revealed by Figure 20, the model is capable of representing an additional driving force for separation that is caused by the effect of intermolecular forces. This stands apart from the driving force that has already been created by the effect of different component vapour pressures.

4.2 Effect of Packing Material Surface Structure on Model Results

Section 4.1 emphasizes that the simulation programme is still in need of some modifications. The model is therefore still in its preliminary, uncalibrated construction phase. However, the potential ability of the model to represent the effect of different surface structures, once it has been successfully calibrated, is explored in this section.

4.2.1 Definition and Classification of Packing Material Surface Structures

The phase boundaries at the start of a simulation are defined by means of algebraic equations in terms of the coordinates on a two-dimensional board. The vertical position (y) is a function of the horizontal position (x). Seeing that x is a vector, these functions are not continuous but discrete. The length of each vector increment is 1 cell and the length of the vector is the total width of the board (in this case 300 cells). Simple geometrical shapes are significantly easier to define and have therefore been used for modelling purposes, although there is a vast number of possible surface geometries in reality.

Figure 21 shows an attempt to classify all the possible configurations for a single tessellation of the three basic shapes, namely the circle, triangle and rectangle (of which the square is a sub-type).

The surface structures in Figure 21 have the same surface area when a constant depth (z) is assumed for a 3 dimensional system. On a 2 dimensional board like the one used for this study, the length of the boundary separating the packing material from the rest of the board, is exactly the same for all configurations. This specification ensures that difference in simulation results for these structures are indeed due to the difference in shape and not due to a difference in surface area (in the xy-plane).

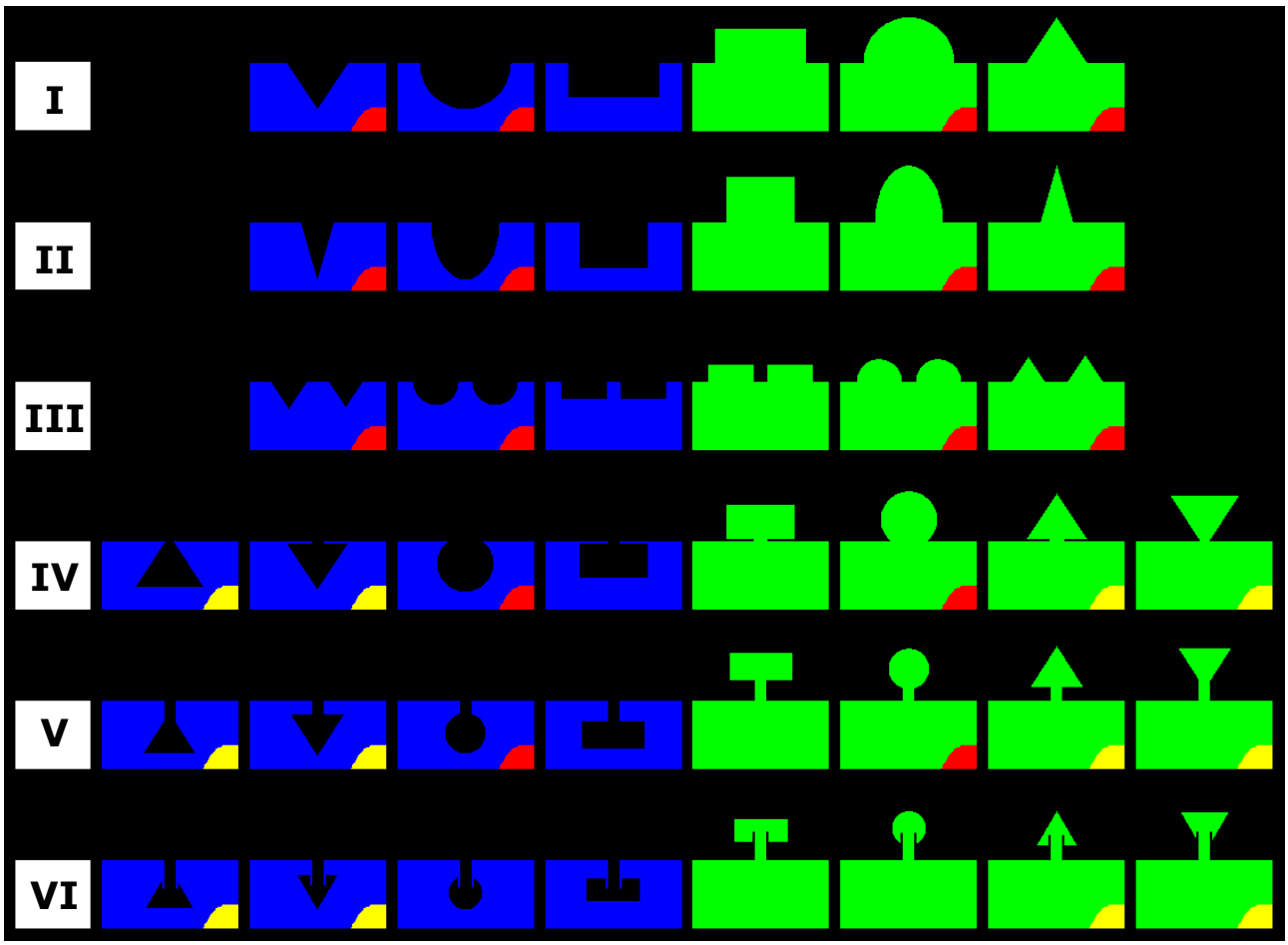

Figure 21: Simple geometric shapes for the packing material surface (blue/green) as viewed in a 2 dimensional model.

Only a few shapes have been selected for this study, seeing that the model yet has to prove itself able to justify the effort of studying all the shapes that have been suggested in Figure 21. The shapes in Figure 21 that have been considered are tagged in red and labelled (numbered) as shown in Figure 22. The shapes will be referred to by means of these labels throughout this chapter. There are numerous types of shape differences that may have an effect on the model results. The following differences have been investigated.

- The effect of different shape types (eg. triangular vs. circular excavations).

- Difference between the effects of sunken (excavated) shapes and equivalent protruding shapes (which are identical in all other aspects): The excavated shapes are blue and the protruding shapes are green in Figure 21 and 22. Note that the blue shapes on the left hand side are "mirrored" by the equivalent green shapes on the right hand side.

- The effect of different excavation or protrusion depths: The excavation or protrusion depth increases from Row I up to Row VI. This excludes Row III in which the shapes are strictly spoken, not single tessellations like the rest of the shapes in Figure 21 and 22, but double tessellations. The apparent decrease in size of the deeper excavations and protrusions keeps the total surface area, represented by the total circumference of the two dimensional shapes in Figure 21 and 22, constant.

- Difference between the effect of a single excavation/protrusion (Row I) and two identical, half-sized excavation/protrusions (Row III).

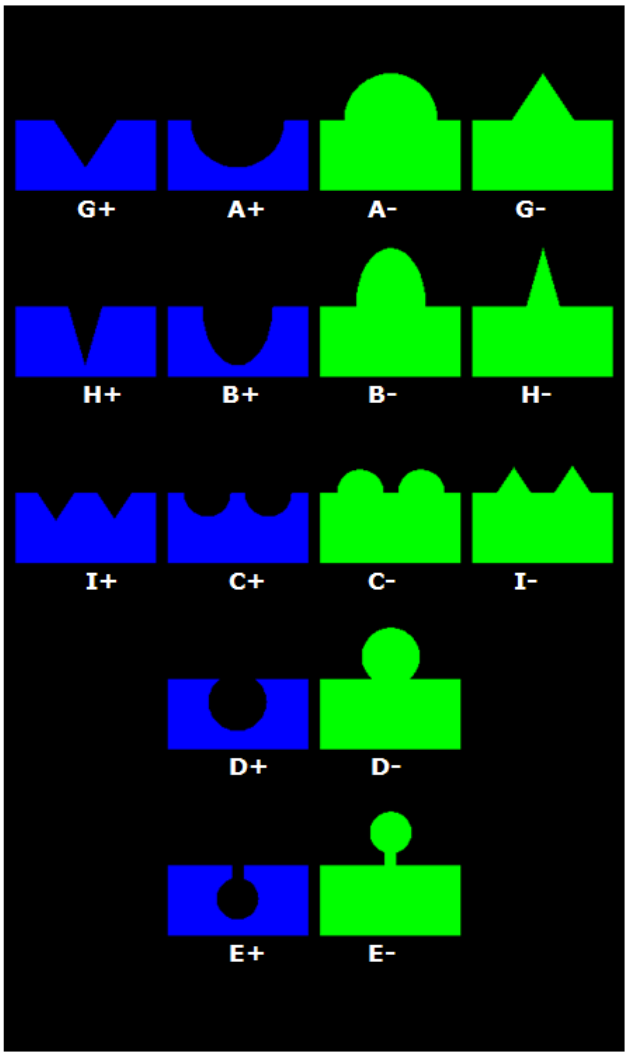

Figure 22: Selected shapes for the representation of various packing material surface geometries.

Note that "depth" for the purposes of this study is a measure of the % of a shape that is "submerged" below the horizontal surface of the otherwise flat packing material surface.

Depth in this context is therefore *not* a measure of the absolute distance that a shape is sunken or protruding from the flat surface. E.g. the protruding semicircle in Shape A- has a depth of -50% relative to that of a full circle, while the excavation in Shape D+, that almost resembles full circle, has a depth of approximately 75% of an equivalent sized full circle, although the absolute distance from the deepest end of Shape D+ to the flat surface is less than that of Shape A-.

Additional aspects regarding shape differences which are not covered in this study include the orientation of a triangular excavation or protrusion.

Examples of shapes containing triangular components that can be rotated in opposite directions are marked with yellow tags in Figure 21. Note that the triangular shape component in a yellow tagged shape, is "flipped" upside down, when it is compared to the adjacent, similarly tagged shape.

The effect of multiple (3 or more) tessellations for the same surface area on the degree of separation achieved, can also be investigated once the model has been sufficiently refined. The model still needs some adjustment to accommodate multiple tessellations in a user friendly manner.

To study the effect of the packing material surface structure on various aspects of the model output, the Type Bias has been held constant with $\alpha_{3,5} = \alpha_{6,5} = 1.5^{m}$ where m=-12. This provides the packing material with a strong enough hydrophilic nature to aid in the separation of the volatile, non-polar substances from the less volatile polar substances, while the programme is still capable to produce reasonable results in spite of the limitations discussed in Section 4.1.2.

4.2.2 Effect of Packing Material Surface Structure on Steady State Conditions and Selectivity Range

The primary focus of this sub-section is the effect of the different surface geometries on the degree of separation achieved (selectivity range) between non-polar, volatile alcohol and polar, less volatile water. For different surface structures, the total volume of the liquid layer might differ slightly from the one shape to the other. Therefore results in terms of NOC cannot be directly compared to one another for different surface areas without compromising the accuracy thereof. To ease comparison between these results, the extent of separation will be evaluated by means of the criteria shown in Table 12. These criteria are based on the hypothetical steady state scenario that would exist for ideal, complete (100%) separation of the alcohol (Type 4) from the water (Type 3 and 6).

For such an ideal separation the following would be true:

- Polar water cells (less volatile) will end up in the liquid layer

  The liquid water (Type 3) cells remain in the liquid layer for the full duration of the simulation run, or it will evaporate only to return to the liquid layer before steady state is reached. In either case, the netto evaporation of the liquid water from the liquid layer to the gas phase will be zero.

  The water vapour (Type 6) cells will condensate and subsequently migrate from the gas phase into the liquid layer (100% netto condensation).

- All volatile, non-polar cells will end up in the gas phase

  The non-polar gas cells (Type 2) will remain in the gas phase (0% netto condensation). Type 2 cells that have initially been suspended in the water layer will completely evaporate (100% netto evaporation).

  The alcohol (Type 4) cells that have initially been in the liquid phase (dissolved within the liquid layer) will completely evaporate (100% netto evaporation).

Table 12: Comparative Measures for Extent of Separation Achieved

Criterion No. (NC)	*Criterion*	*% Increase for Ideal Separation*	*Weight (W)*
1	*% Increase in Liquid Layer for Type 2*	*-100.00%*	*0.5*
2	*% Increase in Liquid Layer for Type 3*	*LPV**	*1.0*
3	*% Increase in Liquid Layer for Type 4*	*-100.00%*	*1.0*
4	*% Increase in Vapour for Type 2*	*LPV**	*0.5*
5	*% Increase in Vapour for Type 6*	*-100.00%*	*1.0*

**Increase of Type 2 in the vapour phase will depend on the number of Type 2 cells initially present in the liquid layer. There is therefore no ideal numerical value, although large, positive values (LPV) are preferred to smaller values.*

W=1 is assigned to criteria that involve Cell Types representing species that are separated (alcohol and water in this case). W = 0.5 is allocated to Criteria involving

species of which the movements are potentially affected by the separation of the other species. Although the primary focus is not on these species (in this case the non polar gases), their movement is indicative of the behaviour of the species to be separated.

The % increase for any substance (Type A) in a given phase (Phase X) is calculated as follows:

$$\% \text{ Increase} = \left(\frac{N_{ss} - N_i}{N_i} \right) \times 100\% \qquad (\mathbf{13})$$

where N_{ss} is the number of Type A cells in Phase X at steady state and
N_i is the initial number of Type A cells in Phase X.

Note that % increase is only defined if Type A were present in Phase X at the initial conditions. A negative % Increase-value indicates a decrease in the number of cells for Phase X.

As previously stated, there are strictly spoken no Type 3 cells (liquid water) present in the initial gas phase and no netto condensation of Type 3 cells is therefore possible. The small amounts of Type 3 condensation shown for example in Table 13 result from the inaccuracies explained in Section 3.4. To account for small amounts of evaporation of Type 3 in spite of these inaccuracies, it is assumed that more "condensation" according to the measured results, correspond to less evaporation. Therefore the largest positive value is ranked in first place.

The low variation in the results of the respective runs and the support to the numerical results that have been provided by the graphical simulation output, deemed five replicate runs acceptable where this would be normally considered insufficient for statistically sound conclusions. Therefore, only five replicate runs have been simulated for each surface structure.

The average separation achieved for each type of surface structure will be compared to the "ideal case" scenario, using the criteria in Table 12. For the purposes of this discussion, "result" refers to the average result of the five replicates that have been run for any given surface structure.

Depending on how closely the steady state results for a particular surface structure represents ideal separation in comparison with that of the other structures, each surface structure has been awarded a scaled separation score (SSS). The SSS has been derived from the criterion score (CS) as follows:

The CS for a given surface structure is a measure of how the numerical result for a specific criterion (e.g. percentage increase in vapour for Type 6) compares to the corresponding results for other surface structures. A rank of 1 will be allocated to the result that differs the least from the ideal result for any given criterion. This can be considered as the "best" result, while the second best result will get a rank of 2, etc. The criterion scores are calculated for all criteria as shown in Equation 14.

$$CS_{NC} = W \times (1 + TNR - IR) \qquad (\mathbf{14})$$

W refers to the weight defined in Table 12. TNR refers to the total number of results (surface structures) that are involved in this comparison, while the Individual Rank

(IR) refers to the rank of the individual result. NC merely refers to the number of the criterion which is given in Table 12.

The USS (unscaled separation score) for any surface structure is calculated by adding up the criterion scores for all the criteria as shown in Equation 15.

$$USS = \sum_{NC=1}^{5} CS_{NC} \qquad (\mathbf{15})$$

Finally, the SSS is calculated for each surface structure in Equation 16.

$$SSS = \frac{USS}{USS_{Min}} \qquad (\mathbf{16})$$

where USS_{Min} refers to lowest USS-value amongst the USS-values from the respective surface structures. For the surface structure with the lowest USS, $USS=USS_{Min}$. Therefore, the surface structure that yields the poorest separation, will have a SSS-value of 1.00, while the SSS for all the other surface structures will exceed 1.00. The Scaled Separation Score will be now be used to compare the degree of separation achieved with the different surface structures in terms of the criteria in Table 12.

To compare the effect of a circular surface geometry with that of a triangular geometry, the average results for Shapes A+, A-, B+, B-, C+ and C- were compared with that of Shapes G+, G-, H+, H-, I+ and I-. The most essential results, with the CS-value for each criterion, are shown in Table 13.

Table 13: ***Calculation and Comparison of the Criterium Scores for Cricular and Triangular Surface Geometries***

NC	***W***	***Average % Increase****		***IR***		***CS_{NC}***	
		Circ.Sh.	*Tri.Sh.*	*Circ.Sh.*	*Tri.Sh.*	*Circ.Sh.*	*Tri.Sh.*
1	*0.5*	*-74.79%*	*-72.99%*	*1*	*2*	*1.0*	*0.5*
2	*1.0*	*7.78%*	*6.33%*	*1*	*2*	*2.0*	*1.0*
3	*1.0*	*-91.39%*	*-92.05%*	*2*	*1*	*1.0*	*2.0*
4	*0.5*	*3.82%*	*3.72%*	*1*	*2*	*1.0*	*0.5*
5	*1.0*	*-6.46%*	*-6.10%*	*1*	*2*	*2.0*	*1.0*

**Ideal Values defined in Table ZYX*

Circ.Sh. refers to all circular shape geometries (A+, A-, B+, B-, C+ and C-), while Tri.Sh. refers to the triangular shapes (G+, G-, H+, H-, I+ and I-).

Table 13 shows that CS_{NC}(Circ.Sh.) > CS_{NC}(Tri.Sh.) for NC = 1,2,4,5 while CS_{NC}(Circ.Sh.) < CS_{NC}(Tri.Sh.) for NC = 3. According to four out of five criteria, better separation results have been obtained for the circular geometry than for the triangular geometry.

These results can be justified by the physical configuration of the shapes as follows: For deep, narrow tips and corners of the triangular shaped cavities, the liquid layer is harder to reach for cells in the gas phase. Exchange between the cells from the respective phases is therefore difficult. On the other hand, the cells within the liquid layer on the relatively smooth surfaces of the circular cavities and protrusions are readily accessible for exchange with cells from the adjacent gas phase.

Note that the criterion scores in Table 13 also account for the weight of each criterion. The criterion scores have in turn been used to calculate the SSS as shown in Equations (14), (15) and (16). For the circular shapes SSS=1.40, while SSS=1.00 for the triangular shapes. These SSS-values confirm that better separation have been achieved with the circular geometry.

To compare the effect of an excavated geometry with that of a protruding geometry, the average results for Shapes A+, B+, C+, D+, E+, G+, H+ and I+ were compared with that of Shapes A-, B-, C-, D-, E-, G-, H- and I-. The essential results for each criterion are shown in Table 14.

Table 14: ***Calculation and Comparison of the Criterion Scores for Excavated (+) and Protruding (-) Surface Geometries***

NC	***W***	***Average % Increase****		***IR***		***CS_{NC}***	
		+	-	+	-	+	-
1	*0.5*	*-70.46%*	*-74.80%*	*2*	*1*	*0.5*	*1.0*
2	*1.0*	*5.64%*	*6.46%*	*2*	*1*	*1.0*	*2.0*
3	*1.0*	*-90.86%*	*-91.98%*	*2*	*1*	*1.0*	*2.0*
4	*0.5*	*4.37%*	*3.49%*	*1*	*2*	*1.0*	*0.5*
5	*1.0*	*-6.93%*	*-5.67%*	*1*	*2*	*2.0*	*1.0*

**Ideal Values defined in Table ZYX*

Table 14 shows that $CS_{NC}(-) > CS_{NC}(+)$ for NC = 1,2,3 while $CS_{NC}(-) < CS_{NC}(+)$ for NC = 4,5. According to three out of the five criteria, better separation results have been obtained for the protruding geometry than for the excavated geometry. This in itself provides not enough ground from which to rank the protruding geometry above the excavated geometry.

The weight of each criterion has been accounted for by means of the CS, after which the SSS is calculated. SSS=1.18 for the protruding shapes, while SSS=1.00 for the excavated shapes. The SSS-values confirm that only slightly better separation have been achieved with the protruding geometries.

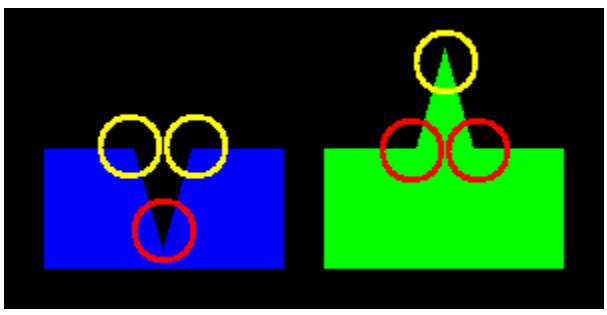

Figure 23: Example of typical surface structures with hard-to-reach areas (red) and easily accessible areas (yellow) for liquid-vapour exchange

The results can be explained by the physical configuration of the respective shapes. Figure 23 shows an example of a typical sunken surface structure (blue) with its protruding complement (green). Areas where liquid-vapour cell exchange is likely to be impaired due to deep cavities or corners are marked with red circles. On the other hand, the complementing tips and corners (marked with yellow circles) provide easy access for exchange of cells between the two respective phases.

For relatively shallow shapes, both the sunken and protruding surfaces provide surfaces of difficult and easy access. Therefore the difference between the sunken and protruding shapes is likely to be small, as the respective SSS-values suggest.

The effect of different shape depths as well as the difference between the effect of a single excavation/protrusion and two identical, half-sized excavation/protrusions has been investigated. (The sizes of N multiple excavations equal the original size divided by N. This measure keeps the total surface area constant.) The most essential results, with the CS-value for each criterion, are shown in Table 15. Note that results of Shape A refer to the average between the results from Shape A+ and Shape A-. The same holds for the results from Shape B up to shape E.

Table 15: Calculation and Comparison of the Criterion Scores for Surface Geometries of Various Configurations

NC	***W***	***Average % Increase****					***IR***					***CS_{NC}***				
		A	*B*	*C*	*D*	*E*	*A*	*B*	*C*	*D*	*E*	*A*	*B*	*C*	*D*	*E*
1	*0.5*	*-76.3*	*-72.9*	*-75.1*	*-71.7*	*-66.0*	*1*	*3*	*2*	*4*	*5*	*2.5*	*1.5*	*2.0*	*1.0*	*0.5*
2	*1.0*	*10.5*	*4.1*	*8.8*	*3.1*	*2.9*	*1*	*3*	*2*	*4*	*5*	*5.0*	*3.0*	*4.0*	*2.0*	*1.0*
3	*1.0*	*-91.8*	*-90.5*	*-91.9*	*-90.8*	*-90.2*	*2*	*4*	*1*	*3*	*5*	*4.0*	*2.0*	*5.0*	*3.0*	*1.0*
4	*0.5*	*4.1*	*3.7*	*3.7*	*4.1*	*4.7*	*3*	*4*	*5*	*2*	*1*	*1.5*	*1.0*	*0.5*	*2.0*	*2.5*
5	*1.0*	*-7.0*	*-6.5*	*-5.9*	*-5.5*	*-7.2*	*2*	*3*	*4*	*5*	*1*	*4.0*	*3.0*	*2.0*	*1.0*	*5.0*

**Ideal Values defined in Table ZYX*

Table 15 shows that CS_{NC}-values for the respective shape configurations and the subsequent ranking thereof differs significantly for the various criteria. There is no obvious favourite amongst these shapes for the best degree of separation. This information in itself provides not enough ground from which to rank the different shape depths.

Again, the weight of each criterion has already been accounted for by means of the CS_{NC}-value, after which the SSS needs to be calculated. The SSS-values for the different shape configurations are shown in Table 16.

Table 16: Unscaled and Scaled Separation Scores (USS and SSS) for Various Surface Configurations

Configuration		*USS*	*SSS*	*Final Rank*
A	*(Shallow)*	*17.00*	*1.89*	*1*
B	*(Elonginated)*	*10.50*	*1.17*	*3*
C	*(2x tessellation of half-sized A)*	*13.50*	*1.50*	*2*
D	*(Submerged)*	*9.00*	*1.00*	*5*
E	*(Deeply submerged)*	*10.00*	*1.11*	*4*

The SSS-values show that better separation have been achieved with shallow geometries (Shapes A and C) than with the deeper geometries (Shapes B, D and E). Once more, the physical configuration of the packing material justifies the results.

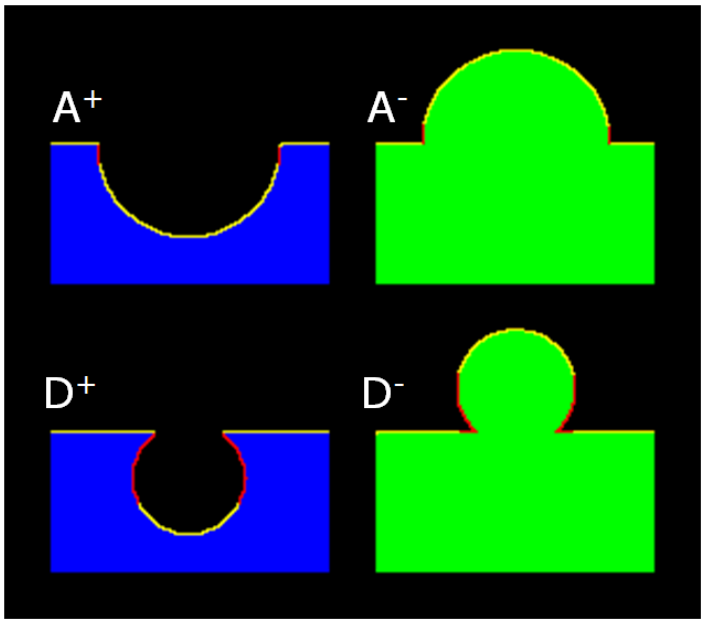

Figure 24 shows examples of shallow surface structures (A+ and A-) and deep surface structures (D+ and D-). The red borders indicate where liquid-vapour interaction is likely to be impaired due to deep cavities or corners. On the other hand, the smooth surfaces (yellow) provide easy access for gas-liquid exchange. Note the increased length of red surfaces relative to the yellow surfaces in the deeper shapes.

Figure 24: Example of typical surface structures with hard-to-reach areas (red) and easily accessible areas (yellow) for liquid-vapour exchange

The increased length of red surfaces relative to the yellow surfaces in the deeper shapes shown in Figure 24 corresponds to an increased ratio of total surface area that is likely to impair the liquid-vapour interaction, to the total surface area that provides easy access for gas-liquid exchange. This ratio increases for the deeper shapes, supporting the quantitative results that have been obtained from the model.

The double tessellation of the shallow shape (Shape C) has a significantly lower scaled separation score (SSS(C)=1.50) than that of Shape A (SSS(A)=1.89). This shows that the use of smaller tessellations for a given shape does not necessary yield better separation than a single, full-sized replica shape. In this study, only the individual, uncombined effects of tessellation and depth are considered.

Once the model has been refined, a factorial approach considering the combined effect of tessellation and depth is likely to yield a relationship between these two factors. For such a study, extensive simulations are necessary, because tessellations of Shapes B, D and E will also be considered in addition to Shape C which is a tessellation of Shape A. Furthermore, as stated earlier on, multiple (3 or more) tessellations still need to be studied.

4.2.3 Effect of Packing Material Surface Structure on Rate at which Steady State is Achieved

The effect of the different surface geometries on the rate of separation between alcohol and water is discussed in this sub-section. The rate of separation can be determined in the same manner as shown in Section 4.1.3 by using any one of the criteria in Table 17.

Table 17: Comparative Measures for Rate of Separation Achieved

Criterion Description		***Approximate NOC_{AX}***		***% Increase****
Type (A)	*Phase (X)*	*Initial Conditions*	*Steady State*	*Refer to Equation 8, p 32*
2	*Vapour*	*1867*	*1939*	*3.86%*
2	*Liquid Layer*	*60*	*16*	*-73.33%*
3	*Liquid Layer*	*426*	*451*	*5.86%*
4	*Liquid Layer*	*357*	*31*	*-91.32%*
6	*Vapour*	*1485*	*1394*	*-6.12%*

** Remember that "% Increase" for any substance (Type A) in a given phase (Phase X) is only defined if Type A were present in Phase X at the initial conditions. A negative % Increase-value indicates a decrease in the NOC for Phase X.*

As previously stated in Section 4.1.3, the approximate NOC_{AX} which undergoes the most radical change would be the most suitable criterion to indicate whether (and when) steady state has been reached.

Table 17 shows again that the % increase in the NOC for Type 4 (alcohol) in the liquid phase has the biggest absolute value. It is therefore assumed that steady state has been achieved when the approximated NOC for liquid alcohol (Type 4) reaches a constant value.

Figure 25 shows the average number of Liquid Type 4 cells for different surface geometries against the elapsed time for the simulation runs.

Figure 25 is equivalent to Figure 19 in Section 4.1.3, except that the surface geometry in stead of the hydrophilic strength of the packing material has been varied in Figure 25.

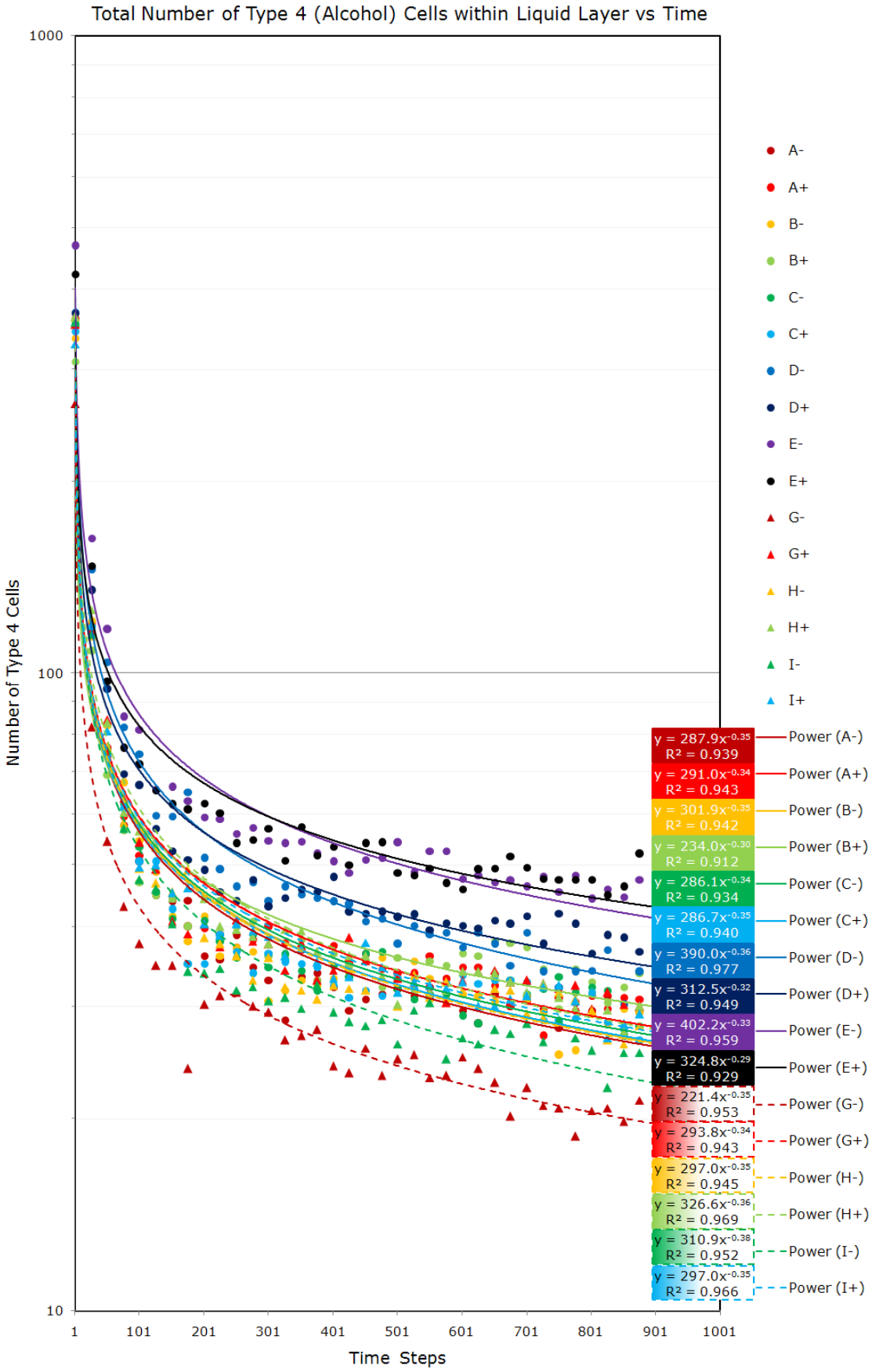

Figure 25: Average number of liquid alcohol cells as a function of time for different surface geometries

The number of liquid Type 4 cells in Figure 25, like in Figure 19, decreases almost logarithmically with time for all types of surface geometries. This behaviour conforms to the theoretical expectations for a system in which the vapour pressure of the liquid phase exceeds that of the gas phase. Such a system will spontaneously strive towards a dynamic steady state equilibrium in which the difference between the component vapour pressure of the gas phase and that of the liquid phase has been minimized through the selective evaporation of the alcohol.

Figure 25 confirms the capability of the model to represent the effect of a declining driving force that is typical for a system which is allowed to reach equilibrium.

The type (triangular vs. circular shape) and orientation (excavation vs. protrusion) of the surface geometry does not seem to have any significant influence on the rate at which steady state has been achieved. This is expected, seeing that these variations do not affect the driving forces which in turn determine the rate at which the Type 4 cells move from the liquid layer to the gas phase, even though these factors *do* influence the steady state conditions as such, as discussed in Section 4.2.2.

The depth of the surface geometry, however, seems to influence the rate at which steady state has been achieved to such an extent that it cannot be ignored. Figure 26 represent the effect of varying surface depths on the rate of alcohol evaporation that corresponds to the decrease in liquid Type 4 cells for various stages during the simulation.

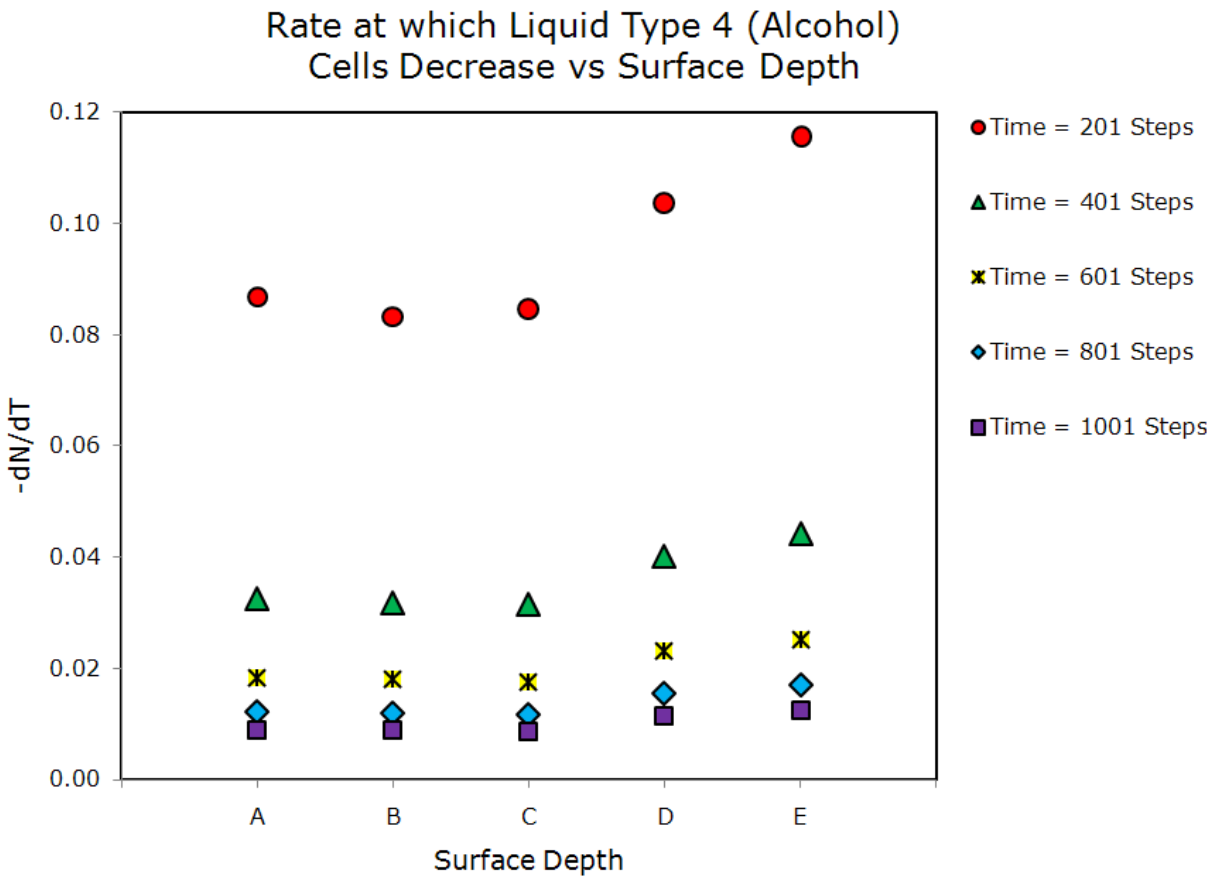

Figure 26: Rate of evaporation for liquid alcohol (Type 4 cells) as a function of packing material surface depth

For any number of completed time steps, the rate of alcohol evaporation seems to be significantly higher for the deeper (according to the definition of "depth" in Section 4.2.1), more "closed" shapes (D and E) than for the shallow, open surfaces.

These results contradict the typical intuitive expectation that the deeper geometries, especially the excavated shapes, would restrict and subsequently slow down the movement of the liquid Type 4 cells from the packing material surface.

Figure 27(a) and (b) accompanied by Table 18 provides a possible explanation for these unexpected results that is based on the dynamic mechanism of the simulation model. Figure 27(a) and (b) are both simplified scenarios which involves a thin liquid film layer consisting of Type 3 cells (turquoise) and Type 4 cells (pink), representing water and alcohol respectively, on a packing material surface (yellow). The dark blue cells represent the large intramolecular space (Type1) which is typical to the gas phase.

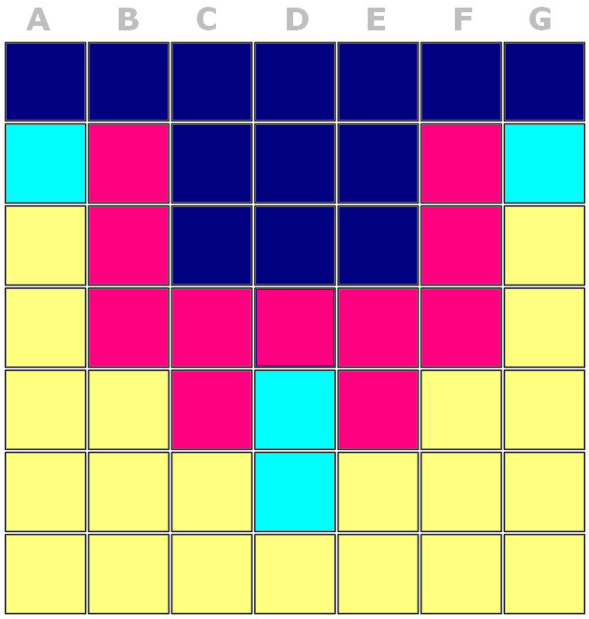

Figure 27 (a): Thin liquid film layer within a wide, relatively open configuration of the packing material surface.

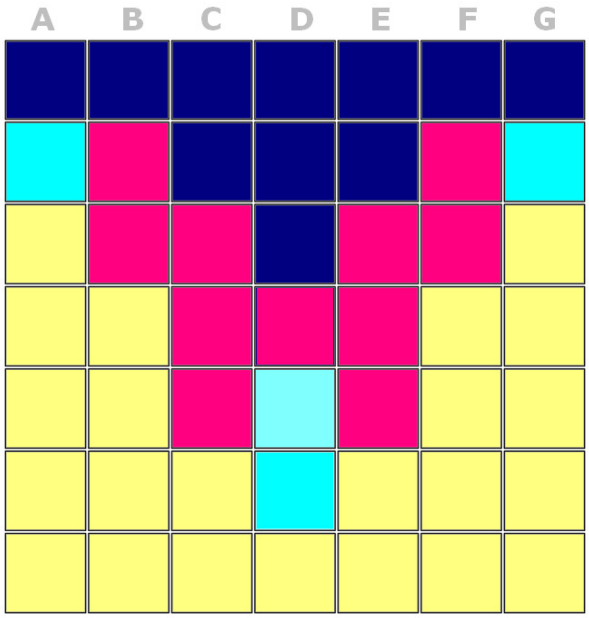

Figure 27 (b): Thin liquid film layer in a slightly narrowed (closed) configuration of the packing material surface.

The rows on the board in Figure 27 are numerically indexed while the columns are alphabetically indexed in aid of the explanation to follow. The individual cells are indexed by these coordinates. For example, the square in the top right hand corner of the board will be referred to as "Position G1".

Table 18 summarizes the nearest neighbours for all the alcohol cells in the liquid films of Figure 27(a) and (b) respectively. Note that the neighbours of an entire R=7 neighbourhood are usually considered when the tendency for a cell to exchange places with any nearest neighbour has to be calculated. For this example, the scenario has been simplified by considering only the nearest neighbours.

The surface of the packing material that touches the liquid, has exactly the same length (15 cells for a Moore neighbourhood) for both the open and narrowed structure. The number of cells present for the different cell types in the liquid film layer, is also exactly the same.

The only difference is the shape of the packing material surface: The left and right sides of the open V-shaped surface in Figure 27(a) have been pushed closer to each other to form the narrowed V-shape in Figure 27(b). The liquid film layer in Figure 27(b) is now bent almost like a hairpin. This has subsequently resulted in an increase in the number of overlapping nearest neighbours for the two different "legs" of the v-shaped liquid layer.

For example, the alcohol cells in Positions B4 and F4, Figure 27(a) initially have had no neighbours in common. In Figure 27(b), they have shifted to Positions C3 and E3 respectively. These two alcohol cells now share the neighbouring cells in Positions D2, D3 and D4. Table 18 shows that the total number of non-empty nearest neighbours for the alcohol cells has increased by four cells due to the increased "sharing" of neighbours by the cells in the liquid layer.

Table 18: Neighbours of the Alcohol Cells for the Open and Closed Packing Material Structures in Figure 27

Position of Type 4 (Alcohol) Cells	***Nearest Neighbours***					
	Type 3 (Water)		*Type 4 (Alcohol)*		*Type 5 (Packing Mat.)*	
	Quantity	*Position(s)*	*Quantity*	*Position(s)*	*Quantity*	*Position(s)*
Open Configuration						
B2	*1*	*A2*	*1*	*B3*	*1*	*A3*
B3	*1*	*A2*	*3*	*B2,B4,C4*	*2*	*A3,A4*
B4	*0*	*-*	*3*	*B3,C4,C5*	*4*	*A3,A4,A5,B5*
C4	*1*	*D5*	*4*	*B3,B4,C5,D4*	*1*	*B5*
C5	*2*	*D5,D6*	*3*	*B4,C4,D4*	*3*	*B5,B6,C6*
D4	*1*	*D5*	*4*	*C4,C5,E4,E5*	*0*	*-*
E5	*2*	*D5,D6*	*3*	*D4,E4,F4*	*3*	*E6,F5,F6*
E4	*1*	*D5*	*4*	*D4,E5,F4,F3*	*1*	*F5*
F5	*0*	*-*	*3*	*E5,E4,F3*	*4*	*F5,G3,G4,G5*
F3	*1*	*G2*	*3*	*E4,F4,F2*	*2*	*G3,G4*
F2	*1*	*G2*	*1*	*F3*	*1*	*G3*
	11		***32***		***22***	
Narrowed Configuration						
B2	*1*	*A2*	*2*	*B3,C3*	*1*	*A3*
B3	*1*	*A2*	*3*	*B2,C3,C4*	*3*	*A3,A4,B4*
C3	*0*	*-*	*4*	*B2,B3,C4,D4*	*1*	*B4*
C4	*1*	*D5*	*4*	*B3,C3,C5,D4*	*2*	*B4,B5*
C5	*2*	*D5,D6*	*2*	*C4,D4*	*4*	*B4,B5,B6,C6*
D4	*1*	*D5*	*6*	*C3,C4,C5,E3, E4,E5*	*0*	*-*
E5	*2*	*D5,D6*	*2*	*D4,E4*	*4*	*E6,F4,F5,F6*
E4	*1*	*D5*	*4*	*D4,E3,E5,F3*	*2*	*F4,F5*
E3	*0*	*-*	*4*	*D4,E4,F2,F3*	*1*	*F4*
F3	*1*	*G2*	*3*	*E3,E4,F2*	*3*	*G3,G4,F4*
F2	*1*	*G2*	*2*	*F3,E3*	*1*	*G3*
	11		***36***		***22***	

For the above stated example, the number of Type 4 (alcohol) cells that act as nearest neighbours have increased from 32 to 36. Table 18 therefore indicates that a larger number of shared neighbours of a certain cell type essentially have the same effect as an increase in the concentration of that cell type in the liquid film layer.

An increased concentration of liquid Type 4 implies an increased vapour pressure for the corresponding component (Alcohol) in the liquid phase. The driving force for cell movement that represents the evaporation of liquid alcohol has increased due to the increased number of shared neighbours within the liquid film layer.

It can therefore be assumed that the increased rate at which the alcohol cells have evaporated in Surface D and E, can be attributed to the increased sharing of alcohol cells by overlapping neighbourhoods from non-adjacent sections of the packing material surface (liquid layer). This overlapping is the consequence of a surface geometry that "folds back on itself" (of which Surface Shapes D and E are examples), with the sides of the fold being in close proximity to one other as shown in Figure 28(a).

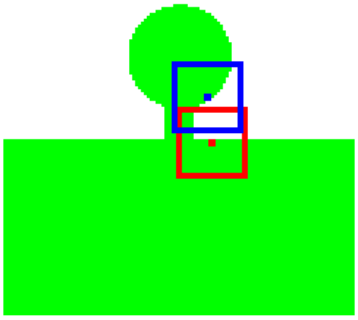

Figure 28 (a): An Example of two overlapping neigh-bourhoods from cells in non-adjacent walls within a narrow fold in the surface of the packing material

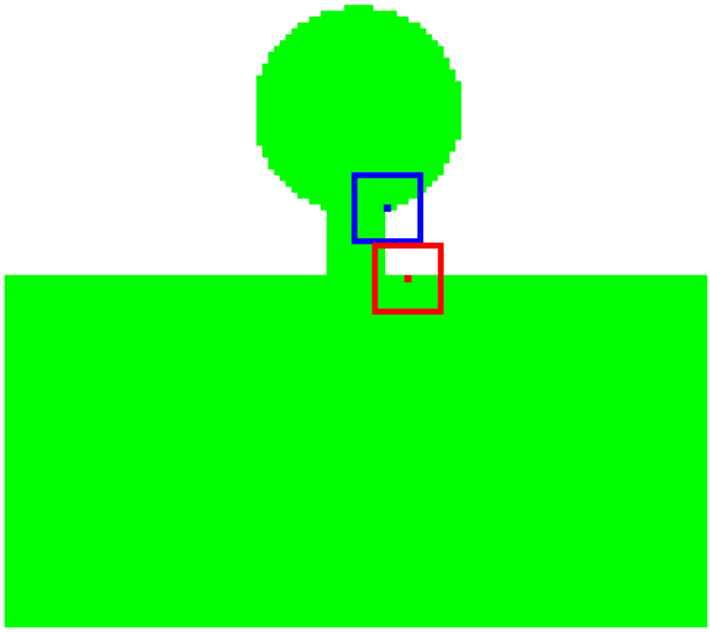

Figure 28 (b): Example of neighbourhoods from cells in non-adjacent walls within a narrow fold in the surface of the packing material: These neighbourhoods do not overlap due to the large scale of the surface geometry with respect to the radius of influence (neighbourhood size)

Depending on the scale of the physical system for which this model might eventually be calibrated, sharing might affect the accuracy of the model negatively. Overlapping neighbourhoods that result in the sharing of neighbours can be effectively reduced by a larger board which will permit the use of bigger geometrical shapes in comparison with the radius of influence. Figure 28 (b) demonstrates that the radius of the smallest bend must still exceed the radius of influence to minimize the possibility of sharing.

4.3 Overview on the Scope and Limitations of the Uncalibrated CA Model

In the preceding subsections the ability of the model to represent simple mass transfer scenarios was put to the test. The model in its uncalibrated state has proven itself capable of the following:

- Representing the effect of the intermolecular forces between the stationary packing material and the other, mobile species during a hypothetical mass transfer scenario.

- Representing the influence of strongly hydrophilic packing materials, not only on the total separation that has been achieved at steady state, but that also on the rate of separation.

- To represent and identify the difference between the densities of (volatile and less volatile) phases and can therefore successfully locate and identify distinctive phases.

- Incorporation of polarization by extending the radius of influence.

- Representing the effect of a declining driving force that is typical of a system which is allowed to reach equilibrium after it has been disturbed.

The model is therefore capable of representing an additional driving force for separation that is caused by the effect of intermolecular forces, apart from the driving force that has already been created by the effect of different component vapour pressures.

The performance of the model was limited due to the following reasons:

- More specific correlation(s) between the model parameters and the properties of the system being modelled needs to be established during the calibration of the model.

- A large neighbourhood combined with high α_{ij} –values, yields very high numerical values for the swapping probabilities. The allowable size range for the α_{ij} –values therefore decreases as the radius of influence (neighbourhood size) increases.

The trade-off between the neighbourhood size and the allowable range of $\alpha_{i,j}$-values, has resulted in a trade-off between the ability of the model to incorporate the effect of polarization and the ability to represent various degrees of separation (in particular the selective condensation of hydrophilic substances for strong hydrophilic packing materials).

Notwithstanding the above stated scope and limitations, the model also displayed the potential ability to represent the effect of different surface structures on the extent of separation achieved at steady state as well as the rate at which such a steady state condition has been achieved. The model must be correctly scaled to minimize inaccurate results due to 'sharing' of neighbourhoods as discussed in Section 4.2.3 and illustrated in Figure 28.

5. Conclusions

The ability of cellular automata to model relatively complex processes or phenomena, in particular thermodynamical scenarios (usually modelled with more conventional methods) was explored and subsequently assessed in this study. The mass transfer in packing materials of distillation columns served as an example for this purpose due to the sufficient level of complexity in the distillation process, and its importance in a wide range of process engineering applications.

The ability of the model to represent transition of solutes from the fluid on the micro-surfaces of packing materials to the by-passing vapour stream in distillation columns, as well as the steady-state equilibrium between evaporation and condensation, has been investigated.

5.1 Conclusions on the Literature Review

The information currently available in books, published journal articles and the internet is summarized in the literature survey.

This literature survey provides a general overview on cellular automata that includes the history and development, definition and characterization, possible structural variations, dynamics, behavioural classification and applications thereof. Some examples of cellular automata models in applications related to the process engineering industry are included.

Cellular automata are at this stage still under-exploited in the process engineering industry as opposed to other modelling techniques like CFD-modelling. At the time this study was undertaken, CA models that specifically deal with the mass transfer in packing materials were non-existent.

Information on other modelling systems with cellular automata proved to be useful only as background knowledge. These shortcomings in the currently available information suggested the need for a cellular automata model (such as the one that has been developed in this study).

5.2 Conclusions on the Model Behaviour

A cellular automata model has been constructed for the modelling of mass transfer in packing materials. The model was incorporated in a computer programme that receives input from the user (model parameters) from which it will calculate the required output (model results). The model parameters include the board dimensions, the number and type of cells present and the rules according to which these cells move (or exchange positions).

The ability of the model to represent simple mass transfer scenarios was put to the test. The following criteria were considered and the simulation programme was accordingly adapted to yield the output necessary for evaluation of the model against these criteria.

5.2.1 General Ability to Model the Effect of Individual and Cumulative Chemical and Thermodynamic Properties

The model in its current state is not able to simulate the individual effects of chemical and thermodynamic properties, for example, intermolecular forces, vapour pressure gradient, etc. It is therefore not always possible to attribute the change in model behaviour that results from adjustments to an input parameter to a single, specific physical or theoretical factor or even a combination thereof.

However, a realistic simulation of the cumulative effect exerted by these factors, or change thereof, on a system, for example the separation of alcohol and water, has been achieved.

The accuracy of the results that have been obtained by using iterated parameters cannot be guaranteed for scenarios that deviate too much from the system that has originally been modelled. This might be resolved by calibration of the model that will allow it to accommodate all systems that are chemically and thermodynamically specified.

5.2.2 Ability to Simulate the Effect of a Strongly Hydrophilic Packing Material on Steady State Conditions

There is a trade-off between the ability of the model to incorporate the effect of polarization, its ability to represent separation, in particular the condensation of hydrophilic substances, for strong hydrophilic packing materials and its ability to incorporate a large number of species. The ultimate consequence of this trade-off is a decreased range of separation scenarios that can be modelled successfully.

The simulation programme needs further modification to avoid these trade-offs that cripples its ability to produce a realistic separation model for scenarios that involve extensive condensation.

5.2.3 Ability to Realistically Represent the Effect of Changing Driving Forces on a Dynamic System

The model has proven itself able to represent the effect of a declining driving force (difference between the component vapour pressure of the gas phase and that of the liquid phase) that is typical of a system which is allowed to reach equilibrium through selective evaporation.

The model suggests that the hydrophilic strength of the packing material not only affects the total separation that has been achieved after steady state has been reached, but that it also affects the rate of separation.

The model is capable of representing an additional driving force for separation caused by the effect of intermolecular forces apart from the effect resulting from the difference in component vapour pressures.

5.2.4 Ability to Realistically Represent the Effect of the Packing Material Shape on the Degree and Rate of Separation Achieved

The surface of the packing material can assume an infinite number of possible shapes. Only carefully selected, simple shapes have been covered in this study. Quantitative criteria were developed and incorporated to ease comparison between the results from different surface geometries.

According to these criteria, better separation is achieved when packing material surfaces with a circular geometry are modelled instead of surfaces with a triangular geometry. Only slightly better separation has been achieved when packing materials with protruding geometries are used instead of packing materials with excavated geometries. Better separation has been achieved with shallow geometries than with the deeper geometries. The type (triangular vs. circular shape) and orientation (excavation vs. protrusion) of the surface geometry does not seem to have any significant influence on the rate at which steady state has been achieved.

These results can be justified by the physical configuration of the shapes which suggests that the above mentioned criteria are sufficient for the purposes of this study.

The depth of the surface geometry, however, seems to influence the rate at which steady state has been achieved to such an extent that it cannot be ignored. The results contradict the typical intuitive expectation that the deeper geometries, especially the excavated shapes, would restrict and subsequently slow down evaporation from the packing material surface. A possible explanation for this contradiction is the overlap between neighbourhoods that results from an incorrectly scaled model. For more accurate results, the radius of the smallest bend in the surface geometry must exceed the radius of influence.

5.3 Ability of the Cellular Automata Model to Represent Basic Characteristics of Mass Transfer in Packing Materials

The ability of a simple cellular automata model to simulate the mass transfer in packing materials has been assessed with reasonable success. Although several adjustments are needed to eliminate some limitations, such as the trade-off between $\alpha_{i,j}$ and R, premature saturation and sharing, the model has proven itself worthy of further development due to its capability to represent the basic characteristics of mass transfer in packing materials. However, extensive fine-tuning and calibration is needed before the model would be suitable for practical applications.

6. References

Bell A., Aoi Y., Terada A., Tsuneda S., Hirata A., Comparison of Spatial Organization in Top-down- and Membrane-aerated Biofilms: A Numerical Study, *Water Science and Technology*, 52(7), 173-180, 2005.

Benjaafar, Saifallah et al., *Cellular Automata for Traffic Flow Modeling*, University of Minnesota, Minneapolis, 1997

Birkhoff G.D., *Dynamical Systems*, American Mathematical Society, Providence, Rhode Island, 1927.

Braga G. , Cattaneo, G., Flocchini, P., Quaranta, C., *Pattern Growth in Elementary Cellular Automata*, Theor. Comp. Sci, 1995.

Brosa U., Direct Simulation of a Permeable Membrane, *Journal de Physique (Paris)*, 51(11), 1051-1053, 1990.

Burks A.W. (ed), *Essays on Cellular Automata*, Univ. of Illinois Press, Illinois, 1968.

Chopard B., Droz M., Study of the A+B to C reaction-diffusion process, *International Journal of Modern Physics C*, 4, 209-215, 1993.

Cochinos R., [3]

Codd E.F., *Cellular Automata*, Academic Press, New York, 1968.

Culik K., Hurd L.P., Yu S., *Computation Theoretic Aspects Of Cellular Automata*, Physica D, 45, 1-3, 357-378, 1990.

Dewdney A.K., *A Cellular Universe of Debris, Droplets, Defects and Demons*, Scientific American, 261:2, 102-105, August 1989.

Dewdney A.K., The Cellular Automata Programs That Create Wireworld, Rugworld and Other Diversions, *Scientific American*, 262:1, 146-149, January 1990.

Dirac P.M., The Evolution of the Physicists, *Scientific American*, 45, May 1963.

Doolen G. (Ed.), Lattice Gas Methods for PDE's, *Physica D*, 47, 1991.

Engelbrecht A.M., Aldrich C., Bredenkamp B., Simulation of Fouling in Membrane Processes with Cellular Automata, *Journal of The Southern African Institute of Mining and Metallurgy*, 107, 2007.

Eppstein D., [4, 5]

Ganguly N., Sikdar B.K., Deutsch A., Canright G., Chaudhuri P.P., *A Survey on Cellular Automata, Technical Report*, Centre for High Performance Computing, Dresden University of Technology, 2003.

Gardner M., The Fantastic Combinations of John Conway's New Solitaire Game of 'Life'. *Scientific American*, 223, 120-123, 1970.

Gardner M., *Wheels, Life, and Other Mathematical Amusements*, W. H. Freeman and Company, New York, 1983.

Gaylord R.J., Nishidate K., *Modeling Nature: Cellular Automata Simulations with Mathematica*, TELOS/Springer-Verlag Publishers, 1996.

Gerhardt M., Schuster H., A Cellular Automaton Describing the Formation of Spatially Ordered Structures in Chemical Systems, *Physica D*, 36, 1989.

Gerhardt M., Schuster H., *Das digitale Universum - Zelluläre Automaten als Modelle der Natur*, Vieweg, Braunschweig/Wiesbaden, 1995.

Grassberger P., Chaos and Diffusion in Deterministic Cellular Automata, *Physica 10D*, 52-58, 1984.

Greenspan D., *Discrete Models*, Addison-Wesley Publishing Company, 1973.

Gottschalk W.H., Hedlund G.A., *Topological Dynamics*, American Mathematical Society, Providence, Rhode Island, 1955.

Gutowitz H. (Ed.), CA FAQ, *Alife Online* [11], Santa Fe Institute, April 1999.

Hapgood F., Let there be Life, *Omni*, 9(7), 40-46, 116-117, April 1987.

Hayes B., *Zelluläre Automaten, Computer Kurzweil, Spektrum der Wissenschaft*, Heidelberg

Hedlund G.A., Endomorphisms and automorphisms of the shift dynamical system, *Mathematical Systems Theory*, 3, 320-375, 1969.

Kauffman S.A., Emergent Properties in Random Complex Automata, *Physica 10D*, 145-156 , 1984.

Kier L.B., Cheng C.K., Testa B., Cellular Automata Models of Biochemical Phenomena, *Future Generation Computer Systems*, 16(2), 273-289, 1999.

Kier L.B., Cheng C.K., A Cellular Automata Model of Membrane Permeability, *Journal on Theoretical Biology*, 186(2), 75-80, 1997.

Kubica K., Cellular Automata for Lipid Membranes, *Applied Mathematics and Computation (New York)*, 63(2-3), 187-199, 1994.

Kuhn T., *The Structure of Scientific Revolutions*, University of Chicago, 1970.

Lan Y.J., Li D.Z., Li Y.Y., A Mesoscale Cellular Automaton Model for Curvature- Driven Grain Growth, *Metallurgical and Materials Transactions*, 73(B), 119-129, 2006.

Langton C.G., Self-Reproduction in Cellular Automata, *Physica 10D*, 135-144, 1984.

Langton C.G., Computation at the edge of chaos: phase transitions and emergent computation, *Physica D,* 42, 12-47, 1990.

Li J., Sanderson R.D., Hurndall M.J., Hallbauer D.K., Hallbauer-Zadorozhnaya V.Y., *Real-Time Observation of Fouling in Membrane Filtration by Non-Invasive Ultrasonic Techniques,* WRC Report No 1166/1/04, Silowa Printers, 2004.

Lim H.A., Lattice Gas Automata of Fluid Dynamics for Unsteady Flow, *Complex Systems*, 2, 45-68, 1988.

Lindenmayer A., Mathematical models for cellular interaction in development, Parts I and II, *Journal of Theoretical Biology*, 1968.

Margolus N., Physics-Like Models of Computation, *Physica 10D*, 81-95, 1984.

Mazoyer J., A six-state minimal time solution to the firing squad synchronization problem, *Theoretical Computer Science 50*, 183—238, 1987.

McCauley J.L., *Chaos, dynamics, and fractals: an algorithmic approach to deterministic chaos*, Cambridge University Press, 1993.

McCulloch W.S., Pitts W., A logical calculus of the ideas immanent in nervous activity, *Bulletin of Mathematical Biophysics,* 5, 115-133, 1943.

McIntosh H. V., [1]

Moore, E. F., "Machine models of self-reproduction". *Proceedings of Symposia in Applied Mathematics* 14, 17–33, 1962.

Moore E. F., Sequential Machines: Selected Papers, *Reading MA,* Addison-Wesley, 213-214, 1962.

Morris S., Games - The game of Life, *Omni*, 7(1), 188-189, October 1984.

Myhill, J. (1963). "The converse of Moore's Garden-of-Eden theorem". *Proceedings of the American Mathematical Society* 14, 685–686, 1963.

Nguyen H.B., Nguyen V.C., Hamacher, Pattern synchronization in two-dimensional cellular spaces,. Information and Control, 26, 12—23, 1974.

Omohundro S., Modelling Cellular Automata with Partial Differential Equations, *Physica 10D*, 128-134, 1984.

Ott E., Sauer T., Yorke J.A., *Coping with chaos : analysis of chaotic data and the exploitation of chaotic systems*, John Wiley, New York, 1994.

Perry K. E., Abstract mathematical art, *Byte*, 11(13), 181-192, December 1986.

Peterson I., The *Mathematical Tourist: Snapshots of Modern Mathematics*. W. H. Freeman, New York, 86-95, 1988.

Rucker R., *The Lifebox, the Seashell and the Soul*, Thunder's Mouth Press/ Avalon Publishing Group, 2005.

Sakoda J.M., The checkerboard model of social interaction, *Journal of Mathematical Sociology 1*: 119–32, 1971.

Sarkar P., A Brief History of Cellular Automata, *ACM Computing Surveys*, v 32, n 1, 80-107, March 2000.

Schatten, A., *Cellular Automata Digital Worlds*, 2006.

Schatten, A., [12]

Schelling T.C., 100% Models of Segregation, *The American Economic Review* v 59, n 2, *Papers and Proceedings of the Eighty-first Annual Meeting of the American Economic Association*, 488-493, 1969.

Schmidhuber J., A Thirty-Five Year Old Kind of Science, *Intl. Journal of High Energy Physics, 43:5, June 2003*

Schmidhuber J., [13]

Sipper M., *Machine Nature: The Coming Age of Bio-Inspired Computing*, McGraw-Hill, New York, 2002.

Sipper M., [2]

Smith III A.R. , Real-time language recognition by one-dimensional cellular automata, J. *Comput. System Sci. 6,* 233 253, 1972.

Sutner K. , Cellular automata and intermediate reachability problems, *Fundamentae Informaticae*, 2002.

Toffoli T., Cellular Automata as an Alternative to (Rather than an Approximation of) Differential Equations in Modelling Physics, *Physica 10D*, 117-127, 1984.
Toffoli T., Margolus N., *Cellular Automata Machines: A New Environment for Modelling*, MIT Press, Cambridge, Massachusetts, 1987.

Ulam S., On some mathematical problems connected with patterns of growth of figures, A.W. Burks (ed.), *Essays on Cellular Automata*, University of Illinois Press, 1970.

Vichniac G.Y., Simulating physics with cellular automata, *Physica D*, 10, 96-116, 1984.

Von Neumann J., *Theory of Self-Reproducing Automata*, A.W. Burks (ed.), University of Illinois Press, Illinois, 1966.

Waksman A., An Optimum Solution to the Firing Squad Synchronization Problem. *Information and Control 9*: 66—78, 1966.

Wainwright R. T. (ed.), *Lifeline*, March 1971, September 1973.

Weaver W., Science and Complexity, *American Scientist*, 36, 536, 1948.

Weisstein E., [6]

Wiener N., *Cybernetics*, John Wiley and Company, New York, 1948.

Willox R., Grammaticos B., Carstea A.S., Ramani A., Epidemic dynamics: discrete-time and cellular automaton models, *Physica A*, 328, 13-22, 2003.

Willson S.J., Growth Rates and Fractional Dimensions in Cellular Automata, *Physica 10D*, 69-74, 1984.

Winfree A.T., Rotating Chemical Reactions, *Scientific American*, 230, 1974.

Wolfram S., Statistical mechanics of cellular automata, *Reviews of Modern Physics,* 55, 601-644, 1983.

Wolfram S., Universality and complexity in cellular automata, *Physica D*, 10, 1-35, 1984.

Wolfram S., *Cellular Automata and Complexity*, Addison-Wesley, Menlo Park, 1994.

Wolfram S., *A New Kind of Science*, Third Printing, Wolfram Media, 2002.

Wolfram S., [7]

Xiao-Guang Wu, Kapral R., Internal fluctuations, period doubling, and chemical chaos, *Physical Review E*, 50, 3560-3568, 1994.

Xuan X., Shao S., Chou K., A probability cellular automaton model for hepatitus B viral infections, *Biochemical and Biophysical Research Communications*, 342(2), 605-610, 2006.

Internet references: January 2008

[1] http://delta.cs.cinvestav.mx/%7Emcintosh/oldweb/lcau/node3.html

[2] http://lslwww.epfl.ch/~moshes/ca.html

[3] http://www.theory.org/complexity/traffic

[4] http://ics.uci.edu/~eppstein/ca/wolfram.html

[5] http://cafaq.com/classify/index.php

[6] http://www.ericweisstein.com/encyclopedias/life

[7] http://mathworld.wolfram.com

[8] http://www.rennard.org/alife/english/acintrogb01.html

[9] http://www.wolframscience.com/reference/notes/876b

[10] http://cocoon.ifs.tuwien.ac.at/info/ca/ca.html

[11] http://alife.santafe.edu/alife/topics/cas/ca-faq/ca-faq.html

[12] http://qspr03.tuwien.ac.at/~aschatt/info/ca/ca.html

[13] http://www.idsa.ch/~juergen/wolfram.html

Appendix

Appendix

Glossary

The following words, terms, acronyms and abbreviations appear frequently in the thesis as well as other related literature sources.

A.1 Basic Terms and Key Words

Term	Explanation
Amphiphilic	Denotes a molecule combining hydrophilic and lipophilic (hydrophobic) properties
Asynchronous	Refers to events that are not synchronized or coordinated in time.
Bio-film	A slime layer which naturally develops when bacteria attach to an inert support that is made of a material such as stone, metal, or wood
Cartesian planes	Area formed by the intersection of two perpendicular, numbered lines.
Cellular automata	Cellular automata are defined as dynamical systems which are discrete in space and time. They operate on a uniform, regular lattice and are characterized by local interactions. Each cell can be in one of a finite number of possible states, updated synchronously in discrete time steps according to a local, identical interaction rule. The state of a cell is determined by the previous state of itself as well as that of the surrounding neighbourhood of cells.
Deterministic	Causing a fixed outcome, given initial conditions (as opposed to stochastic).
Diffusion	Intermingling of molecules in gases and liquids as a result of random thermal agitation.
Distillation	Distillation is a method for separating the components of a liquid mixture that depends on differences in the ease of vaporization of the components. The process involves heating of the mixture to separate the more volatile from the less volatile parts, and then condensing fractions of the resulting vapour so as to produce a more nearly pure or refined substance.
Dissociation	The process by which the action of a solvent or a change in physical condition, as in pressure or temperature, causes a molecule to split into simpler groups of atoms, single atoms, or ions.
Dissolution	Dissolution is the process by which a solid or liquid enters its aqueous phase. This can be explained simply as a breakdown of the crystal lattice into individual ions, atoms or molecules.
Distillation column	Equipment for fractional distillation in which a liquid mixture is separated into its component parts by heating. See also definition for 'Distillation'
Elementary cellular automata	The simplest class of one dimensional cellular automata.
Filter	A porous material through which a liquid or gas is passed in order to separate the fluid from suspended particulate matter. (Or: A device containing such a material, especially one used to extract impurities from air or water.)
Filtration	To pass (a liquid or gas) through a filter.
Fouling	To clog or obstruct.
Glider	The glider is a pattern in Conway's *Game of Life* that travels (diagonally) across the board.

Term	Explanation
Hydrophilic	Having an affinity for water; readily absorbing or dissolving in water.
Hydrophobic	Repelling, tending not to combine with or incapable of dissolving in water.
Hypothesis	A tentative explanation for an observation, phenomenon, or scientific problem that can be tested by further investigation.
Iteration	A computational procedure in which a cycle of operations is repeated, often to approximate the desired result more closely.
Lipophilic	Having an affinity for, tending to combine with, or capable of dissolving in lipids
Membrane	A thin sheet of natural or synthetic material that is permeable to substances in solution.
Micelle	A sub-microscopic aggregation of molecules, as a droplet in a colloidal system.
Model	A schematic description of a system, theory, or phenomenon that accounts for its known or inferred properties and may be used for further study of its characteristics.
Osmosis	Diffusion of fluid through a semi-permeable membrane from a solution with a low solute concentration to a solution with a higher solute concentration until there is an equal concentration of fluid on both sides of the membrane.
Osmotic effect	See Osmosis (The tendency of fluids to diffuse in such a manner.)
Permeable	That can be permeated or penetrated, especially by liquids or gases
Probabilistic	Refer to 'stochastic'.
Selectivity range	Ability of model to represent different degrees of separation.
Simulation	Imitation or representation, as of a potential situation or in experimental testing. (Or: Representation of the operation or features of one process or system through the use of another.)
Stochastic	Involving or containing a random variable or variables. Involving chance or probability.
Tessellation	A repetitive pattern of polygons that covers (or tiles) a plane with no gaps and no overlaps.
Universal	Universal automata are able to model the behaviour of any other automata.
Wolfram rules	Refers to the elementary cellular automaton rules introduced by Wolfram in 1983.

A.2 Acronyms, Abbreviations and Symbols

Term	Explanation
$\alpha_{i,j}$	Weight Contribution to Swapping Probability of Cell x with Cell y with i = State of Cell y and j = State of Neighbour of Cell y
β_y	Swapping Probability of Cell x with Neighbouring Cell y
IR	Individual Result
CA	Cellular Automata
CS	Criterion Score
ID	State (Identity) of Cell
M	Membrane
MATLAB	Matrix Laboratory (Name of computer programme used for mathematical simulation and modelling)
n	Side Length of Square Matrix with n x n Dimensions
NOC	Number of Cells
SSS	Scaled Separation Score
TNR	Total Number of Results
$\overline{V}$	Directional Bias Vector
VLSI	Very Large Scale Integration
WRC	Water Research Commission
$\overline{\Omega}_y$	State Bias Matrix of Cell y
x	Index Number of Centre Cell within Moore Neighbourhood